Development of Peptides as Potential Drug Leads for the Treatment of Inflammatory Bowel Diseases

Claudia Cobos Caceres

B.Sc. (Hons.) Chemistry

For the degree of Doctor of Philosophy in Medical and Molecular Sciences

College of Public Health, Medical and Veterinary Sciences

James Cook University, Cairns, Australia

1st May 2018

Acknowledgments

Applying to be a PhD candidate at James Cook University in Cairns was the perfect place to start this journey. Nothing better than working in a great place in the middle of paradise. I wish to express my deepest gratitude to my University and the College of Public Health, Medical and Veterinary Sciences for letting me become a Doctor in Medicinal and Biological Science, thank you for the scholarships that made this dream come true.

I also would like to continue by expressing how immensely grateful I am to my primary supervisor **Professor Norelle Daly**, who took me under her wing and guided with all her knowledge, patience, motivation, enthusiasm for science and provided me all the support necessary to pursue my goals. This work would not have been possible without her.

I would also like to thank my secondary supervisor **Professor Alex Loukas** for always having the door open for me when I needed him with his scientific advice and extremely knowledgeable suggestions that helped me during these years of work.

Thank you also to my co-supervisor **Dr. David Wilson**, who was there for me every time I needed help when something went wrong in the lab. He made my life easier every time the HPLC or Mass Spectrometer stopped working. He was always able to fix them, making my life stress free.

I am also extremely grateful to my co-supervisor **Dr. Paramjit Bansal**. Paramjit who taught me everything he knows about peptide synthesis. He helped me every step through this journey. When I did not know what to do, he always knew! Sharing every day with him was an amazing experience. He would make a wonderful role model for every chemist in the world and I am now lucky to call him my friend. Thank you for all those years of knowledge and Punjabi stories!

I also would like to thank to **Dr. Paul Giacomin** and **Dr. Severine Navarro** for their support in all my biological experiments. Paul gave me perfect advice every time I did not

understand something. Severine helped me to learn animal experiments and statistical analysis of results. As this was not my expertise as a chemist, I now have extra skills, thanks to both of you.

I am extremely happy that I was part of Daly's group, and although it was a small group, it was a perfect combination of minds. Thank you **Mrs. Mohadeseh Dastpeyman** for your friendship, support, and always being there with a smile to help me organise my thoughts. You are an inspiration and I am happy to be your friend.

Also, even though I am not part of the Immunology Loukas' team, I feel part of them. **Mrs. Linda Jones (Ryan)**, thank you for all your help with mouse experiments. Your support was invaluable, and I am extremely grateful for the time we shared all these years. You are an amazing scientist and friend. Thank you to **Ms. Geraldine Buitrago** for your help, (laud) laughs, conversations, scientific advice, and everyday support. Thank you for your friendship. You will be an amazing Dr. in immunology! Also thank you to **Dr. Phurpa Wangchuk** who was there every time I needed help with statistical analysis or animal experiments. **Mr. Rafid Al-Hallaf**, thank you for offering your help every time I needed it. I am very grateful to you and **Mrs. Zainab Agha** for your constant help and support.

Also, my gratitude to all the other part of Loukas group: **Ms. Bemnet Tedla**, **Dr. Ramon Eichenberger**, **Ms. Stephanie Ryan**, **Ms. Sally Troy**. Thank you for your assistance and encouragement. To **Mr. Atik Susianto** and **Mr. Bjorn Hauge a** big thank you for all the technical help.

Also, my deepest gratitude to administrative staff of AITHM: **Ms. Mel Campbell** and **Mrs. Trilby Butcher,** I am eternally grateful for your patience and assistance and **Mrs. Julie Woodward**, for your encouraging smile and your extra help during the final stages. You are the heart of AITHM.

Thank you very much for the help and opportunities that my College of Public Health, Medical and Veterinary Sciences di. A special thank you to: **Mr. Tina Cornell, A/Prof Kerrianne Watt, Mrs. Kerry Knight, Mr. Shane Walker and Prof. Alan Baxter.**

Finally, and most importantly, I especially thank **my family**. I have the most hard-working **mum** in the world who made great sacrifices for myself and my brother Sebastian. This is all happening because of you and I love you. To **Seba**, I am so proud of you. To my **dad**, I am here for you always. You and my mum are the inspiration for my desire to become a scientist. To my **siblings**, you are my best friends that have supported me even when we are an ocean and thousands of kilometers apart, I miss you all. To my **Caceres and Cobos family**, you are my everything and I am so happy to be part of your life. Your love and support has always been with me even from the other side of the world. To my **granddad**, I miss you every day and I wish you were here to share this moment with me. To my other family in Australia, **The Casella family**. You "adopted" me almost like a daughter. **Lyndell** and **Fred** have been my support in Australia, I do not have words enough to say how much you mean to me. Thank you for your love. To **Ben** and **Aaron**, my other brothers, thank you for accepting me with love into your family.

Finally, this is for you, the love of my life, my soul-mate and future husband, **Evan Casella**. These years living in Cairns, starting a PhD in another language, in a foreign country was the most difficult and amazing thing that I have ever done. All because of you. Following from the other side of the world to this paradise was the best decision I have ever made, and I would do it all over again. You have been a true partner, my biggest supporter, who with unconditional love guided me in good and bad times. Always with a hug and a kiss with the perfect word when I needed it most. These years have made us stronger and I know have the best man in the world walking through life by my side. I love you.

This thesis is dedicated to my mum, my family in Chile, my family in Australia,

and to my soul-mate *Evan.*…

*"**It always seems impossible until it's done**"*-Nelson Mandela

Statement of The Contribution of Others

During my PhD candidature my thesis work has included:

1) Synthesis of the peptides (synthesis, purification, mass analysis, oxidation)

2) Structural analysis of peptides using NMR spectroscopy

3) Biological assays (mouse assays, cell culture, tissue collection, histological analysis)

4) Thesis write up

I have had great support from the AITHM team, a JCU scholarship and travel grants. I have attached a list outlining the contributions from others in the following table.

Nature of Assistance	Contribution	Name and Affiliations
Intellectual support	Project Plan and Development	1) Prof. Norelle Daly, AITHM 2) Prof. Alex Loukas, AITHM
	Data Analysis Assistance	1) Prof. Norelle Daly, AITHM 2) Prof. Alex Loukas, AITHM 3) Dr. Severine Navarro, AITHM 4) Dr. Paul Giacomin, AITHM
	Editorial Support	1) Prof. Norelle Daly, AITHM 2) Prof. Alex Loukas, AITHM 3) Dr David Wilson, AITHM 4) Dr Severine Navarro, AITHM 5) Dr Paul Giacomin, AITHM
Financial support	Research Costs	1) Fellowship from NHMRC (1020114) 2) Australian Research Council and National Health and Medical Research Council via a Future Fellowship (110100226) 3) Fellowship (1117504) 4) Program Grant (1037304) 5) Janssen R&D, US
	Stipend	1) James Cook University Postgraduate Scholarship (APA) 2) College Scholarship, College of Public Health, Medical and Veterinary Science, James Cook University

	Conference Travel Assistance	1) Robert Logan Memorial Bursary Scholarship, JCU 2) HDRES Round 1 Grant, JCU 3) Student travel bursary 3rd International Conference on Circular Peptides 4) Student Travel Bursary 11th Australian Peptide Conference 5) Australian Institute of Tropical Health and Medicine
	Write-Up Grant	Doctoral Completion Grant, College of Public Health, Medical and Veterinary Science, James Cook University
Data collection	Research Assistance	1) Dr David Wilson (mass spectrometry) 2) Dr Paramjit Bansal (peptide synthesis) 3) Ms Linda Jones (animal assays)
	Mouse Histology Analysis Assistance	1) Dr. Ramon M. Eichenberger 2) Dr Paul Giacomin
Technical support	Peptide Synthesis Assistance	1) Dr Paramjit Bansal
	Mouse Samples Collection Assistance	1) Ms. Linda Jones

Published Works by the Author Incorporated into the Thesis

Chapter 2. An engineered cyclic peptide alleviates symptoms of inflammation in a Murine model of inflammatory bowel disease

Reference:

Cobos Caceres, C., Bansal, P. S., Navarro, S., Wilson, D., Don, L., Giacomin, P., Loukas, A., and Daly, N. L. (2017) An engineered cyclic peptide alleviates symptoms of inflammation in a murine model of inflammatory bowel disease. *J. Biol. Chem.* 292, 10288-10294

Author contributions: AL and NLD designed the study and wrote the paper, along with CCC. CCC, PSB, DW and LD synthesized and purified the peptides. DW carried out the mass spectrometry analyses. CCC and NLD determined the structure of the cyclic peptide. CCC, SN and PG carried out the animal experiments. All authors analyzed the results and approved the final version of the manuscript

Collaboration in other projects:

Reference:

Bansal, P. S., Smout, M. J., Wilson, D., **Caceres, C. C**., Dastpeyman, M., Sotillo, J., Seifert, J., Brindley, P. J., Loukas, A., and Daly, N. L. (2017) Development of a Potent Wound Healing Agent Based on the Liver Fluke Granulin Structural Fold. *J. Med. Chem.* **60**, 4258-4266

Unpublished Works by the Author Incorporated into the Thesis

Chapter 4 and Chapter 5 contain unpublished data, that will be submitted for publication following IP protection.

.

Chapter 3. Engineering of an anti-inflammatory peptide based on the disulfide-rich linaclotide scaffold (accepted at Biomedicines, September 2018)

Author contributions: AL and NLD designed the study and wrote the paper, along with CCC. CCC and PSB synthesized and purified the peptides. CCC and DW carried out the mass spectrometry analyses. CCC and NLD determined the structure of the peptide. CCC, LJ and PW carried out the animal experiments. All authors analyzed the results and approved the final version of the manuscript.

Chapter 4. Peptides derived from hookworm anti-inflammatory proteins suppress inducible colitis in mice and inflammatory cytokine production by human cells

Author contributions: AL and NLD designed the study and wrote the paper, along with CCC. CCC and PSB synthesized and purified the peptides. CCC, PB and DW carried out the mass spectrometry analyses. CCC and NLD determined the structure of the peptide. CCC, LJ, PG, SN carried out the animal experiments. CCC, PG and RE carried out histological evaluation. MF, NLD and CCC modelled proteins using I-TASSER. RR, CR and JM carried out human immune cells and BD™ Cytometric Bead Array. CCC carried out serum stability assay. All authors analyzed the results and approved the final version of the manuscript

Chapter 5. Engineering of an anti-inflammatory peptide based on MHC-II binding predictions

Author contributions: SN and NLD designed the study and wrote the paper, along with CCC and AL. CCC and PSB synthesized and purified the peptides. CCC, PSB and DW carried out the mass spectrometry analyses. CCC and NLD determined the structure of the peptide. SN, NLD and CCC carried out statistical analysis using Immune Epitope Database Analysis Resource. CCC and RE carried out histological evaluation. CCC, LJ and SN carried out the animal experiments.

Abstract

This thesis focuses on the study of peptides as potential drug leads for inflammatory bowel disease (IBD). IBD is a chronic and debilitating disease, that affects millions of people globally and costs billions to health systems. There is currently no cure for any form of IBD. Peptides have significant advantages for the design of novel therapeutics as they can have high potency and specificity, low immunogenicity and can be cheaper to manufacture compared with protein-based drugs.

Peptides as small as three residues have been shown to have efficacy in mouse models of colitis but they require very high concentrations presumably because of a lack of stability *in vivo*. Chapter 2 of this thesis describes the stabilization of MC-12, a tri-peptide derived from annexin A1, that is active in a TNBS mouse model of colitis. Grafting the tri-peptide sequence into the cyclic peptide SFTI-1 significantly improved the potency of the peptide in the TNBS mouse model of colitis, and significantly improved the stability *in vitro*. In Chapter 3 a similar grafting approach was used but in this study MC-12 was grafted into the linaclotide framework. Linaclotide is an orally active, disulfide-rich peptide used in the treatment irritable bowel syndrome. This is the first study to show that linaclotide can be used as framework and can adopt a novel bioactivity.

The second part of the thesis focused on hookworm protein-derived bioactive peptides. The low prevalence of parasites such as hookworms in developed countries, appears to be correlated with the rise in autoimmune conditions. This correlation has led to studies of parasite excreted proteins in autoimmune conditions such as inflammatory bowel disease (IBD). These studies

suggest that these excretory/secretory (ES) products in hookworms are a source of compounds with potential in the treatment of inflammatory bowel diseases.

AIP proteins from hookworms have been shown to have significant potential for the treatment of IBD. Using a “downsizing” approach Chapters 4 and 5 provided indications to regions of AIP proteins that might be important for the activity. Despite the sequence diversity in the AIP proteins, a conserved region containing a EXXXL motif conserved helical was identified that appears to be associated with the anti-inflammatory effects. This region appears to be helical in the full-length proteins, and interestingly one of the derived peptides forms a well-defined helical structure in solution without the need for covalent constraints such as disulfide bonds. In Chapter 5 a method based on MHC II peptide binding prediction was used to identify a bioactive sequence derived from an AIP protein. This peptide displayed significant protective effects in a chemically-induced acute colitis in mice. Despite the small size of the peptides (20 residues or less) identified in Chapters 4 and 5, they displaced potent activity *in vivo* when administered via intraperitoneal injection. These peptides have potential in the development of lead molecules as they are likely to have lower immunogenicity, greater tissue penetration and cheaper manufacturing compared to proteins. Further study is required to determine optimal routes for administration and if further stabilization is required to produce viable drug leads.

Overall this thesis has highlighted different strategies for the design of new peptide-based drug leads for the treatment of inflammatory bowel diseases. Furthermore, insight into the structure/function relationships of AIP proteins has also been gained. Future directions are likely to focus on the identification of the biological targets and mechanism of action involved in the anti-inflammatory activity.

Table of Contents

1. CHAPTER 1

Introduction

1.1. Development of peptides as potential drug leads

The fields of contemporary chemistry, biology and biochemistry have expanded the knowledge of biological and physiological processes. This expansion has led to the exploration of new drug targets that might help to improve the quality of human lives. However, one of the major challenges is the discovery and/or design of suitable new drugs for treatment and diagnosis of disease (1).

One method to meet the drug development challenge is the use of nature as an inspiration. Powerful new medicines can be created based on naturally occurring molecules. Natural products are the result of evolutionary pressure to preserve and improve the lives of the organisms that produce them (2). Such biological evolution has created complex compounds with specific bioactivities. These bioactive compounds include amino acids, peptides, proteins, carbohydrates and lipids (3,4), and have been shown to have an effect on human health (5).

Peptides, one of the many bioactive compound classes, are molecules that consist of amino acids linked together through amide bonds. They display a range of potentially useful biological functions such as anti-inflammatory (6), anti-cancer (7), anti-HIV (8), antimicrobial (9) and insecticidal (10) activities, among others. Peptides as drug leads have a range of advantages including target specificity, low toxicity and immunogenicity, but one major limitation for small, unstructured peptides is a lack of stability *in vivo* (1). The principal reasons for the fast elimination of peptides from the circulation are enzymatic degradation and/or fast renal clearance (11-13). The ability to reproduce peptides chemically in laboratories has led to modifications that enhance their activity and remedy their lack of stability. This approach

has the potential to improve the bioavailability of these drugs, and increase their pharmacological efficacy (14-16).

The use of disulfide-rich peptides and backbone cyclization is currently being explored to improve the stability and therapeutic potential of peptide based drug leads (17). Disulfide-rich peptides and backbone cyclic peptides have been used successfully for therapeutic applications as mentioned in the Cemazar et al review (18). For example, Prialt® (Ziconotide) is a synthetic version of the cone-snail venom peptide MVIIA and is currently on the market for the treatment of chronic pain (19). This cone-snail venom peptide is a calcium channel antagonist, containing 25 residues and three-disulfide bonds in a cystine knot motif (20). Another example is the 12-residue cyclic peptide cyclosporine that has famously revolutionised organ transplant therapy due to its potent immunosuppressant activities (21). These examples highlight the potential for using peptides constrained by disulfide bonds and/or cyclization for a range of therapeutic applications.

In addition to using naturally occurring peptides such as MVIIA and cyclosporine as drugs or drug leads, another approach for the identification of peptide based drug leads is the "downsizing" of proteins. The main idea behind downsizing proteins is to reproduce the functional potency of the protein but in a small peptide, which can simplify synthesis (making this cheaper), improve chemical stability (i.e. they can be useful for mimetics studies) and limit the potential for immunogenicity. This approach can also be useful for elucidating structure/function relationships. Protein downsizing has been applied to the human inflammatory protein C3a, and resulted in a peptide that presented the same specificity and potency with the receptor and also same cellular responses as the C3a protein. (22). The peptide also displayed an improvement in stability in plasma and bioavailability. The approach of

downsizing proteins can lead to the identification of small peptides, that might be sufficiently stable to use as drug leads or can be used as starting points for the development of more stable lead molecules. Another example was the study of the granulin protein from the human parasitic liver fluke *Opisthorchis viverrini*, known as *Ov*-GRN-1. *Ov*-GRN-1 accelerates wound repair in mice, but is difficult to express in high yields which limits its potential as a therapeutic agent (23). Bioactive peptides from the N-terminal region of *Ov*-GRN-1 have been engineered with the same potency as the full-length protein in a mouse wound healing assay (24). These peptides are likely to be less immunogenic and easier to more produced compared to the full-length recombinant protein.

The studies outlined in thesis use cyclic/disulfide rich peptides as structural scaffolds, and the downsizing of proteins, for the development of novel drug leads and elucidation of structure/function relationships. Background related to cyclic peptides and their use as scaffolds is given in section 1.1. In section 1.2 the rationale for studying hookworm proteins as anti-inflammatory agents is given. In this thesis, these proteins have been used in the downsizing approach to derive bioactive peptides and provide insight into the structure/function relationships.

1.1.1. Cyclic Peptides from Plants

1.1.1.1. Cyclotides

Cyclotides are an example of a naturally occurring family of peptides that are both disulfide-rich and contain a cyclic backbone. These peptides are plant-derived, have approximately 30 residues, and in addition to a head-to-tail cyclic backbone have a knotted arrangement of the three disulfide bonds (25). This structural motif has been referred to as the cyclic cystine knot (CCK) (25). Cyclotides have six inter-cysteine loops and generally have hydrophobic residues situated on their surface, as a result of the disulfide bonds being in the interior of the peptide structure (26).

Cyclotides were originally discovered when an indigenous medicinal application was studied by the Norwegian doctor Lorents Gran (27). Women in Africa used a tea made from the Rubiaceae plant *Oldenlandia affinis* to accelerate childbirth (27,28). Gran analysed the tea and demonstrated that the medicinal activity was due to a polypeptide of 29 amino acids in length, called kalata B1 (27). However, it was not until 1995 that the cyclic nature of kalata B1 was discovered (29). There are now hundreds of cyclotides that have been characterized from a range of plant families.

A range of bioactivities has been associated with cyclotides. For example, the circulins, cyclotides isolated from an extract of the tropical tree *Chassalia parvifolia*, were found in a screen aimed at elucidating novel anti-HIV agents (30). Cyclotides with antimicrobial activity against Gram-positive *Staph. aureus* and Gram-negative bacteria *P. aeruginosa* and *E. coli* have also been characterised (9), as well as potent serine protease inhibitors isolated from the seeds of the tropical plant *M. cochinchinensis* (31). The natural function of cyclotides in plants

is thought to be for defence against insects and other pests based on the insecticidal activity observed for kalata B1 and kalata B2 (32).

Cyclotides are highly resistant to enzyme degradation in contrast to some linear peptides, which have free N- and C-termini, making them targets for cleavage by exopeptidases (17). The sequence diversity associated with the cyclotides coupled with their resistance to denaturation and enzymatic degradation has led to several studies exploring the potential of cyclotides as leads for drug development (15).

1.1.1.2. Sunflower Trypsin Inhibitor

Sunflower Trypsin Inhibitor 1 (SFTI-1) is another example of a cyclic peptide from plants. SFTI-1 is present in the seeds of sunflowers (*Helianthus annuus*) (Figure 1.1), but in contrast to cyclotides, it only has 14 amino acids and a single disulfide bond (Figure 1.2.). Edman-degradation was used in an attempt to determine the SFTI-1 sequence but was unsuccessful because of the lack of an N-terminal residue. Consequently, the sequence was eventually determined by analysis of X-ray crystallography data and the cyclic backbone discovered (33). The structure of SFTI-1 comprises two short antiparallel β-strands that are linked by the single disulfide bond (33). SFTI-1 is now known to be part of a family of natural products that are encoded within genes that also contain a seed storage albumin (34,35). Cleavage of the peptide from the precursor protein and cyclization utilise enzymes involved in albumin maturation. Importantly, an asparaginyl endopeptidase is involved in ligation of the N-terminal Gly to the C-terminal Asp, and in this way forming the cyclic peptide SFTI-1(34,35). Although other plant derived cyclic peptides are not encoded within seed storage albumin genes, they is

evidence they also involve asparaginyl endopeptidases, highlighting the importance of this enzyme in cyclic peptide production (34).

Figure 1.1. *Helianthus annuus* (Sunflower).

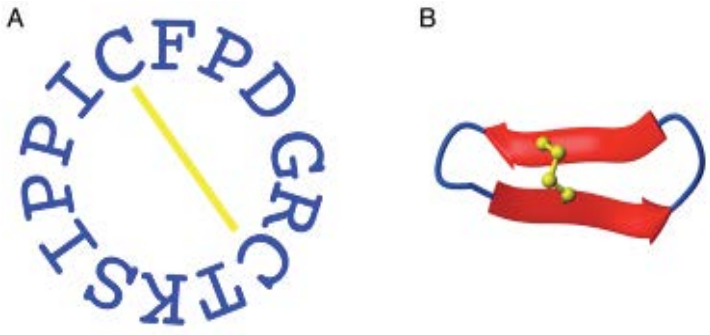

Figure 1.2. Sequence and structure of SFTI-1. (A) The sequence of SFTI-1 is drawn to represent the cyclic structure and the disulfide bond represented with a yellow line. (B) Ribbon representation of the three-dimensional structure of SFTI-1 (PDB code 1SFI).

SFTI is one of the most potent Bowman-Birk trypsin inhibitors (BBI) known and also inhibits other serine proteases including cathepsin G (33). BBIs are typically large peptides of approximately 60-90 residues with one loop targeting trypsin and one targeting chymotrypsin. This family of protease inhibitors was characterized by Birk in 1967 (36). The potency and specificity that defines BBIs is related to the nature of the P1 residue within the binding loop (37,38). Arg or Lys as the P1 residue can result in potent trypsin inhibitory activity (39). SFTI has a binding loop which contains the P1 residue, as well as a second loop that is involved with cyclization; hence, SFTI-1 is called a bicycle peptide. SFTI-1 has been shown to tolerate amino acid substitutions, while being highly stable as a result of its cyclic backbone and its disulfide bond, making it a promising stable peptide drug scaffold (33,40,41).

1.1.1.3. New horizons for disulfide rich peptides. Engineering cyclic/linear peptides

In addition to taking advantage of the intrinsic bioactivities of disulfide-rich and/or cyclic peptides, using them as grafting templates or scaffolds for the design of novel drug leads has also received significant attention in the literature recently. Protein grafting comprises the relocation of a bioactive epitope onto the surface of a stable folded peptide/protein in order to enhance its stability. There are now several examples where cyclic and linear peptides have been used as scaffolds to engineer non-native bioactivities. For example, an engineered form of SFTI-1 has been developed that targets the prostate cancer associated trypsin-like serine protease - KLK4 (40); the sequence is shown in Figure 1.4. The cyclotide framework has been used as a stable framework to graft peptide epitopes from central nervous system proteins, with potential in the treatment of multiple sclerosis (42). Both SFTI-1 and the *Momordica cochinchinensis* trypsin inhibitor-II (MCoTI-II) cyclotide have been used in the development of novel angiogenic peptides (41) (Figure 1.3). In this case, peptides from laminin-α1,

osteopontin and a peptide that mimics the VEGF helix region, were grafted onto MCoTI-II and SFTI-1. All grafted peptides were stable after being incubated in human serum and a grafted SFTI-1 analogue was developed that had nanomolar activity in an angiogenic assay.

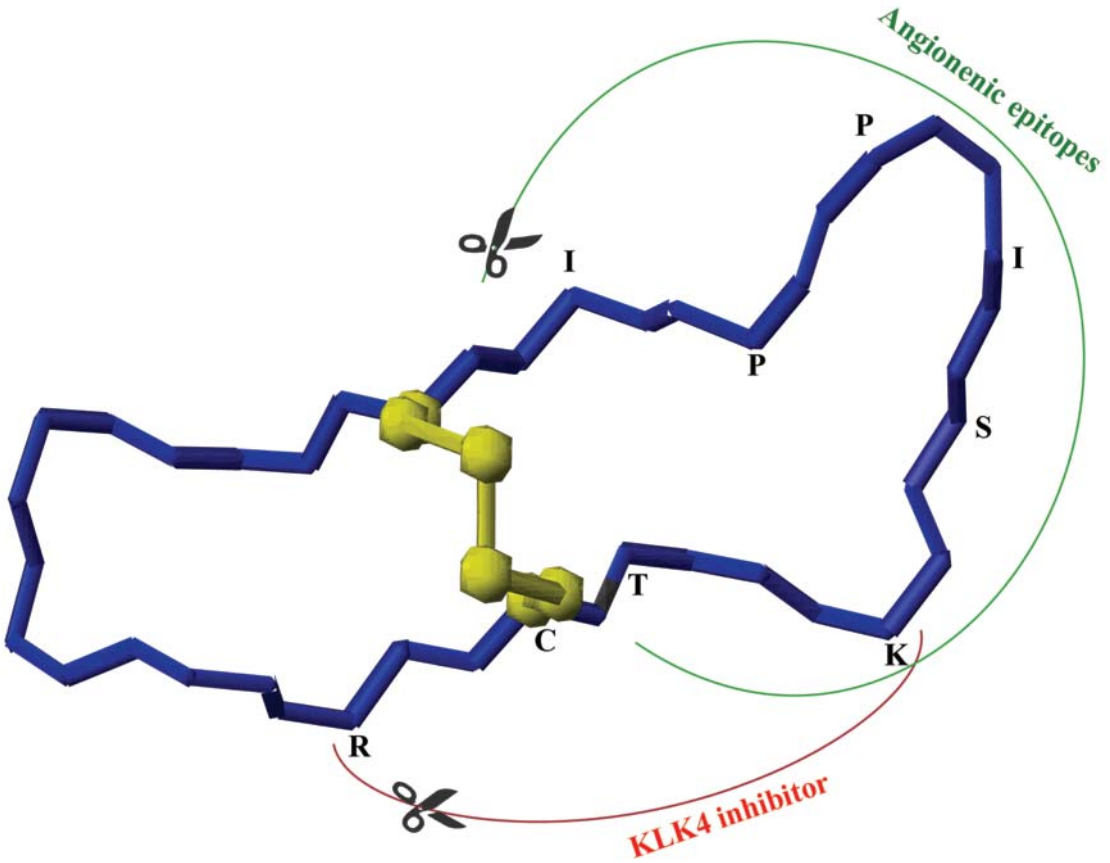

Figure 1.3. SFTI-1 engineering. The image shows regions of SFTI-1 that have been replaced with different bioactive sequences, using the peptide as backbone scaffold. In red is highlighted the sequence replaced by KLK4 inhibitor sequences. In green is shown the sequence replaced from SFTI-1 by angiogenic sequences.

Kalata B1 has also been used in several grafting and mutagenesis studies, including the grafting of a poly-Arg epitope into four of the backbone loops (16). The peptide with the poly-Arg sequence grafted into loop 3 showed the most anti-angiogenesis activity in a cell-based assay, highlighting that the grafting into different loops can have an influence on bioactivity.

Interestingly, the natural hemolytic activity of kalata B1 was abolished in all of the analogues. Kalata B1 has also been used to graft small bioactive peptides with bradykinin receptor antagonist activity (43). Analogues with oral activity in a mouse model were designed in this study with potential in treating inflammatory pain.

It is not only cyclic peptides that have been used as grafting templates - linear peptides have also been used for this purpose. For example, agatoxin (AgTx), a peptide inhibitor of voltage-activated calcium channels found in spider venom (44) has been used as an engineering scaffold (45). The grafted peptide was designed based on similarities between AgTx and the neuropeptide AgRP (46). A disulfide-constrained loop from AgRP was grafted into AgTx to enable it to bind integrins, demonstrating that linear disulfide-rich peptides can be engineered as well as the cyclic.

Although there are successful examples of engineering cyclic and linear peptides with novel bioactivities, with many of these peptides displaying enhanced *in vitro* stability, there is limited information on effect of these peptides *in vivo*. Further study is required to explore the *in vivo* bioactivity and bioavailability of grafted cyclic peptides.

1.1.2. Anti-inflammatory proteins from hookworms

Anti-inflammatory proteins from hookworms have significant potential therapeutic applications. The intrinsic activities these proteins display in autoimmune diseases makes them remarkable targets for drug development.

The incidence of autoimmune diseases has risen sharply during the past few decades (47-49). Autoimmune diseases such as inflammatory bowel disease (IBD), Crohn's disease and colitis, have increased in younger populations of developed countries/regions such as Australia, New Zealand, Northern Europe and the USA (50). The hypothesis behind why this is happening began in 1968 with Greenwood who published information about extremely low rates of autoimmune diseases in Nigeria (51). He studied the relationship between the low occurrence of autoimmune diseases, such as rheumatoid arthritis, in tropical areas of Nigeria, and the rates of multiple parasitic infections. In 1989, Strachan published findings regarding first-born children who had more allergic rhinitis and dermatitis compared with their siblings born after them (52). These two findings were the beginning of the "hygiene hypothesis".

The hygiene hypothesis is based on regions with high levels of parasites having low rates of autoimmune diseases (53-55). Intriguingly, countries where the hygiene levels are high and parasitic diseases have essentially been eradicated, autoimmune diseases are increasing at an alarming rate (50). This correlation also includes people who migrate from undeveloped countries to developed nations before adolescence as they also show high rates of some autoimmune diseases (56,57).

The hygiene hypothesis lead to the initial idea that parasites could be protecting undeveloped nations from autoimmune diseases (58,59). Subsequent studies have shown that eradication of parasites such as hookworms, appears to be correlated with the rise in autoimmune conditions in developed countries (60-62).

The excretory/secretory (ES) products in hookworms are an interesting source of compounds with potential in the treatment of both IBD and asthma (63,64). ES products comprise a

complex mixture of proteins, carbohydrates, small molecules and lipids secreted by the parasite (65). More than 250 different proteins have been sequenced from the ES products from the dog hookworm *Ancylostoma caninum* (65,66). Several of these proteins have sequence homology to a family of mammalian proteins known as tissue inhibitors of matrix-metalloproteinases (TIMPs), among these Ac-TIMP-1 and Ac-TIMP-2 were part of the list (67). Ac-TIMP-1 and Ac-TIMP-2 have subsequently been named as *Ac*-AIP-1 and *Ac*-AIP-2, with AIP referring to anti-inflammatory protein. *Ac*-AIP-1 and *Ac*-AIP-2 have been tested in mouse models of colitis (68) and asthma (69) respectively. Recombinant AIP-2 induced the expansion of Tregs that promoted long-term protection against allergic responses in asthma models (70). These proteins improved the symptoms of the disease states in the mice models, but the biological targets of these proteins are not known, and there is no information available on the structure/function relationships.

1.1.3. Inflammatory Bowel Disease

The grafting studies on cyclotides and SFTI-1 highlight the potential of this approach for a range of disease states. Furthermore, the approach of downsizing proteins is also applicable to a wide range of applications, depending on the bioactivity of the protein. In this thesis both of these approaches were applied to the development of lead molecules for inflammatory bowel disease (IBD).

IBDs are a set of complex, chronic and devastating lifelong diseases, for which there is no satisfactory treatment (71). The two major forms of IBD are ulcerative colitis and Crohn's disease (72). Ulcerative colitis involves the rectum and colon, whereas Crohn's disease involves the entire gastro intestinal tract from the mouth to the anus (73). The burden that patients who suffer from these diseases are as follows: bloody diarrhoea, fever, intestinal pain and cramping, vomiting, loss of appetite, loss of weight, ulcerations and fatigue (as reviewed by Health Direct Australian Government (71)). The aetiologies of the diseases are largely unknown, though recent schools of thought believe both types of IBD may be caused by an inappropriate immune response in individuals genetically prone to intestinal microbial species, along with environmental factors. However, the site and nature of inflammation differ between the two diseases (74-76). Even though the estimated cost of these diseases is 2.7 billion dollars annually in Australia, there are still no satisfactory treatments for any form of IBD (71). The current treatments for IBD rely on nonspecific immunosuppressive drugs, such as steroids, antibiotics, and immunomodulators targeting TNF pathway or the gut-homing integrin α4β7 (77-79). However, the repetitive cycles of acute inflammation followed by temporary remission in IBD result over time in severe impairment of gut function, motility and tissue remodelling (80,81). Despite promising clinical trial end points, TNF-α inhibitors are not effective in all

patients and do not prevent relapse (82). A recent review summarises the current biologic and small molecules used in IBD and highlighting the challenges for tailoring treatments for individuals (83). To make matters worse, the incidence of the diseases in Australia has been rising, corresponding with the increasing level of incidence in other first world countries that have genetic and lifestyle similarities (84). Furthermore, for reasons still unclear, the rate of childhood-onset IBD has been the highest observed over the past two decades (85). In addition to the unbearable symptoms associated with the disease, children affected by early-onset IBD suffer significant malabsorption and nutritional deficiencies resulting in growth failure, skeletal impairment, and significant psychological and developmental delays (86). These recent observations emphasize the urgent necessity for novel therapeutic approaches to be developed.

In addition to proteins such as the AIP proteins mentioned in section 1.2, recent studies have shown a range of peptides may have potential in the design of novel drug leads for the treatment of IBD. For example, a tripeptide (MC-12) has been shown to be effective in the treatment of experimental colitis in mice (87). MC-12 is a region of annexin A1, a protein that regulates anti-inflammatory responses (88). MC-12 has anti-inflammatory effects in two experimental models of colitis, dextran sodium sulfate (DSS) and 2,4,6-trinitrobenzene sulfonic acid (TNBS). However, small peptides are likely to be unstable and thus, non-viable drug leads. This prediction is supported by the finding that MC-12 was more effective when injected as opposed to oral administration.

Improving the stability of MC-12 and related peptides through grafting them into a stable cyclic peptides and disulfide-rich peptide scaffold may enhance their therapeutic potential. This approach has successfully been used for the design of a range of bioactive peptides, as

mentioned in section 1.1. It is therefore of valid interest to apply this approach to the development of novel drug leads for inflammatory diseases.

1.1.4. Peptide synthesis and structure characterisation

To be able analyse the potential of peptides as therapeutics they have to be produced in sufficient quantities. Several methods are available for the production of peptides, but solid phase peptide synthesis (SPPS) is one of the most commonly used and robust methods. Two types of chemistry are generally used for peptide synthesis, namely Fmoc (fluorenylmethyloxycarbonyl) and Boc (tert-butyloxycarbonyl) chemistry. Fmoc chemistry is more straightforward to establish in a laboratory than Boc chemistry because it does not require the use of hydrogen fluoride (HF) which can be very hazardous and requires specialist manifolds (89). Fmoc chemistry can provide good yields without the use of HF and has been previously shown to be appropriate for the synthesis of SFTI-1 (90) - one of the peptides of interest in this study.

Both cyclic and linear peptides can be produced using SPPS, with native chemical ligation useful for the synthesis of cyclic peptides (89,90). Some of the early studies that used native chemical ligation allowed the production of cyclotides (9). Native chemical ligation requires a C-terminal thioester and an N-terminal cysteine residue which react to ultimately form a native peptide bond and in the case of the cyclotides, formed the cyclic backbone. Cyclic peptides such as the cyclotides and SFTI are well suited to this method given the high proportion of cysteine residues in the peptides.

Structural analysis of peptides at high resolution is primarily carried out using X-ray crystallography or NMR spectroscopy. Small peptides (less than 50 residues) are highly suited with the latter technique because they are often highly soluble and have limited overlap in the NMR spectra making it relatively straightforward to determine if the peptide is structured or not. The analysis can be done in solution, and therefore minimal sample manipulation, such as crystallisation, is required. Recent reviews on structure determination protocols are given in Comprehensive natural products II: Chemistry and biology(91) for general peptides, and Mobli and King have summarised methods for the analysis of disulfide rich peptides(92).

1.1.5. Scope of thesis

SFTI-1 is a particularly attractive scaffold for grafting tripeptides with anti-inflammatory activity, due to its small size and presence of only a single disulfide bond. These features can enhance yields and simplify the oxidative folding process. **Chapter 2** reports the engineering of SFTI-1 to improve the stability of the tri-peptide MC-12. The broad objective of this chapter was to develop a novel anti-inflammatory agent based on a naturally occurring cyclic peptide scaffold. The specific aims were to design and synthesize a grafted cyclic peptide incorporating a small bioactive sequence with anti-inflammatory activity, structurally characterise the grafted peptides and analyse the bioactivity and stability of the grafted peptide. The hypothesis underlying this study was that cyclic peptide scaffolds are valuable drug leads based on their intrinsic stability and ability to adopt novel bioactivities as proven in previous studies.

The anti-inflammatory activity was assessed in a TNBS mouse model of colitis (93,94) This model has previously been shown to be effective screen for determining compounds with potential in IBD treatment and requires minimal amounts of peptide for testing (95).

This study has been published in the Journal of Biological Chemistry doi: 10.1074/jbc.M117.779215 (96) .

Chapter 3 describes studies that utilize another disulfide-rich peptide as a grafting scaffold for the design of drug leads for IBD. Similar to Chapter 2, the objective of this study was to develop novel anti-inflammatory agents based on a disulfide-rich peptide scaffold.

The scaffold used was linaclotide, a linear peptide that contains three disulfide bonds and only 14-residues. Linaclotide is a heat-stable enterotoxin receptor agonist, which is currently used for the treatment of irritable bowel syndrome with constipation and chronic idiopathic constipation (97,98). This highly disulfide-rich peptide has oral activity making it a very attractive framework for grafting studies. This chapter is unpublished data, written in a paper format ready to be submitted.

Chapter 4 and Chapter 5 correspond to the study of downsizing hookworm proteins into bioactive peptides, termed AIP peptides. The broad objective for these chapters was to downsize AIP proteins into peptides with anti-inflammatory activity and potential as lead molecules for clinical development in IBD. The downsizing approach is primarily based on synthesising discrete elements of secondary structure within the larger protein and determining if the peptide in isolation has bioactivity. This requires determination of the three-dimensional structure, generally using X-ray crystallography or molecular modelling. The specific aim was

to design and characterise AIP peptides, and analyse their activity as anti-inflammatory agents. The studies were made following the hypothesis that developing AIP peptides as therapeutics holds significant promise, as they are likely to be more stable than the full-length proteins, have greater tissue penetration, be less immunogenic and cheaper to manufacture. In this chapter the structures of these peptides were analysed using NMR spectroscopy, serum stability determined, and *in vitro* an *in vivo* activity assessed.

These chapters contain unpublished data, that will be submitted for publication following IP protection.

1.2. References

1. Adessi, C., and Soto, C. (2002) Converting a peptide into a drug: strategies to improve stability and bioavailability. *Curr. Med. Chem.* **9**, 963-978

2. Tringali, C. (2012) *Bioactive compounds from natural sources: natural products as lead compounds in drug discovery*, Second Edition ed., CRC Press, Florida, US

3. Silverstein, K. A. T., Moskal, W. A., Wu, H. C., Underwood, B. A., Graham, M. A., Town, C. D., and VandenBosch, K. A. (2007) Small cysteine-rich peptides resembling antimicrobial peptides have been under-predicted in plants. *Plant J.* **51**, 262-280

4. Lewis, R. J., and Garcia, M. L. (2003) Therapeutic potential of venom peptides. *Nat. Rev. Drug Discov.* **2**, 790-802

5. Hamilton, G. R., and Baskett, T. F. (2000) In the arms of Morpheus: the development of morphine for postoperative pain relief. *Can. J. Anaesth.* **47**, 367-374

6. Yang, Y. L., Hua, K. F., Chuang, P. H., Wu, S. H., Wu, K. Y., Chang, F. R., and Wu, Y. C. (2008) New cyclic peptides from the seeds of Annona squamosa L. and their anti-inflammatory activities. *J. Agric. Food Chem.* **56**, 386-392

7. Svangard, E., Goransson, U., Hocaoglu, Z., Gullbo, J., Larsson, R., Claeson, P., and Bohlin, L. (2004) Cytotoxic cyclotides from Viola tricolor. *J. Nat. Prod.* **67**, 144-147

8. Gustafson, K. R., McKee, T. C., and Bokesch, H. R. (2004) Anti-HIV cyclotides. *Curr. Protein Peptide Sci.* **5**, 331-340

9. Tam, J. P., Lu, Y. A., Yang, J. L., and Chiu, K. W. (1999) An unusual structural motif of antimicrobial peptides containing end-to-end macrocycle and cystine-knot disulfides. *Proc. Natl. Acad. Sci. U. S. A.* **96**, 8913-8918

10. Pinto, M. F. S., Fensterseifer, I. C. M., Migliolo, L., Sousa, D. A., de Capdville, G., Arboleda-Valencia, J. W., Colgrave, M. L., Craik, D. J., Magalhaes, B. S., Dias, S. C., and Franco, O. L. (2012) Identification and structural characterization of novel cyclotide with activity against an insect pest of sugar cane. *J. Biol. Chem.* **287**, 134-147

11. Pollaro, L., and Heinis, C. (2010) Strategies to prolong the plasma residence time of peptide drugs. *MedChemComm* **1**, 319-324

12. Zorzi, A., Middendorp, S. J., Wilbs, J., Deyle, K., and Heinis, C. (2017) Acylated heptapeptide binds albumin with high affinity and application as tag furnishes long-acting peptides. *Nat. Commun.* **8**, 16092

13. Werle, M., and Bernkop-Schnürch, A. (2006) Strategies to improve plasma half life time of peptide and protein drugs. *Amino Acids* **30**, 351-367

14. Clark, R. J., Akcan, M., Kaas, Q., Daly, N. L., and Craik, D. J. (2012) Cyclization of conotoxins to improve their biopharmaceutical properties. *Toxicon* **59**, 446-455

15. Gould, A., Ji, Y. B., Aboye, T. L., and Camarero, J. A. (2011) Cyclotides, a Novel Ultrastable Polypeptide Scaffold for Drug Discovery. *Curr. Pharm. Des.* **17**, 4294-4307

16. Gunasekera, S., Foley, F. M., Clark, R. J., Sando, L., Fabri, L. J., Craik, D. J., and Daly, N. L. (2008) Engineering stabilized vascular endothelial growth factor-A antagonists: synthesis, structural characterization, and bioactivity of grafted analogues of cyclotides. *J. Med. Chem.* **51**, 7697-7704

17. Colgrave, M. L., and Craik, D. J. (2004) Thermal, chemical, and enzymatic stability of the cyclotide kalata B1: The importance of the cyclic cystine knot. *Biochemistry* **43**, 5965-5975

18. Cemazar, M., Kwon, S., Mahatmanto, T., Ravipati, A. S., and Craik, D. J. (2012) Discovery and Applications of Disulfide-Rich Cyclic Peptides. *Curr. Top. Med. Chem.* **12**, 1534-1545

19. Miljanich, G. P. (2004) Ziconotide: neuronal calcium channel blocker for treating severe chronic pain. *Curr. Med. Chem.* **11**, 3029-3040

20. Basus, V. J., Nadasdi, L., Ramachandran, J., and Miljanich, G. P. (1995) Solution structure of omega-conotoxin MVIIA using 2D NMR spectroscopy. *FEBS Lett.* **370**, 163-169

21. Ito, C., Ribeiro, R. C., Behm, F. G., Raimondi, S. C., Pui, C. H., and Campana, D. (1996) Cyclosporine a induces apoptosis in childhood acute lymphoblastic leukemia cells. *Blood* **88**, 261-261

22. Reid, R. C., Yau, M. K., Singh, R., Hamidon, J. K., Reed, A. N., Chu, P. F., Suen, J. Y., Stoermer, M. J., Blakeney, J. S., Lim, J., Faber, J. M., and Fairlie, D. P. (2013) Downsizing a human inflammatory protein to a small molecule with equal potency and functionality. *Nat. Commun.* **4**

23. Smout, M. J., Mulvenna, J. P., Jones, M. K., and Loukas, A. (2011) Expression, refolding and purification of Ov-GRN-1, a granulin-like growth factor from the carcinogenic liver fluke, that causes proliferation of mammalian host cells. *Protein Expr. Purif.* **79**, 263-270

24. Bansal, P. S., Smout, M. J., Wilson, D., Caceres, C. C., Dastpeyman, M., Sotillo, J., Seifert, J., Brindley, P. J., Loukas, A., and Daly, N. L. (2017) Development of a Potent Wound Healing Agent Based on the Liver Fluke Granulin Structural Fold. *J. Med. Chem.* **60**, 4258-4266

25. Craik, D. J., Daly, N. L., Bond, T., and Waine, C. (1999) Plant cyclotides: A unique family of cyclic and knotted proteins that defines the cyclic cystine knot structural motif. *J. Mol. Biol.* **294**, 1327-1336

26. Craik, D. J., Daly, N. L., Mulvenna, J., Plan, M. R., and Trabi, M. (2004) Discovery, structure and biological activities of the cyclotides. *Curr. Protein Peptide Sci.* **5**, 297-315

27. Gran, L. (1973) Effect Of A Polypeptide Isolated From Kalata-Kalata (Oldenlandia-Affinis Dc) On Estrogen Dominated Uterus. *Acta Pharmacol. Toxicol. (Copenh.)* **33**, 400-408

28. Gran, L., Sandberg, F., and Sletten, K. (2000) Oldenlandia affinis (R&S) DC - A plant containing uteroactive peptides used in African traditional medicine. *J. Ethnopharmacol.* **70**, 197-203

29. Saether, O., Craik, D. J., Campbell, I. D., Sletten, K., Juul, J., and Norman, D. G. (1995) Elucidation of the primary and 3-dimensional structure of the uterotonic polypeptide kalata b1. *Biochemistry* **34**, 4147-4158

30. Gustafson, K. R., Walton, L. K., Sowder, R. C., Johnson, D. G., Pannell, L. K., Cardellina, J. H., and Boyd, M. R. (2000) New circulin macrocyclic polypeptides from Chassalia parvifolia. *J. Nat. Prod.* **63**, 176-178

31. Hernandez, J. F., Gagnon, J., Chiche, L., Nguyen, T. M., Andrieu, J. P., Heitz, A., Hong, T. T., Pham, T. T. C., and Nguyen, D. L. (2000) Squash trypsin inhibitors from Momordica cochinchinensis exhibit an atypical macrocyclic structure. *Biochemistry* **39**, 5722-5730

32. Jennings, C., West, J., Waine, C., Craik, D., and Anderson, M. (2001) Biosynthesis and insecticidal properties of plant cyclotides: The cyclic knotted proteins from Oldenlandia affinis. *Proc. Natl. Acad. Sci. U. S. A.* **98**, 10614-10619

33. Luckett, S., Garcia, R. S., Barker, J. J., Konarev, A. V., Shewry, P. R., Clarke, A. R., and Brady, R. L. (1999) High-resolution structure of a potent, cyclic proteinase inhibitor from sunflower seeds. *J. Mol. Biol.* **290**, 525-533

34. Mylne, J. S., Colgrave, M. L., Daly, N. L., Chanson, A. H., Elliott, A. G., McCallum, E. J., Jones, A., and Craik, D. J. (2011) Albumins and their processing machinery are hijacked for cyclic peptides in sunflower. *Nat. Chem. Biol.* **7**, 257-259

35. Franke, B., Mylne, J. S., and Rosengren, K. J. (2018) Buried treasure: biosynthesis, structures and applications of cyclic peptides hidden in seed storage albumins. *Nat. Prod. Rep.* **35**, 137-146

36. Birk, Y., Gertler, A., and Khalef, S. (1967) Further Evidence For A Dual Independent Activity Against Trypsin And Alpha-Chymotrypsin Of Inhibitor Aa From Soybenas. *Biochim. Biophys. Acta* **147**, 402-404

37. Chen, P., Rose, J., Love, R., Wei, C. H., and Wang, B. C. (1992) Reactive Sites Of An Anticarcinogenic Bowman-Birk Proteinase-Inhibitor Are Similar To Other Trypsin-Inhibitors. *J. Biol. Chem.* **267**, 1990-1994

38. Schechter, I., and Berger, A. (2012) On The Size Of The Active Site In Proteases. I. Papain (Reprinted From Biochemical And Biophysical Research Communications, Vol 27, Pg 157, 1967). *Biochem. Biophys. Res. Commun.* **425**, 497-502

39. Laskowski, M., and Kato, I. (1980) Protein Inhibitors Of Proteinases. *Annu. Rev. Biochem.* **49**, 593-626

40. Swedberg, J. E., Nigon, L. V., Reid, J. C., de Veer, S. J., Walpole, C. M., Stephens, C. R., Walsh, T. P., Takayama, T. K., Hooper, J. D., Clements, J. A., Buckle, A. M., and Harris, J. M. (2009) Substrate-guided design of a potent and selective kallikrein-related peptidase inhibitor for kallikrein 4. *Chem. Biol.* **16**, 633-643

41. Chan, L. Y., Gunasekera, S., Henriques, S. T., Worth, N. F., Le, S. J., Clark, R. J., Campbell, J. H., Craik, D. J., and Daly, N. L. (2011) Engineering pro-angiogenic peptides using stable, disulfide-rich cyclic scaffolds. *Blood* **118**, 6709-6717

42. Wang, C. K., Gruber, C. W., Cemazar, M., Siatskas, C., Tagore, P., Payne, N., Sun, G. Z., Wang, S. H., Bernard, C. C., and Craik, D. J. (2014) Molecular grafting onto a stable framework yields novel cyclic peptides for the treatment of multiple sclerosis. *ACS Chem. Biol.* **9**, 156-163

43. Wong, C. T. T., Rowlands, D. K., Wong, C. H., Lo, T. W. C., Nguyen, G. K. T., Li, H. Y., and Tam, J. P. (2012) Orally Active Peptidic Bradykinin B-1 Receptor Antagonists Engineered from a Cyclotide Scaffold for Inflammatory Pain Treatment. *Angew. Chem. Int. Ed. Engl.* **51**, 5620-5624

44. Adams, M. E., Mintz, I. M., Reily, M. D., Thanabal, V., and Bean, B. P. (1993) Structure And Properties Of Omega-Agatoxin-Ivb, A New Antagonist Of P-Type Calcium Channels. *Mol. Pharmacol.* **44**, 681-688

45. Moore, S. J., Leung, C. L., Norton, H. K., and Cochran, J. R. (2013) Engineering Agatoxin, a Cystine-Knot Peptide from Spider Venom, as a Molecular Probe for In Vivo Tumor Imaging. *PLoS One* **8**, e60498

46. Silverman, A. P., Levin, A. M., Lahti, J. L., and Cochran, J. R. (2009) Engineered Cystine-Knot Peptides that Bind alpha(v)beta(3) Integrin with Antibody-Like Affinities. *J. Mol. Biol.* **385**, 1064-1075

47. Gibson, P. R. (2009) Overview of inflammatory bowel disease in Australia in the last 50 years. *J. Gastroenterol. Hepatol.* **24**, S63-S68

48. Lionetti, E., Gatti, S., Pulvirenti, A., and Catassi, C. (2015) Celiac disease from a global perspective. *Best Pract. Res. Clin. Gastroenterol.* **29**, 365-379

49. Benchimol, E. I., Fortinsky, K. J., Gozdyra, P., Van den Heuvel, M., Van Limbergen, J., and Griffiths, A. M. (2011) Epidemiology of Pediatric Inflammatory Bowel Disease: A Systematic Review of International Trends. *Inflamm. Bowel Dis.* **17**, 423-439

50. M'koma, A. E. (2013) Inflammatory Bowel Disease: An Expanding Global Health Problem. *Clin. Med. Insights Gastroenterol.* **6**, 33-47

51. Greenwoo.Bm. (1968) Autoimmune disease and parasitic infections in nigerians. *Lancet* **2**, 380-382

52. Strachan, D. P. (1989) Hay-fever, hygiene, and household size. *Br. Med. J.* **299**, 1259-1260

53. Okada, H., Kuhn, C., Feillet, H., and Bach, J. F. (2010) The 'hygiene hypothesis' for autoimmune and allergic diseases: an update. *Clin. Exp. Immunol.* **160**, 1-9

54. Caraballo, L. (2018) The tropics, helminth infections and hygiene hypotheses. *Expert Rev. Clin. Immunol.* **14**, 99-102

55. Yazdanbakhsh, M., Kremsner, P. G., and van Ree, R. (2002) Immunology - Allergy, parasites, and the hygiene hypothesis. *Science* **296**, 490-494

56. Hammond, S. R., English, D. R., and McLeod, J. G. (2000) The age-range of risk of developing multiple sclerosis - Evidence from a migrant population in Australia. *Brain* **123**, 968-974

57. Bodansky, H. J., Staines, A., Stephenson, C., Haigh, D., and Cartwright, R. (1992) Evidence for an environmental-effect in the etiology of insulin-dependent diabetes in a transmigratory population. *Br. Med. J.* **304**, 1020-1022

58. Bach, J.-F. (2017) The hygiene hypothesis in autoimmunity: the role of pathogens and commensals. *Nat. Rev. Immunol.* **18**, 105

59. Weinstock, J. V., and Elliott, D. E. (2009) Helminths and the IBD Hygiene Hypothesis. *Inflamm. Bowel Dis.* **15**, 128-133

60. Molodecky, N. A., Soon, I. S., Rabi, D. M., Ghali, W. A., Ferris, M., Chernoff, G., Benchimol, E. I., Panaccione, R., Ghosh, S., Barkema, H. W., and Kaplan, G. G. (2012) Increasing Incidence and Prevalence of the Inflammatory Bowel Diseases With Time, Based on Systematic Review. *Gastroenterology* **142**, 46-54

61. Prescott, S., and Allen, K. J. (2011) Food allergy: Riding the second wave of the allergy epidemic. *Pediatr. Allergy Immunol.* **22**, 155-160

62. Weinstock, J. V., Summers, R. W., Elliott, D. E., Qadir, K., Urban, J. F., and Thompson, R. (2002) The possible link between de-worming and the emergence of immunological disease. *J. Lab. Clin. Med.* **139**, 334-338

63. Navarro, S., Pickering, D. A., Ferreira, I. B., Jones, L., Ryan, S., Troy, S., Leech, A., Hotez, P. J., Zhan, B., Laha, T., Prentice, R., Sparwasser, T., Croese, J., Engwerda, C. R., Upham, J. W., Julia, V., Giacomin, P. R., and Loukas, A. (2016) Hookworm recombinant protein promotes regulatory T cell responses that suppress experimental asthma. *Sci. Transl. Med* **8,** 362ra143

64. Ferreira, I., Smyth, D., Gaze, S., Aziz, A., Giacomin, P., Ruyssers, N., Artis, D., Laha, T., Navarro, S., Loukas, A., and McSorley, H. J. (2013) Hookworm excretory/secretory products induce interleukin-4 (IL-4)(+) IL-10(+) CD4(+) T cell responses and suppress pathology in a mouse model of colitis. *Infect. Immun.* **81**, 2104-2111

65. Mulvenna, J., Hamilton, B., Nagaraj, S. H., Smyth, D., Loukas, A., and Gorman, J. J. (2009) Proteomics Analysis of the Excretory/Secretory Component of the Blood-feeding Stage of the Hookworm, Ancylostoma caninum. *Mol. Cell. Proteomics* **8**, 109-121

66. Morante, T., Shepherd, C., Constantinoiu, C., Loukas, A., and Sotillo, J. (2017) Revisiting the Ancylostoma Caninum Secretome Provides New Information on Hookworm-Host Interactions. *Proteomics* **17**

67. Cantacessi, C., Hofmann, A., Pickering, D., Navarro, S., Mitreva, M., and Loukas, A. (2013) TIMPs of parasitic helminths - a large-scale analysis of high-throughput sequence datasets. *Parasit. Vectors* **6**

68. Ferreira, I. B., Pickering, D. A., Troy, S., Croese, J., Loukas, A., and Navarro, S. (2017) Suppression of inflammation and tissue damage by a hookworm recombinant protein in experimental colitis. *Clin. Transl. Immunology* **6**, e157

69. Navarro, S., Pickering, D. A., Ferreira, I. B., Jones, L., Ryan, S., Troy, S., Leech, A., Hotez, P. J., Zhan, B., Laha, T., Prentice, R., Sparwasser, T., Croese, J., Engwerda, C. R., Upham, J. W., Julia, V., Giacomin, P. R., and Loukas, A. (2016) Hookworm recombinant protein promotes regulatory T cell responses that suppress experimental asthma. *Sci. Transl. Med.* **8**, 14

70. Navarro, S., Pickering, D. A., Ferreira, I. B., Jones, L., Ryan, S., Troy, S., Leech, A., Hotez, P. J., Zhan, B., Laha, T., Prentice, R., Sparwasser, T., Croese, J., Engwerda, C. R., Upham, J. W., Julia, V., Giacomin, P. R., and Loukas, A. (2016) Hookworm recombinant protein promotes regulatory T cell responses that suppress experimental asthma. *Sci Transl Med* **8**, 362ra143

71. Health Direct Australian Government. (2013) Crohn's disease and ulcerative colitis.

72. Ament, M. E. (1975) Inflammatory disease of the colon: ulcerative colitis and Crohn's colitis. *J. Pediatr.* **86**, 322-334

73. Lennardjones, J. E. (1989) Classification Of Inflammatory Bowel-Disease. *Scand. J. Gastroenterol.* **24**, 2-6

74. Saleh, M., and Trinchieri, G. (2011) Innate immune mechanisms of colitis and colitis-associated colorectal cancer. *Nat Rev Immunol* **11**, 9-20

75. Van Limbergen, J., Radford-Smith, G., and Satsangi, J. (2014) Advances in IBD genetics. *Nat Rev Gastroenterol Hepatol* **11**, 372-385

76. Xu, X. R., Liu, C. Q., Feng, B. S., and Liu, Z. J. (2014) Dysregulation of mucosal immune response in pathogenesis of inflammatory bowel disease. *World J. Gastroenterol.* **20**, 3255-3264

77. Coskun, M., Vermeire, S., and Nielsen, O. H. (2017) Novel Targeted Therapies for Inflammatory Bowel Disease. *Trends Pharmacol Sci* **38**, 127-142

78. Furfaro, F., Bezzio, C., Ardizzone, S., Massari, A., de Franchis, R., and Maconi, G. (2015) Overview of biological therapy in ulcerative colitis: current and future directions. *J Gastrointestin Liver Dis* **24**, 203-213

79. McLean, M. H., Neurath, M. F., and Durum, S. K. (2014) Targeting interleukins for the treatment of inflammatory bowel disease-what lies beyond anti-TNF therapy? *Inflamm Bowel Dis* **20**, 389-397

80. Peyrin-Biroulet, L., Loftus, E. V., Jr., Colombel, J. F., and Sandborn, W. J. (2011) Long-term complications, extraintestinal manifestations, and mortality in adult Crohn's disease in population-based cohorts. *Inflamm Bowel Dis* **17**, 471-478

81. Ruffolo, C., Scarpa, M., Faggian, D., Basso, D., D'Inca, R., Plebani, M., Sturniolo, G. C., Bassi, N., and Angriman, I. (2010) Subclinical intestinal inflammation in patients with Crohn's disease following bowel resection: a smoldering fire. *J Gastrointest Surg* **14**, 24-31

82. Danese, S., Colombel, J. F., Peyrin-Biroulet, L., Rutgeerts, P., and Reinisch, W. (2013) Review article: the role of anti-TNF in the management of ulcerative colitis -- past, present and future. *Aliment Pharmacol Ther* **37**, 855-866

83. Reinglas, J., Gonczi, L., Kurt, Z., Bessissow, T., and Lakatos, P. L. (2018) Positioning of old and new biologicals and small molecules in the treatment of inflammatory bowel diseases. *World J. Gastroenterol.* **24**, 3567-3582

84. Wilson, J., Hair, C., Knight, R., Catto-Smith, A., Bell, S., Kamm, M., Desmond, P., McNeil, J., and Connell, W. (2010) High Incidence of Inflammatory Bowel Disease in Australia: A Prospective Population-Based Australian Incidence Study. *Inflamm. Bowel Dis.* **16**, 1550-1556

85. Malmborg, P., and Hildebrand, H. (2016) The emerging global epidemic of paediatric inflammatory bowel disease--causes and consequences. *J Intern Med* **279**, 241-258

86. Conrad, M. A., and Rosh, J. R. (2017) Pediatric Inflammatory Bowel Disease. *Pediatr Clin North Am* **64**, 577-591

87. Ouyang, N., Zhu, C., Zhou, D., Nie, T., Go, M. F., Richards, R. J., and Rigas, B. (2012) MC-12, an annexin A1-based peptide, is effective in the treatment of experimental colitis. *PLoS One* **7**, e41585

88. Zhang, Z. Q., Huang, L. Q., Zhao, W. P., and Rigas, B. (2010) Annexin 1 induced by anti-inflammatory drugs binds to NF-kappa B and inhibits its activation: anticancer effects in vitro and in vivo. *Cancer Res.* **70**, 2379-2388

89. Camarero, J. A., and Mitchell, A. R. (2005) Synthesis of proteins by native chemical ligation using Fmoc-based chemistry. *Protein Peptide Lett.* **12**, 723-728

90. Gunasekera, S., Aboye, T. L., Madian, W. A., El-Seedi, H. R., and Goransson, U. (2013) Making ends meet: Microwave-accelerated synthesis of cyclic and disulfide rich proteins via in situ thioesterification and native chemical ligation. *Int. J. Pept. Res. Ther.* **19**, 43-54

91. King, G. F., and Mobli, M. (2010) 9.09 - Derivation of Peptide and Protein Structure using NMR Spectroscopy. in *Comprehensive Natural Products II* (Liu, H.-W., and Mander, L. eds.), Elsevier, Oxford. pp 279-325

92. Mobli, M., and King, G. F. (2010) NMR methods for determining disulfide-bond connectivities. *Toxicon* **56**, 849-854

93. Wirtz, S., Neufert, C., Weigmann, B., and Neurath, M. F. (2007) Chemically induced mouse models of intestinal inflammation. *Nat. Protoc.* **2**, 541-546

94. Chassaing, B., Aitken, J. D., Malleshappa, M., and Vijay-Kumar, M. (2014) Dextran sulfate sodium (DSS)-induced colitis in mice. *Curr. Protoc. Immunol.* **104,** Unit 15.25.

95. Ruyssers, N. E., De Winter, B. Y., De Man, J. G., Loukas, A., Pearson, M. S., Weinstock, J. V., Van den Bossche, R. M., Martinet, W., Pelckmans, P. A., and Moreels, T. G. (2009) Therapeutic Potential of Helminth Soluble Proteins in TNBS-induced Colitis in Mice. *Inflamm. Bowel Dis.* **15**, 491-500

96. Cobos Caceres, C., Bansal, P. S., Navarro, S., Wilson, D., Don, L., Giacomin, P., Loukas, A., and Daly, N. L. (2017) An engineered cyclic peptide alleviates symptoms of inflammation in a murine model of inflammatory bowel disease. *J. Biol. Chem.* **292**, 10288-10294

97. Roque, M. V., and Camilleri, M. (2011) Linaclotide, a synthetic guanylate cyclase C agonist, for the treatment of functional gastrointestinal disorders associated with constipation. *Expert Rev. Gastroenterol. Hepatol.* **5**, 301-310

98. Wensel, T. M., and Luthin, D. R. (2011) Linaclotide: A Novel Approach to the Treatment of Irritable Bowel Syndrome. *Ann. Pharmacother.* **45**, 1535-1543

2. CHAPTER 2

An Engineered Cyclic Peptide Alleviates Symptoms of Inflammation in a Murine Model of Inflammatory Bowel Disease

Claudia Cobos Caceres, Paramjit S. Bansal, Severine Navarro, David Wilson, Laurianne Don, Paul Giacomin, Alex Loukas, and Norelle L. Daly

2.1. Abstract

Inflammatory bowel diseases (IBDs) are a set of complex and debilitating diseases, for which there is no satisfactory treatment. Recent studies have shown that small peptides show promise for reducing inflammation in models of IBD. However, these small peptides are likely to be unstable and rapidly cleared from the circulation, and therefore, if not modified for better stability, represent non-viable drug leads. We hypothesized that improving the stability of these peptides by grafting them into a stable cyclic peptide scaffold may enhance their therapeutic potential. Using this approach, we have designed a novel cyclic peptide, which comprises a small bioactive peptide from the annexin A1 protein grafted into a sunflower trypsin inhibitor cyclic scaffold. We used native chemical ligation to synthesize the grafted cyclic peptide. This engineered cyclic peptide maintained the overall fold of the naturally occurring cyclic peptide, was more effective at reducing inflammation in a mouse model of acute colitis than the bioactive peptide alone, and showed enhanced stability in human serum. Our findings suggest that the use of cyclic peptides as structural backbones offers a promising approach for the treatment of IBD and potentially other chronic inflammatory conditions.

2.2. Introduction

Inflammatory bowel diseases (IBD) are a set of chronic inflammatory disorders of the gastrointestinal tract and the two major forms are ulcerative colitis and Crohn's disease (1). Although there are several medications on the market for IBD, they generally only provide temporary relief and 70% of IBD patients require surgical intervention (2). Because the current treatments are not satisfactory, new drug leads are being sought from a range of sources, including small molecules from plants and bioactive regions of larger proteins (3-6).

Intriguingly, several small peptides, some comprising only three residues, have been shown to be effective in the treatment of experimental colitis in mice (7-11). One example is a tripeptide (MC-12) derived from annexin A1, a calcium-dependent phospholipid binding, anti-inflammatory protein (12). Annexin A1 mediates expression of cytokines such as TNG-α, IL-6 and IL-10. It is required for the inhibition of NF-kB activity by anti-inflammatory drugs (13), and has recently been shown to be a potential biomarker of therapeutic efficacy for IBD (14). The N-terminal region of annexin A1 comprising residues 2-26 (Ac2-26) has been well studied (15,16) and appears to have the same biological effects as the full-length protein (17). Analysis of a series of peptides based on the N-terminal sequence of annexin A1 showed that MC-12 (Ac-Gln-Ala-Trp) was the most potent inhibitor of NF-kB activity in SW480 cells (13).

Small peptides such as MC-12 are likely to be unstable and not viable drug leads, supported by the finding that high doses (25 mg/kg) of MC-12 were required to elicit an *in vivo* response in mouse colitis models, and it was more effective when injected compared to oral administration (18). Improving the stability of MC-12 and related peptides may enhance their therapeutic potential.

A range of approaches have been used to improve the stability of peptides, including backbone cyclization, and grafting into cyclic peptide scaffolds. Both approaches are based on the inherent stability observed for naturally occurring cyclic peptides such as cyclosporine, an 11 residue cyclic peptide, used clinically as an immunosuppressant agent. Sunflower trypsin inhibitor 1 (SFTI-1) is an example of a cyclic peptide that has proven useful in grafting studies. SFTI-1 was originally isolated from the seeds of sunflowers (*Helianthus annuus)*, contains 14 residues and is one of the most potent trypsin inhibitors known (19). The structure comprises two short antiparallel β-strands that are linked by a single disulfide bond. The two loops formed by the cyclic backbone and disulfide bond are termed the "binding" loop, which contains the active-site lysine residue for binding to trypsin, and the "cyclization" loop, which contains the residues involved in the backbone cyclization. In addition to the cyclic backbone and disulfide bond, SFTI-1 contains a network of hydrogen bonds, all of which make the peptide highly stable (19). Amino acid substitutions are structurally well tolerated, and the protease inhibitory activity can be removed by mutation of the active-site lysine residue from the binding loop (20). The stability and tolerance to sequence changes makes SFTI-1 a promising peptide drug scaffold (19,21,22). Engineered forms of SFTI-1 have been developed as inhibitors of the serine proteases KLK4, KLK5 and KLK7, which are possible targets for cancer treatment (21,23), as well as in the development of angiogenic agents (22), anti-angiogenic agents (24) and matriptase inhibitors (25).

Here we show that grafting the tripeptide MC-12 into the SFTI-1 scaffold improves its therapeutic efficacy in a murine model of chemically-induced acute colitis, while also improving its *in vitro* stability. A schematic representation of the grafting approach is shown in **Figure 2.1**, highlighting the helical structure of MC-12 in annexin A1. A range of peptides

were synthesised to explore the importance of the cyclic backbone and the loop into which the sequence was grafted.

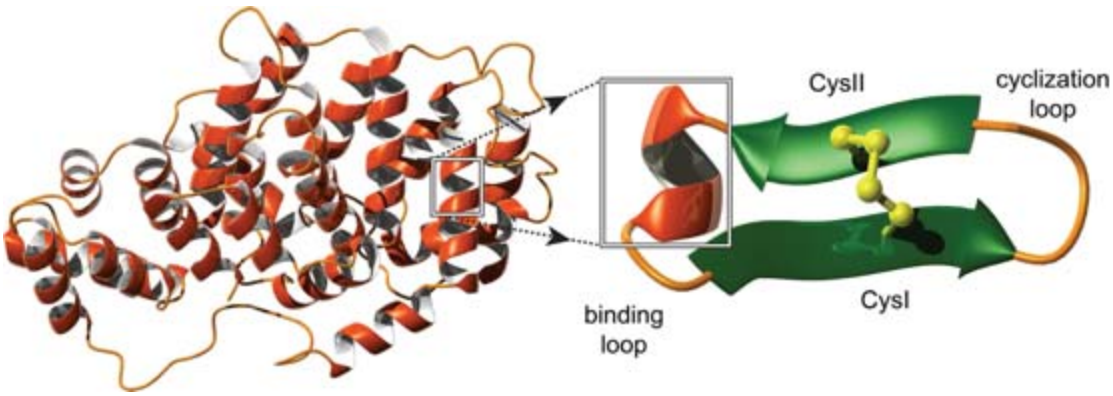

FIGURE 2.1. Schematic representation of grafting into the SFTI-1 scaffold. The three-dimensional structure of annexin A1 is shown on the left of the diagram (PDB ID code 1HM6). MC-12, highlighted on the structure of annexin A1, forms a helical structure in the full-length protein. The helical region of MC-12 is schematically represented as grafted into the binding loop of SFTI-1. SFTI-1 comprises two β-strands connected by a disulfide bond. The cyclization loop is also labelled on the diagram. The figure was generated using MOLMOL (37).

2.3. Experimental Procedures

2.3.1. Peptide synthesis and purification

The peptides were synthesized using fluorenylmethyloxycarbonyl (Fmoc) chemistry based solid phase peptide synthesis chemistry on a 0.1 mmole scale. Linear peptides were synthesised on 2-chlorotrityl chloride resin. Amino acids (2 equiv.) were activated in 5 equiv HBTU and 10 equiv. DIPEA in DMF (1.5 mL). Deprotection was carry out in two repetitions: Starting with 2 min of 20% pipiridine in DMF (5 ml), followed by 3 mins of the same solution. The first amino acid was coupled manually to the resin (Arg was double coupled), and the remainder of the peptide assembled using a Protein Technologies PS3 synthesiser following FMOC approach. Peptides were cleaved from the resin using trifluoroacetic acid (TFA)/water/ triisopropylsilane (95:2.5:2.5) for 2-3 h, precipitated with diethylether, dissolved in 50% acetonitrile/0.05% TFA and subsequently lyophilised. The resulting crude peptides were purified with RP-HPLC on a C-18 preparative column (Phenomenex Jupiter 250 x 21.2 mm) using a 1% gradient of solvent B (solvent A: 0.05% TFA; solvent B: 90% acetonitrile, 0.05% TFA). Peptides were oxidised in 0.1M ammonium bicarbonate pH 8-8.5, purified using RP-HPLC and the mass analysed using MALDI mass spectrometry.

The cyclic peptide was synthesised using native chemical ligation (32) on Dawson Dbz AM resin (100-200 mesh). The Dawson resin was deprotected with 20% piperidine in dimethylformamide (DMF) (2 x 5 min washes) and then washed with DMF prior to addition of the first residue. Prior to cleavage of the cyclic peptide, acylation of Dbz linker was achieved by adding 4-nitrophenylchloroformate in dichloromethane (16 equiv, room temperature) to the dry resin under N_2 for 1 h. The resin was then washed with DMF. *N*,*N*-Diisopropylethylamine

(195 equiv.) in DMF was added for 1 h at room temperature for activation. After activation, the Nbz-peptide was washed with DMF and dried. Cyclization was carried out in 200 mM 4-mercaptophenylacetic acid and 20 mM *tris*(2-carboxyethyl) phosphine in 200 mM phosphate buffer at room temperature for 48 hours. The cyclic peptide was purified using RP-HPLC on a C-18 semi preparative column (250 x 10 mm Phenomenex Jupiter C18 column) and mass was analysed on a 5800 MALDI TOF-TOF (SCIEX) mass spectrometer. The cyclic peptide was subsequently oxidised using 0.1 M NH_4HCO_4. The sample was then purified with RP-HLPC and finally analysed with NMR.

2.3.2. NMR spectroscopy

Lyophilized peptides were resuspended to a final concentration of ~0.2 mM in 90%H_2O:10%D_2O. 2D ^{1}H-^{1}H TOCSY, ^{1}H-^{1}H NOESY, ^{1}H-^{1}H DQF-COSY, ^{1}H-^{15}N HSQC, and ^{1}H-^{13}C HSQC spectra were acquired at 290 K using a 600 MHz AVANCE III NMR spectrometer (Bruker, Karlsruhe, Germany) equipped with a cryogenically cooled probe. All spectra were recorded with an interscan delay of 1 s. NOESY spectra were acquired with mixing times of 200-300 ms, and TOCSY spectra were acquired with isotropic mixing periods of 80 ms. Standard Bruker pulse sequences were used with an excitation sculpting scheme for solvent suppression. Slowly exchanging amide protons were detected by acquiring a series of one-dimensional and TOCSY spectra over a 24-hour period, following dissolution of the peptides in D_2O. Exchange rates were calculated as previously described for comparison of acyclic and cyclic peptides (33).

The 2D NOESY spectra of cyc-MC12 were automatically assigned and an ensemble of structures calculated using the program CYANA (34). Torsion-angle restraints from TALOS+

were used in the structure calculations. Procheck (35) and Promotif (36) were used to analyse the stereochemical quality of the final structures, which were visualized using MOLMOL (37).

2.3.3. TNBS colitis assay

All animal experiments were conducted in accordance with the James Cook University Animal Ethics Committee approved guidelines under the project #A2003. Groups of five male C57BL/6 were used (5 weeks old). Mice were purchased from the Animal Resources Centre (Perth, Australia) and housed in the animal care facility unit at James Cook University under specific pathogen free conditions (Cairns). Mice were placed inside plastic cages with unlimited access to food and water.

Mice were divided randomly into 7 groups: Naïve, 2,4,6-trinitrobenzenesulfonic acid (TNBS), cyc-MC12, SFTI-1, lin-MC12(n), lin-MC12(p), MC12 and annexin A1 (2-26). Experimental mice received intraperitoneal (i.p) injections of peptides at a dosage of 3 mg/kg body weight. The mice were anaesthetized prior to administration of TNBS using mild ketamine/xylazine solution. After anaesthesia, each mouse received 100 μL of 5% (w/v) TNBS solution in 60% ethanol by intra-colonic instillation using a 20 gauge soft catheter (Terumo), which was inserted into the colon. Following the procedure, the animals were kept vertical for 30 seconds. Mice were monitored daily for piloerection, survival, body weight, decreased motor activity, rectal bleeding and stool consistency. Macroscopic pathology score was calculated for each colon after the mice were culled. Briefly, colons were harvested, opened longitudinally and washed with sterile phosphate buffer saline, then placed under a microscope (Olympus SZ61, 0.67-4.5x). The tissues were assessed for changes in macroscopic appearance, and scored for pathological changes as follows: adhesion (0 to 3), bowel wall thickening (0 to 3), mucosal

oedema (0 to 3), ulceration (0 to 3), and colon length as described previously (38). All animal experiments were conducted in duplicate to ensure reproducibility of the findings.

2.3.4. Serum stability assay

The stability of the peptides was tested in human male AB plasma (Sigma-Aldrich) using methods previously described (22). Peptides (final concentration of 200 μM) were incubated in serum or PBS at 37°C and 40 μL aliquots taken at 0 h, 3 h and 8 h. The aliquots of serum were quenched with 40 μL of 20% TFA and incubated for 10 minutes at 4°C to precipitate serum proteins. PBS received the same treatment as serum. The samples were then centrifuged at 17000 *g* for 10 min and 90 μL of supernatant analysed by RP-HPLC at a flow rate of 0.3 mL/min using an Phenomenex Jupiter C12 analytical column (150 x 2.00 mm, 4 μm, 90Å) using a linear 1% min^{-1} acetonitrile gradient (0-50% solvent B). The eluent was observed by dual wavelength UV detector set to 214 and 280 nm.

2.4. Results

2.4.1. Peptide design and synthesis

The tripeptide MC-12 was grafted into the SFTI-1 cyclic scaffold with the aim of improving its stability and potency. MC-12 was grafted into the binding loop of SFTI-1 as this resulted in removal of the P1 lysine residue. Acyclic versions of SFTI-1 incorporating the MC-12 sequence were also designed to examine the influence of the cyclic backbone, and loop grafted, on structure and activity. Ac2-26 was also synthesized using FMOC chemistry to provide additional insight into the structure function relationships of the MC-12 sequence. The sequences of the synthetic peptides are shown in **Figure 2.2**.

FIGURE 2.2. Sequences of the grafted peptides. The sequences of SFTI-1 (19) and the grafted peptides are shown. The active site Lys residue in SFTI-1 is italicized. The MC-12 sequence is highlighted in bold. The disulfide bond linking the two cysteine residues is shown in grey and the cyclic backbone shown with a black line. SFTI-1 is the original peptide sequence; cyc-MC12 has MC12 grafted into the binding loop of SFTI-1; lin-MC12(n) corresponds to the linear form of cyc-MC-12 with the N- and C- termini equivalent to the

precursor of SFTI-1; lin-MC12 (p) is a permuted form of cyc-MC-12 where they termini are not equivalent to the precursor of SFTI-1. Lin-MC12(l2) refers to MC-12 grafted into the cyclization in loop of SFTI-1.

2.4.2. Structural analysis using NMR spectroscopy

The structures of all the peptides were analysed using NMR spectroscopy. In general, the peptides displayed significant dispersion in the amide region, and a single set of resonances for each residue, consistent with peptides containing β-sheet structure and one well defined conformation. By contrast, lin-MC12(p) had significant overlap in the amide region, which prevented assignment of the resonances. With the exception of lin-MC12(p), two-dimensional spectra (TOCSY and NOESY) allowed assignment of the resonances and the secondary chemical shifts (secondary shifts) were determined by subtracting random coil chemical shifts (26) from the αH chemical shifts. A comparison of the secondary shifts is shown in Figure 2.3. The secondary shifts are similar between cyc-MC12 and lin-MC12(n), but lin-MC12(l2) has significantly different shifts for the cysteine residues compared to the other two peptides. The cysteine residues form part of the β-hairpin in the native peptide and consequently have downfield shifted α protons. The lack of downfield shifted α protons for the cysteine residues in lin-MC12(l2) suggests that the overall fold differs from the native peptide.

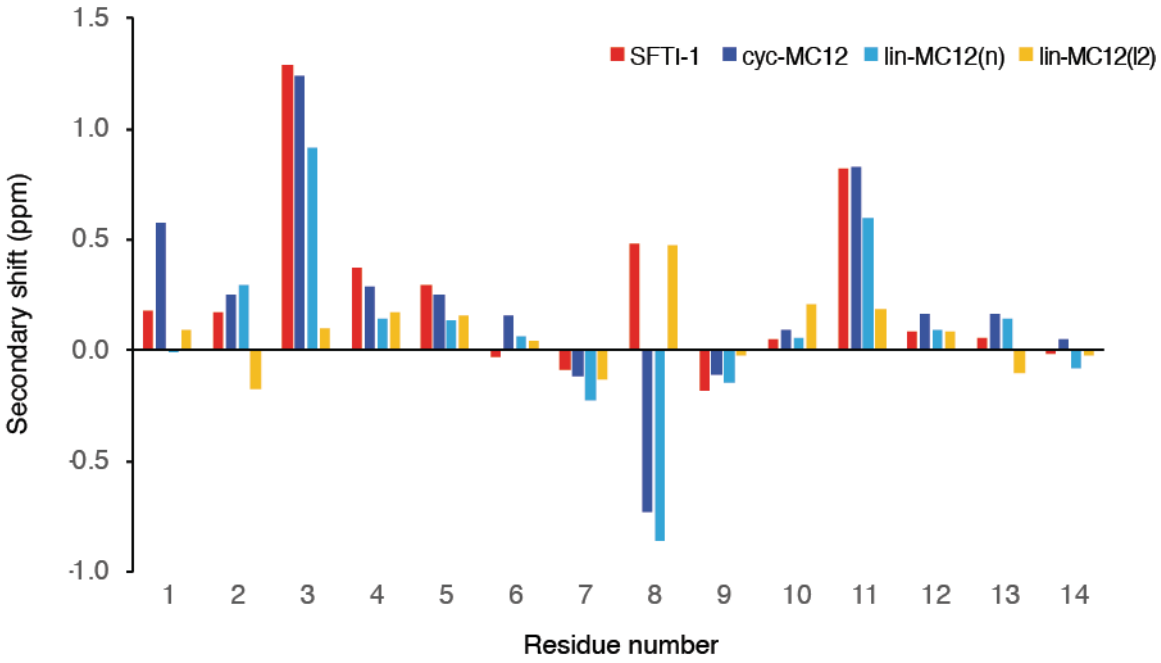

FIGURE 2.3. Secondary shift analysis of peptides. The secondary shifts for SFTI-1 are shown in red, cyc-MC12 in blue, lin-MC12(n) in cyan and lin-MC12(l2) in yellow. The secondary shifts were calculated by subtracting the random coil shifts (39) from the αH shift. The overall shifts are similar for all peptides with the exception of lin-MC12(l2) where the shifts for the cysteine residues (residues 3 and 11) differ significantly from the other peptides. Despite the similarities in secondary shifts between cyc-MC12 and lin-MC12(n), analysis of the amide exchange rates shows a significant difference as shown in Table 1. The exchange rates for lin-MC12(n) are higher than those observed for cyc-MC12 indicating that the overall structural stability has been decreased.

Table 2.1. Experimental amide exchange rates (k_{ex} min^{-1}) for cyc-MC12 and lin-MC12 (n)

Residue	cyc-MC12 ($x10^{-3}$)	lin-MC12(n) ($x10^{-3}$)
Gly 1	2.2	
Cys 3	0.56	
Thr 4	1.2	61
Ala 6	1.8	
Trp 7		13
Ile 10	0.37	1.2
Cys 11	3.5	69
Phe 12	0.53	33

The three-dimensional structures of cyc-MC12 and Ac2-26 were determined using the program CYANA based on distance restraints from the NOESY spectrum and angle restraints derived from TALOS+. The 20 lowest energy structures were chosen to represent the structures of cyc-MC12 and Ac2-26. Cyc-MC12 has a well-defined structure, including the loop containing the grafted residues as shown in Figure 2.4. The structure overlaps with the backbone atoms of SFTI-1 with an RMSD of 1.32 Å, highlighting the similarity between the two peptides. The structure statistics are provided Table 2. The structures of Ac2-26 are most well defined over the first 13 residues with an RMSD of 0.08 Å over the backbone atoms as shown in Figure 2.5. An α-helix is present from residues 7-10, with residues 9 and 10 corresponding to the Gln and Ala of MC-12. A 310 helix is also present between residues 15-17.

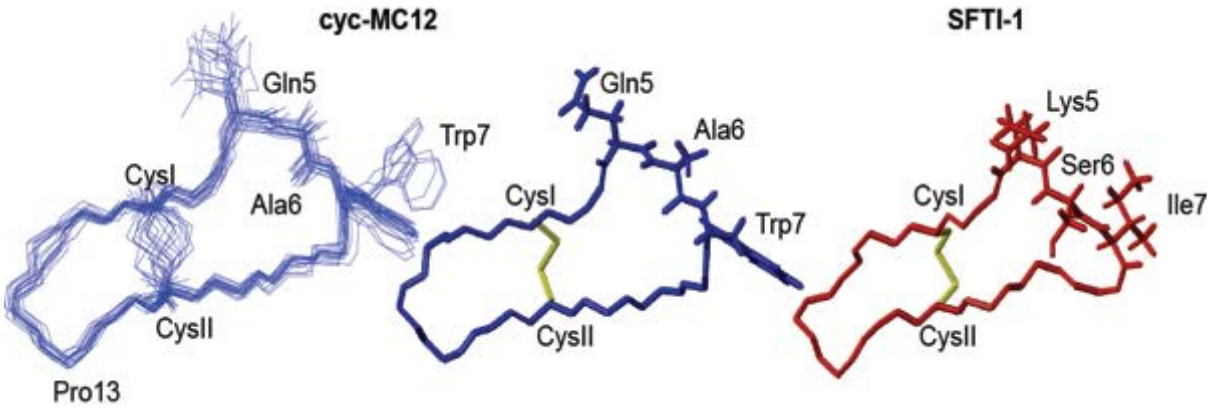

FIGURE 2.4. Structural analysis of cyc-MC12. The three-dimensional structure of the 20 lowest energy structures of cyc-MC12 is shown on the left of the diagram, highlighting the well-defined nature of the peptide, including the grafted region. The PDB ID code is 5VAV and the BMRB code is 30274. The lowest energy structure for cyc-MC12 is shown in the middle of the diagram with the sidechains of the grafted residues included. The structure of SFTI-1 is shown on the right of the diagram with the sidechains of the residues replaced with MC-12 shown. The figure was made using MOLMOL (37).

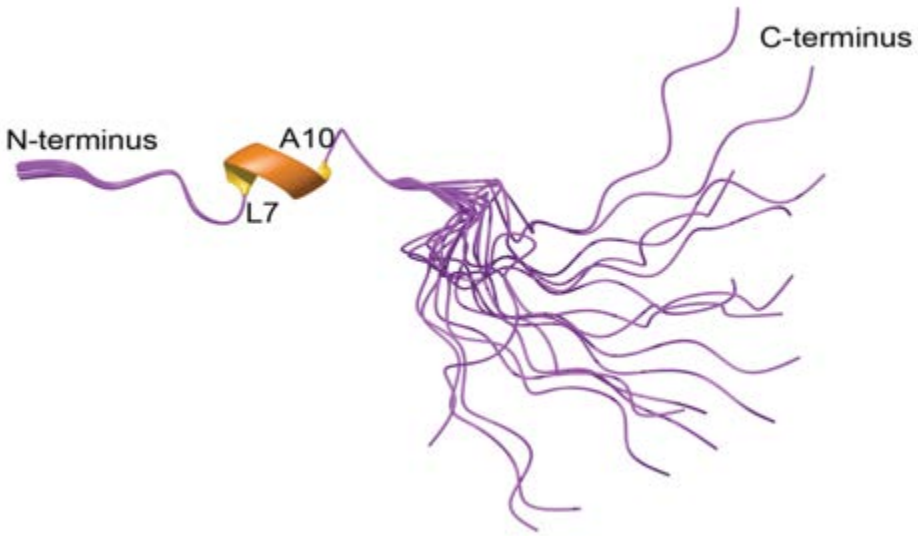

FIGURE 2.5. Three-dimensional structure of Ac2-26. The three-dimensional structure of the 20 lowest energy structures determined using NMR derived constraints. The helical region is shown with a thickened ribbon. The PDB ID code is 5VFW and the BMRB code is 30281. The figure was made using MOLMOL (37) .

Table 2.2. Structural statistics for the cyc-MC12 ensemble

Experimental restraints	
Interproton distance restraints	74
Intraresidue	40
Sequential	22
Medium range (i-j < 5)	5
Long range (i-j ≥5)	7
Disulfide-bond restraints	3
Dihedral-angle restraints	18
R.m.s. deviations from mean coordinate structure (Å)	
Backbone atoms	0.43 ± 0.17
All heavy atoms	1.27 ± 0.19
Ramachandran Statistics	
% in most favoured region	89.6
% in additionally allowed region	10.4

2.4.3. TNBS mouse model

The TNBS-induced murine colitis model was used to test the biological activities of all peptides. Mice were either left untreated (naïve) or were treated with peptide 5 hours prior to administration of TNBS. On day three of the experiment, all mice were euthanased by gas asphyxiation and examined. Mice treated with TNBS alone lost weight within one day of TNBS administration and continued to lose weight until day three. Initial experiments used 1 mg/kg dosage for cyc-MC12, but only partial protection in the TNBS model was observed (results not shown), and subsequent experiments used 3 mg/kg. Mice that were treated with 60 μg (3 mg/kg) of cyc-MC12 prior to administration of TNBS displayed significantly reduced weight loss at day 3, while all other peptides tested, including the linear form of the MC-12 peptide, had no significant effect (Figure 2.6A). Consistent with enhanced protection against TNBS-induced colitis, cyc-MC12-treated mice had visibly longer, healthier looking colons than untreated control mice administered TNBS (Figure 2.6B). The length of the colon in cyc-MC12-treated mice was similar to that of naïve mice (Figure 2.6C). Colons were then scored macroscopically by the following parameters: adhesions, bowel wall thickening, mucosal oedema, ulceration, necrosis, and colon length (macroscopic score), and demonstrated that cyc-MC12-treated mice displayed a significantly reduced macroscopic score (Figure 2.6D). SFTI-1 displayed no protective effect, indicating that the effect observed as a result of administering cyc-MC12 was related to the grafted region rather than the native scaffold. The tripeptide MC-12 administered at a dose of 60 μg did not have an influence on weight loss, or macroscopic score. However, the colon length of MC-12-treated mice was significantly longer than the TNBS-only treated mice, albeit not to the same extent as the cyc-MC12 peptide. The colon length and the macroscopic scores of mice treated with Ac2-26 showed a protective effect, but not to the same extent as cyc-MC12.

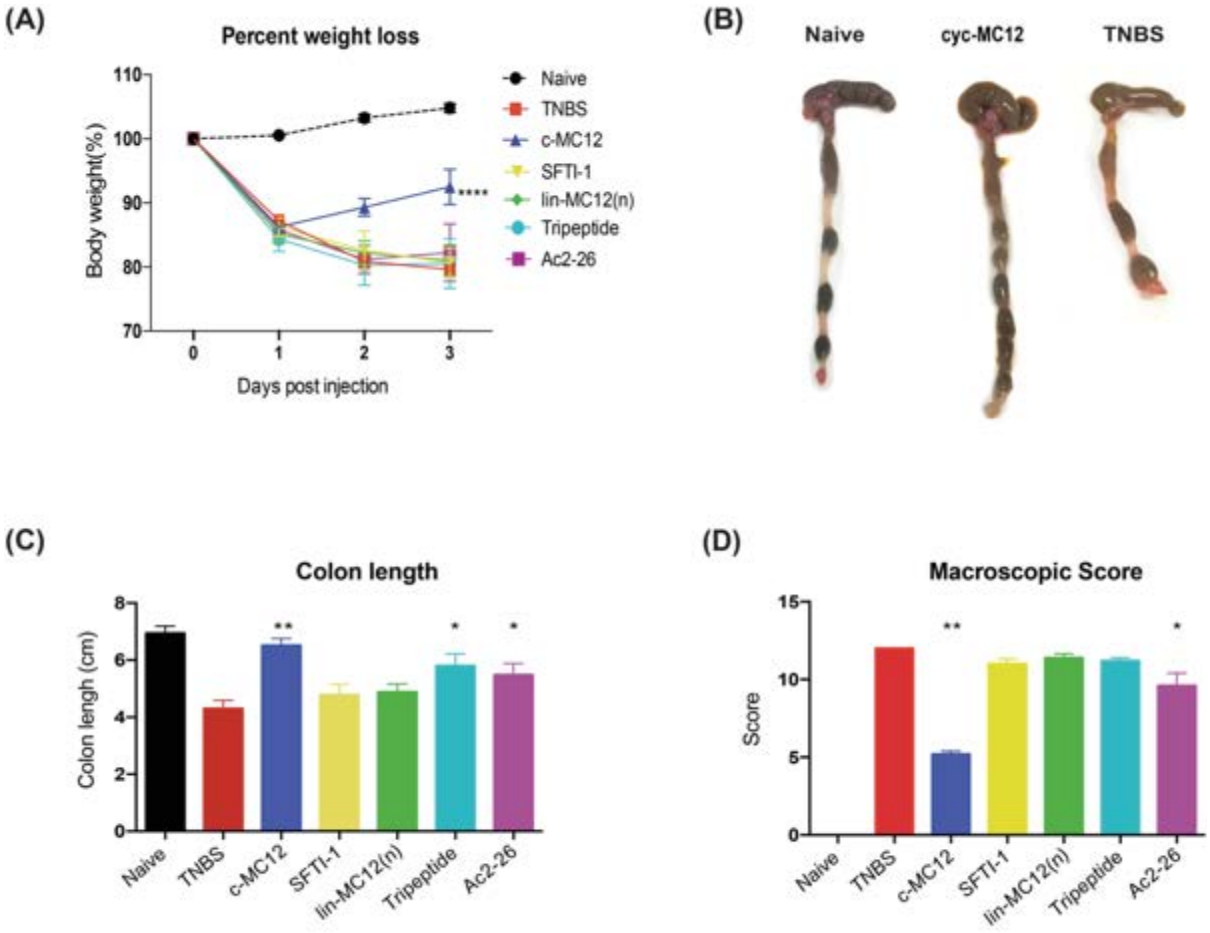

FIGURE 2.6. Protective effects of cyc-MC12 against weight loss and clinical symptoms induced by TNBS colitis. Mice were treated with TNBS at day 0 and weighed daily before termination at day 3. A) Percent weight loss (****P< 0.0001). B) Representative photomicrographs of colons at day 3. C) Colon lengths at day 3 (**P=0.0079, *P=0.0397). D) Macroscopic score of colon pathology at day 3 (**P=0.0079, *P= 0.0476). All peptides were administered at a dosage of 3 mg/kg corresponding to injection solution with molar concentrations of approximately 0.18 mM for the grafted peptides and 0.1 mM for Ac2-26. Data show the mean ± SEM from a representative experiment of three, with n = 5.

2.4.4. Serum stability

The stability of the peptides in human serum was assessed over an 8-hour period as shown in Figure 2.7. MC-12 and annexin A1(2-26) were completely degraded after 8 hours. By contrast, cyc-MC12 was stable in human serum over the time course of the experiment. The acyclic peptides were more stable than MC-12 and Ac2-26, but were degraded to ~60% of the initial concentration within the first three hours of incubation. The lower stability of the linear peptides demonstrates that the disulfide bond alone is not sufficient to confer high stability and that the cyclic backbone enhances the stability of the grafted peptides in human serum.

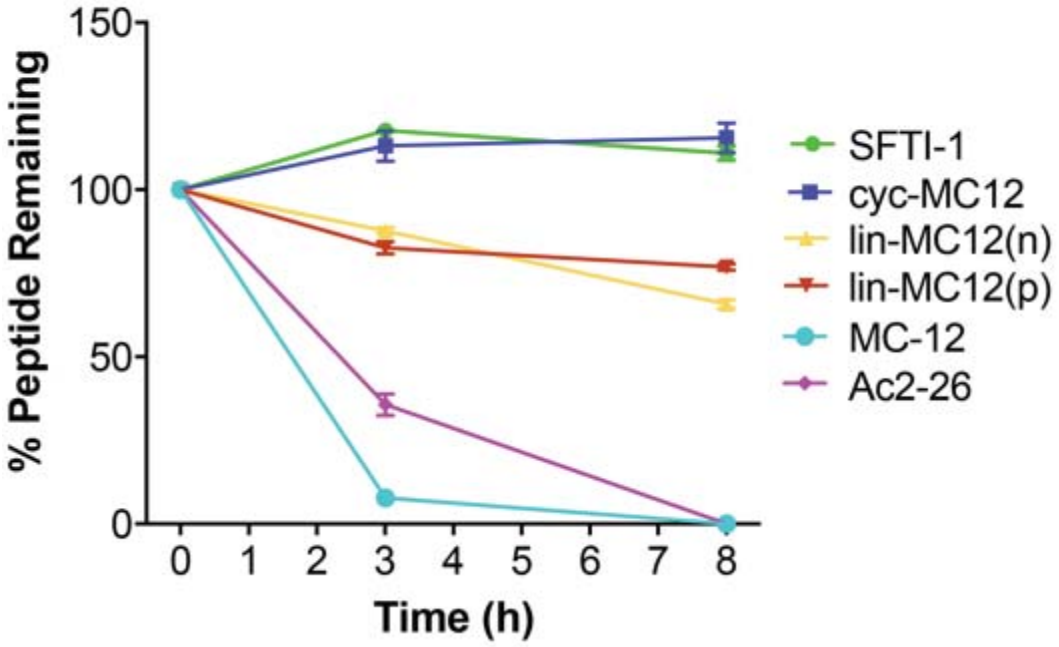

FIGURE 2.7. Serum stability of SFTI-1 grafted peptides. The percentage of peptide remaining in the serum stability assay as assessed by RP-HPLC. The grafted peptides, and SFTI-1, showed better stability than MC-12 and the longer Ac2-26 peptide. All data are represented as mean ± SD and were recorded in triplicate

2.5. Discussion

This study broadens the knowledge on grafting bioactive sequences into stable cyclic peptide scaffolds. Grafting MC-12 into the SFTI-1 cyclic scaffold enhances its bioactivity in a mouse model of acute colitis and stability in human serum, indicating that this approach might be useful for the design of novel drug leads for the treatment of colitis and other inflammatory diseases.

Cyc-MC12 had a significant effect on weight loss, macroscopic score and colon length in the TNBS mouse colitis model. By contrast, MC-12 did not improve weight loss or the macroscopic score relative to the TNBS treated mice. A significant difference was observed between the colon length of MC-12-treated mice and TNBS-only treated mice, but not to the same extent as cyc-MC12. Both MC-12 and cyc-MC12 were injected into mice at a dose of 3 mg/kg but MC-12 has a significantly lower molecular weight than cyc-MC12 (MC-12: 445.47 g/mol; cyc-MC12 1570.81 g/mol) corresponding to a higher molar concentration. The original study on MC-12 in colitis required a dose of 25 mg/kg to elicit an influence on macroscopic score and colon length in a TNBS mouse model (18); no effect on weight loss was observed. This improvement in bioactivity of MC-12 *in vivo* upon grafting in the cyclic scaffold is likely to be related to the significant improvement in stability in serum of cyc-MC12 compared to MC-12.

The three-dimensional structure of cyc-MC12, determined by NMR spectroscopy, is well-defined, including the grafted Gln-Ala-Trp sequence. The residues corresponding to MC-12 form a helical structure in the annexin A1 protein (27) as shown in **Figure 2.1**, but do not form a helix when grafted into the cyclic scaffold. This is not surprising given the tightly folded

structure of SFTI-1 resulting from the cyclic backbone and cross-bracing of the disulfide bond. Given the well-defined nature of the cyclic peptide, it is unlikely it can change conformation significantly to interact with a binding partner. However, based on the activity observed in the TNBS mouse model, the turn structure induced by grafting into the cyclic backbone appears to be sufficient to allow binding to the biological target. The biological target for cyc-MC12 is unknown but the original studies on the MC-12 tripeptide suggested that NF-κB, a central mediator of gastrointestinal inflammation in IBD might be involved (18,28). Further study on these peptides is required to elucidate the mechanism of action.

Although the binding partner of MC-12 has not been conclusively shown, our current study provides significant insight into the structure function relationships involved in the anti-inflammatory activity. The importance of the cyclic backbone in SFTI-1 grafting has been highlighted in the current study. Previous studies have shown that the disulfide bond and network of hydrogen bonds are sufficient to maintain the native fold (29). However, in the current study we have shown that although the native fold is maintained in the absence of the cyclic backbone in lin-MC12(n), the bioactivity is not maintained. Cyc-MC12 is structurally more stable than lin-MC12(n) based on the slower amide exchange rates and is more biologically stable in human serum than lin-MC12(n). This lack of stability of lin-MC12(n) might account for the lack of bioactivity *in vivo*. Interestingly, when the MC-12 peptide is grafted into the SFTI-1 binding loop, without backbone cyclization in lin-MC12(p), the chemical shift analysis indicates that the overall fold of the native peptide is not maintained. This peptide has a large extended N-terminal tail that presumably prevents the native structure from forming.

Further insight into the structure function relationships of MC-12 have come from analysis of Ac2-26. Ac2-26 is effective in a range of anti-inflammatory assays including models of ocular inflammation and asthma at doses of 1 mg/kg (30,31) but the structure has not been reported. We show here that the N-terminal region, including the MC-12 sequence (residues 9-11), is well defined in contrast to the C-terminal region of the peptide (**Figure 2.5**). Residues 9-11 in Ac2-26 overlay well with the corresponding residues in the full length annexin A1 protein as shown in **Figure 2.8,** but the adjacent residues in Ac2-26 do not overlay with the full length protein. The conservation of the native structure of MC-12 in the Ac2-26 peptide suggests there will be less entropic losses upon binding to the biological target and consequently why this tripeptide has previously been shown to be so important in anti-inflammatory activity (13). In the current study we have shown that Ac2-26 is not as effective as cyc-MC12 in the colitis model and this lower efficacy is likely to be related to the lower biological stability; Ac2-26 is degraded rapidly in human serum.

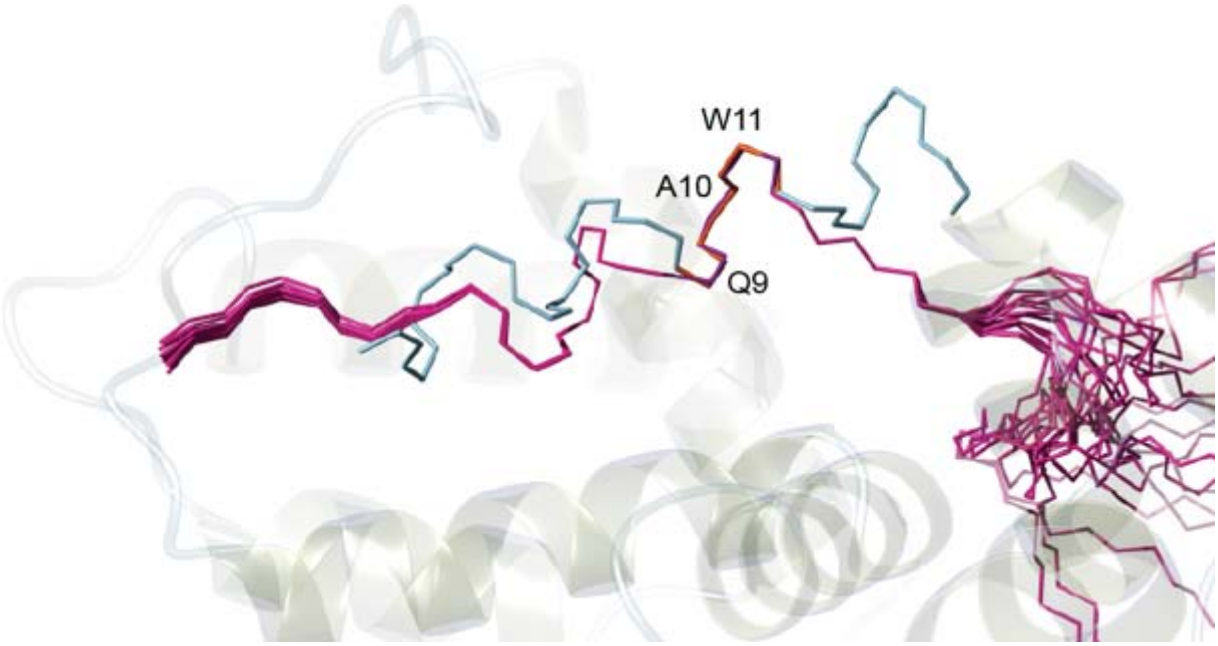

FIGURE 2.8. Overlay of Ac2-26 with annexin A1 (PDB ID code 1HM6). Structures were superimposed over residues 9-11 in Ac2-26 and residues 10-12 in annexin A1 (these residues

correspond to the MC-12 sequence Gln-Ala-Trp). The labelling corresponds to the numbering in cyc-MC12. The figure was made using MOLMOL (37).

In summary, the potency and stability of the MC-12 tripeptide was improved by incorporation into the SFTI-1 scaffold. The cyclic backbone is important for structural and biological stability and consequently biological activity. Overall, our results indicate that SFTI-1 is a promising scaffold for the design of novel lead molecules for IBD and other diseases that result from a dysregulated immune system.

Conflict of interest: The authors declare that they have no conflicts of interest with the contents of this article.

2.6. References

1. Ament, M. E. (1975) Inflammatory disease of colon - ulcerative-colitis and crohns colitis. J. Pediatr. 86, 322-334

2. SA, S. (2001) Surgical management of Crohn's disease. in Surgical Treatment: Evidence-Based and Problem-Oriented (Mannick, R. G. H. J. A. ed.), Munich: Zuckschwerdt. pp

3. Navarro, S., Ferreira, I., and Loukas, A. (2013) The hookworm pharmacopoeia for inflammatory diseases. Int. J. Parasitol. 43, 225-231

4. Molnar, T., Farkas, K., Szepes, Z., Nagy, F., Szucs, M., Nyari, T., Balint, A., and Wittmann, T. (2014) Long-term outcome of cyclosporin rescue therapy in acute, steroid-refractory severe ulcerative colitis. United European Gastroenterol. J. 2, 108-112

5. Wangchuk, P., Navarro, S., Shepherd, C., Keller, P. A., Pyne, S. G., and Loukas, A. (2015) Diterpenoid alkaloids of Aconitum laciniatum and mitigation of inflammation by 14-O-acetylneoline in a murine model of ulcerative colitis. Sci. Rep. 5, 10

6. Leoni, G., Neumann, P. A., Kamaly, N., Quiros, M., Nishio, H., Jones, H. R., Sumagin, R., Hilgarth, R. S., Alam, A., Fredman, G., Argyris, I., Rijcken, E., Kusters, D., Reutelingsperger, C., Perretti, M., Parkos, C. A., Farokhzad, O. C., Neish, A. S., and Nusrat, A. (2015) Annexin A1-containing extracellular vesicles and polymeric nanoparticles promote epithelial wound repair. J. Clin. Invest. 125, 1215-1227

7. Dalmasso, G., Charrier-Hisamuddin, L., Nguyen, H. T. T., Yan, Y., Sitaraman, S., and Merlin, D. (2008) PepT1-mediated tripeptide KPV uptake reduces intestinal inflammation. Gastroenterology 134, 166-178

8. Akgul, S., Erbil, Y., Giris, M., Alis, H., Yanik, B. T., Olgac, V., and Toker, G. A. (2006) The effect of octreotide on pancreatic damage in TNBS-induced colitis. Surg. Innov. 13, 102-108

9. Wada, S., Sato, K., Ohta, R., Wada, E., Bou, Y., Fujiwara, M., Kiyono, T., Park, E. Y., Aoi, W., Takagi, T., Naito, Y., and Yoshikawa, T. (2013) Ingestion of low dose pyroglutamyl leucine improves dextran sulfate sodium-induced colitis and intestinal microbiota in mice. J. Agric. Food Chem. 61, 8807-8813

10. Bettenworth, D., Buyse, M., Bohm, M., Mennigen, R., Czorniak, I., Kannengiesser, K., Brzoska, T., Luger, T. A., Kucharzik, T., Domschke, W., Maaser, C., and Lugering, A. (2011) The tripeptide KdPT protects from intestinal inflammation and maintains intestinal barrier function. Am. J. Pathol. 179, 1230-1242

11. Kovacs-Nolan, J., Zhang, H., Ibuki, M., Nakamori, T., Yoshiura, K., Turner, P. V., Matsui, T., and Mine, Y. (2012) The PepT1-transportable soy tripeptide VPY reduces intestinal inflammation. Biochim. Biophys. Acta-General Subjects 1820, 1753-1763

12. Flower, R. J. (1988) 11th gaddum memorial lecture - lipocortin and the mechanism of action of the glucocorticoids. Br. J. Pharmacol. 94, 987-1015

13. Zhang, Z. Q., Huang, L. Q., Zhao, W. P., and Rigas, B. (2010) Annexin 1 induced by anti-inflammatory drugs binds to NF-kappa B and inhibits its activation: anticancer effects in vitro and in vivo. Cancer Res. 70, 2379-2388

14. de Paula-Silva, M., Barrios, B. E., Maccio-Maretto, L., Sena, A. A., Farsky, S. H. P., Correa, S. G., and Oliani, S. M. (2016) Role of the protein annexin A1 on the efficacy of anti-TNF treatment in a murine model of acute colitis. Biochem. Pharmacol. 115, 104-113

15. Cirino, G., Cicala, C., Sorrentino, L., Ciliberto, G., Arpaia, G., Perretti, M., and Flower, R. J. (1993) antiinflammatory actions of an n-terminal peptide from human lipocortin-1. Br. J. Pharmacol. 108, 573-574

16. Stuqui, B., de Paula-Silva, M., Carlos, C. P., Ullah, A., Arni, R. K., Gil, C. D., and Oliani, S. M. (2015) Ac2-26 mimetic peptide of annexin A1 inhibits local and systemic inflammatory processes induced by bothrops moojeni venom and the Lys-49 phospholipase A(2) in a rat model. PLoS One 10, 18

17. Perretti, M., and D'Acquisto, F. (2009) Annexin A1 and glucocorticoids as effectors of the resolution of inflammation. Nat. Rev. Immunol. 9, 62-70

18. Ouyang, N. T., Zhu, C. H., Zhou, D. Y., Nie, T., Go, M. F., Richards, R. J., and Rigas, B. (2012) MC-12, an annexin A1-based peptide, is effective in the treatment of experimental colitis. PLoS One 7, 11

19. Luckett, S., Garcia, R. S., Barker, J. J., Konarev, A. V., Shewry, P. R., Clarke, A. R., and Brady, R. L. (1999) High-resolution structure of a potent, cyclic proteinase inhibitor from sunflower seeds. J. Mol. Biol. 290, 525-533

20. Daly, N. L., Chen, Y. K., Foley, F. M., Bansal, P. S., Bharathi, R., Clark, R. J., Sommerhoff, C. P., and Craik, D. J. (2006) The absolute structural requirement for a proline in the P3 '-position of Bowman-Birk protease inhibitors is surmounted in the minimized SFTI-1 scaffold. J. Biol. Chem. 281, 23668-23675

21. Swedberg, J. E., Nigon, L. V., Reid, J. C., de Veer, S. J., Walpole, C. M., Stephens, C. R., Walsh, T. P., Takayama, T. K., Hooper, J. D., Clements, J. A., Buckle, A. M., and Harris, J. M. (2009) Substrate-guided design of a potent and selective kallikrein-related peptidase inhibitor for kallikrein 4. Chem. Biol. 16, 633-643

22. Chan, L. Y., Gunasekera, S., Henriques, S. T., Worth, N. F., Le, S. J., Clark, R. J., Campbell, J. H., Craik, D. J., and Daly, N. L. (2011) Engineering pro-angiogenic peptides using stable, disulfide-rich cyclic scaffolds. Blood 118, 6709-6717

23. Jendrny, C., and Beck-Sickinger, A. G. (2016) Inhibition of kallikrein-related peptidases 7 and 5 by grafting serpin reactive-center loop sequences onto sunflower trypsin inhibitor-1 (SFTI-1). ChemBioChem 17, 719-726

24. Chan, L. Y., Craik, D. J., and Daly, N. L. (2016) Dual-targeting anti-angiogenic cyclic peptides as potential drug leads for cancer therapy. Sci. Rep. 6, 13

25. Quimbar, P., Malik, U., Sommerhoff, C. P., Kaas, Q., Chan, L. Y., Huang, Y. H., Grundhuber, M., Dunse, K., Craik, D. J., Anderson, M. A., and Daly, N. L. (2013) High-affinity cyclic peptide matriptase inhibitors. J. Biol. Chem. 288, 13885-13896

26. Wishart, D. S., Bigam, C. G., Holm, A., Hodges, R. S., and Sykes, B. D. (1995) 1H, 13C and 15N random coil NMR chemical shifts of the common amino acids. I. Investigations of nearest-neighbor effects. J. Biomol. NMR 5, 67-81

27. Perretti, M., D'Acquisto, F., and Flower, R. J. (2013) Chapter 86 - Annexin-A1 peptide Ac2–26 A2 - Kastin, Abba J. in Handbook of Biologically Active Peptides (Second Edition), Academic Press, Boston. pp 631-639

28. Tambuwala, M. M. (2016) Natural nuclear factor kappa beta inhibitors: safe therapeutic options for inflammatory bowel disease. Inflamm. Bowel Dis. 22, 719-723

29. Korsinczky, M. L. J., Schirra, H. J., and Craik, D. J. (2004) Sunflower trypsin inhibitor-1. Curr. Protein Peptide Sci. 5, 351-364

30. Girol, A. P., Mimura, K. K. O., Drewes, C. C., Boonheis, S. M., Solito, E., Farsky, S. H. P., Gil, C. D., and Oliani, S. M. (2013) Anti-inflammatory mechanisms of the annexin A1 protein and its mimetic peptide Ac2-26 in models of ocular inflammation in vivo and in vitro. J. Immunol. 190, 5689-5701

31. Wang, L. M., Li, W. H., Xu, Y. C., Wei, Q., Zhao, H., and Jiang, X. F. (2011) Annexin 1-derived peptide Ac2-26 inhibits eosinophil recruitment in vivo via decreasing prostaglandin D-2. Int. Arch. Allergy Immunol. 154, 137-148

32. Gunasekera, S., Aboye, T. L., Madian, W. A., El-Seedi, H. R., and Goransson, U. (2013) Making ends meet: Microwave-accelerated synthesis of cyclic and disulfide rich proteins via in situ thioesterification and native chemical ligation. Int. J. Pept. Res. Ther. 19, 43-54

33. Daly, N. L., and Craik, D. J. (2000) Acyclic permutants of naturally occurring cyclic proteins - Characterization of cystine knot and beta-sheet formation in the macrocyclic polypeptide kalata B1. J. Biol. Chem. 275, 19068-19075

34. Güntert, P. (2004) Automated NMR structure calculation with CYANA. in Protein NMR Techniques (Downing, A. K. ed.), Humana Press, Totowa, NJ. pp 353–378

35. Laskowski, R. A., Macarthur, M. W., Moss, D. S., and Thornton, J. M. (1993) Procheck - A program to check the stereochemical quality of protein structures. J. Appl. Crystallogr. 26, 283-291

36. Hutchinson, E. G., and Thornton, J. M. (1996) PROMOTIF - A program to identify and analyze structural motifs in proteins. Protein Sci. 5, 212-220

37. Koradi, R., Billeter, M., and Wuthrich, K. (1996) MOLMOL: A program for display and analysis of macromolecular structures. J. Mol. Graphics 14, 51-&

38. Ferreira, I., Smyth, D., Gaze, S., Aziz, A., Giacomin, P., Ruyssers, N., Artis, D., Laha, T., Navarro, S., Loukas, A., and McSorley, H. J. (2013) Hookworm excretory/secretory products induce interleukin-4 (IL-4)(+) IL-10(+) CD4(+) T cell responses and suppress pathology in a mouse model of colitis. Infect. Immun. 81, 2104-2111

39. Wishart, D. S., Bigam, C. G., Holm, A., Hodges, R. S., and Sykes, B. D. (1995) H-1, C-13 and N-15 random coil NMR chemical-shifts of the common amino-acids .1. investigations of nearest-neighbor effects. J. Biomol. NMR 5, 67-81

3. CHAPTER 3

Engineering of an Anti-Inflammatory Peptide Based on the Disulfide-Rich Linaclotide Scaffold

Claudia Cobos Caceres, Paramjit S. Bansal, Linda Jones, Phurpa Wangchuk, David Wilson, Alex Loukas, Norelle L. Daly*

3.1. Abstract

Inflammatory bowel diseases are a set of complex and debilitating diseases, for which there is no satisfactory treatment. Peptides as small as three amino acids have been shown to have anti-inflammatory activity in mouse models of colitis, but they are likely to be unstable limiting their development as drug leads. Here we have grafted a tripeptide from the annexin A1 protein into linaclotide, a 14-amino-acid peptide with three-disulfide bonds, which is currently in clinical use for patients with chronic constipation or Irritable Bowel Syndrome. This engineered disulfide-rich peptide maintained the overall fold of the original synthetic guanylate cyclase C agonist peptide, and reduced inflammation in a mouse model of acute colitis. This is the first study to show that this highly disuflide-rich peptide can be used as a scaffold to confer a new bioactivity.

3.2. Introduction

Peptides display a range of potentially useful biological functions such as anti-inflammatory (1), anti-cancer (2), anti-HIV (3), antimicrobial (4) and insecticidal (5) activities, among others. Peptides as drug leads have a range of advantages over small molecules and proteins, including target specificity, low toxicity and immunogenicity, but one major limitation for small, unstructured peptides is a lack of stability *in vivo* (6). Small, unconstrained peptides can be degraded within a few minutes in the blood, which decreases their potential as therapeutic agents.

Advances in medicinal chemistry has led to a range of approaches for stabilizing peptides, including the use of disulfide bonds and backbone cyclization (7). These studies have involved the use of naturally occurring peptides as well as engineering studies (8,9). Examples of peptides that are currently used in the clinic, include Prialt® (Ziconotide), which is a synthetic version of the cone-snail venom peptide MVIIA and is currently used for the treatment of chronic pain (10). This cone-snail venom peptide is a calcium channel antagonist, containing 25 residues and three-disulfide bonds in a cystine knot motif (11). Another example is the 12-residue cyclic peptide cyclosporine that has famously revolutionised organ transplant therapy due to its potent immunosuppressant activities (12). Linaclotide, a 14-amino-acid peptide with three-disulfide bonds, which in oral administration interacts with guanylate cyclase-C, generating cyclic guanosine monophosphate (cGMP), is currently in clinical use for patients with chronic constipation or Irritable Bowel Syndrome (13). Linaclotide improves bowel function and abdominal discomfort (14).

We have recently shown that a tri-peptide (MC-12), originally derived from annexin A1, can be stabilized by grafting into the SFTI-1 framework (15). SFTI-1 is a 14-residue cyclic peptide isolated from the seeds of sunflowers (*Helianthus annuus*), and is one of the most potent trypsin inhibitors known (16). It contains two short antiparallel β-strands linked by a single disulfide bond, and the structure contains a network of hydrogen bonds which makes it extremely stable for engineering modifications (17,18). We grafted MC-12 into the so called binding loop of SFTI-1 to remove the trypsin inhibitory activity. Our grafted peptide, termed (cyc-MC12), improved the therapeutic efficacy in a murine model of chemically-induced acute colitis, and also improved the *in vitro* stability of MC-12 (15).

Inflammatory bowel diseases (IBD) are a set of debilitating chronic inflammatory disorders of the gastrointestinal tract. The two major forms for IBD are ulcerative colitis and Crohn's disease (19). Current treatments are not satisfactory, and consequently new drug leads are being sought from a range of sources, including small molecules from plants and bioactive regions of larger proteins (20-23).

To further explore the potential of using disulfide rich/cyclic peptide scaffolds for IBD applications we have used the linaclotide scaffold for grafting the MC-12 sequence. The linaclotide scaffold is highly constrained and orally active, making it interesting to explore its potential for acting as a scaffold for engineering novel bioactivities. Linaclotide regulates guanylate cyclase C (GCC) and is used in the treatment of inflammatory bowel syndrome (IBS), but has not been demonstrated to regulate autoimmune diseases such as inflammatory bowel disease (IBD), making this study the first to examine its potential as a scaffold in IBD.

3.3. Experimental procedures

3.3.1. Peptide synthesis and purification

The peptides were synthesized using fluorenylmethyloxycarbonyl (Fmoc) chemistry based solid phase peptide synthesis. The resin used for the peptides was 2-chlorotrityl chloride resin on a 0.1 mmole scale. Amino acids (2 equiv.) were activated in 5 equiv HBTU and 10 equiv. DIPEA in DMF (1.5 mL). Deprotection was carry out in two repetitions: Starting with 2 min of 20% pipiridine in DMF (5 ml), followed by 3 mins of the same solution. The C-terminal amino acid was coupled manually to the resin, and the remainder of the peptide assembled using a Protein Technologies PS3 synthesiser following FMOC approach. Peptides were cleaved from the resin using a mixture of trifluoroacetic acid/water/triisopropylsilane (95:2.5:2.5) for 2-3 h. Each peptide was precipitated with diethylether after cleavage, dissolved in 50% acetonitrile/0.05% TFA, and then lyophilised. RP-HPLC was used for purification on a C_{18} preparative column (Phenomenex Jupiter 250 x 21.2 mm, 10 µm, 300 Å) with 1% gradient of solvent B (solvent A: 0.05% TFA; solvent B: 90% acetonitrile, 0.05% TFA). Masses were analysed using MALDI-TOF mass spectrometry. The reduced peptides were oxidised for in 0.1 M ammonium bicarbonate (pH8.5) buffer solution containing 2 mM reduced glutathione for 24 hours at room temperature. The oxidized peptides were purified in RP-HPLC and masses analysed using MALDI-TOF mass spectrometry.

3.3.2. NMR spectroscopy and structural analysis

After purification, the peptides were resuspended at a final concentration of ~0.2 mM in 90%H_2O:10%D_2O, or 100 mM deuterated SDS dissolved in 90%H_2O:10%D_2O. 2D ^{1}H-^{1}H

TOCSY, ^{1}H-^{1}H NOESY, ^{1}H-^{1}H DQF-COSY, ^{1}H-^{15}N HSQC, and ^{1}H-^{13}C HSQC spectra were acquired at 290 K using a 600 MHz AVANCE III NMR spectrometer (Bruker, Karlsruhe, Germany). NOESY spectra were acquired with mixing times of 200-300 ms, and TOCSY spectra were acquired with isotropic mixing periods of 80 ms. Standard Bruker pulse sequences were used with an excitation sculpting scheme for solvent suppression. Spectra were referenced to internal 4,4-dimethyl-4-silapentane-1-sulfonic acid (DSS).

NMR assignments were made using established protocols (24), and the secondary shifts derived by subtracting the random coil αH shift from the experimental αH shifts (25). The 2D NOESY spectra of MC12-linaclotide was automatically assigned and an ensemble of structures calculated using the program CYANA(26). Dihedral-angle restraints were derived based on the $J_{\alpha N}$ coupling constants measured from the one-dimensional spectra. The final structures were visualized using MOLMOL (27).

3.3.3. TNBS colitis assay

The animal experiments were conducted in accordance with the James Cook University Animal Ethics Committee approved guidelines. Five male BALB/c were used for each group (5 weeks old). Mice were purchased from the Animal Resources Centre (Perth, Australia) and housed in the animal care facility unit at James Cook University in Cairns under specific pathogen free conditions, with unlimited access to food and water in their cages. Mice were divided randomly into 4 groups: Naïve, 2,4,6-trinitrobenzenesulfonic acid (TNBS), MC12-linaclotide plus TNBS and linaclotide plus TNBS. Mice received intraperitoneal (i.p) injections of peptides at a dosage of 3 mg/kg body weight. Prior to intra-rectal administration of TNBS, mice were anaesthetized using mild ketamine/xylazine solution. After anaesthesia, each mouse received 100 μL of 5%

(w/v) TNBS solution in 60% ethanol by intra-colonic instillation using a 20 gauge soft catheter (Terumo), which was inserted into the anus and up to the colon. Mice were monitored daily for body weight, piloerection, survival, decreased motor activity, rectal bleeding and stool consistency. Mice were humanely euthanased using gas asphyxiation, where CO_2 was applied directly to the individual cage for approximately 1.5 minutes and animals removed from the cage and death confirmed. After cull, macroscopic pathology score was calculated for each colon. Briefly, colons were harvested, opened longitudinally and washed with sterile phosphate buffer saline. The tissues were assessed for changes in macroscopic appearance, and scored for pathological changes as follows: adhesion (0 to 3), bowel wall thickening (0 to 3), mucosal oedema (0 to 3), ulceration (0 to 3), and colon length as described previously (28). All animal experiments were conducted in duplicate to ensure reproducibility of the findings.

3.3.4. Tissue p-IκB-α (Ser32) and p-NF-κB p65 (Ser536) measurements

The levels of phosphorylated inhibitors phosphorylated nuclear factor kappa-light-chain-enhancer of activated B cells p65 (Ser536) (phospho-NF-κB p65 (Ser536)) and phosphorylated inhibitor of κB-α (Ser32) (phospho-IκBα (Ser32)) were measured using tissue homogenates prepared at 4 °C using phosphate buffer as per the manufacturer's instructions using a manual tissue grinder. Results were determined by ELISA using PathScan® kits (Cell Signalling Technology), and absorbances were read using POLARstar Omega spectrophotometer (BMG Labtech). Statistical analyses were performed using four groups of mice (naïve, TNBS only, linaclotide + TNBS, and MC12-linaclotide + TNBS), with a total of 20 mice. Error bars represent ± SEM.

3.4. Results

3.4.1. Peptide design and synthesis

The linaclotide sequence contains three inter-cysteine loops, comprising two or three residues. To avoid changing the inter-cysteine loop sizes we grafted MC-12 into the second loop, which contains three residues, as shown in Figure 3.1. Linaclotide and the grafted peptide (MC12-linaclotide) were synthesised by Fmoc solid phase peptide synthesis, purified using RP-HPLC and the mass analysed with MALDI-TOF mass spectrometry. The purified, reduced peptides were oxidised in ammonium bicarbonate with glutathione as a shuffling reagent, and a single major product was evident based on RP-HPLC analysis. This major isomer was purified and the mass confirmed.

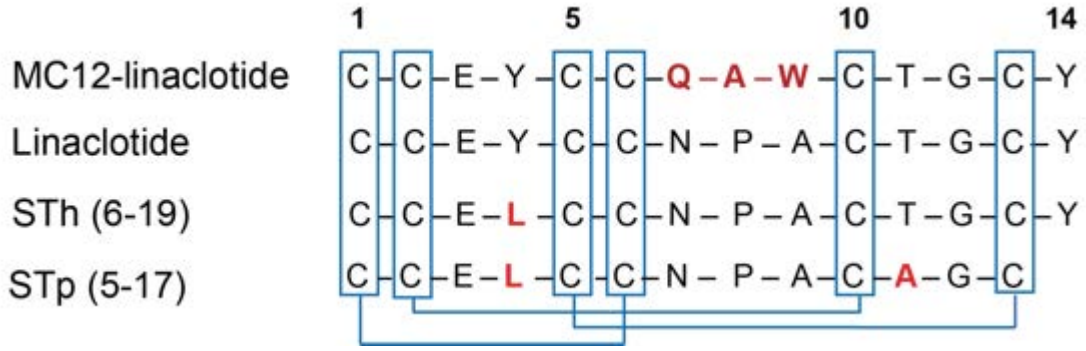

Figure 3.1. Sequences of MC-12-linaclotide, linaclotide, STh (6-19) and STp (5-17) (the latter two peptides are **linaclotide related peptides**). The differences in sequences are highlighted in red. The disulfide bonds are highlighted in blue.

3.4.2. Structural analysis

The structures of linaclotide and MC12-linaclotide were analysed using NMR spectroscopy. NMR spectra were recorded in aqueous solution. Two-dimensional TOCSY and NOESY spectra allowed assignment of the majority of the resonances, and the secondary chemical shifts were determined by subtracting random coil chemical shifts from the αH chemical shifts (25). Cys1, Cys 2, Cys5 and Cys6 could not be assigned for either linaclotide or MC12-linaclotide. It is likely that these residues have very broad peaks, which prevented detection. A comparison of the secondary shifts for the assigned residues is shown in Figure 3.2A. The secondary shifts are similar between MC12-linaclotide and linaclotide, indicating that the peptides have the same overall fold. To confirm the fold of the synthetic peptides was similar to related peptides, and therefore likely to have the native disulfide connectivity, we compared the secondary shifts to STh (6-19), which is a toxin that only differs from linaclotide by one residue; linaclotide contains a tyrosine at residue 4, whereas STh (6-19) contains a leucine (Figure 3.1). The chemical shifts of STh (6-19) have previously been published, and the structure reported has the same disulfide connectivity as linaclotide (29). STh (6-19) also has incomplete shifts for residues 1, 2, 5 and 6. All three peptides have similar secondary shifts consistent with them having the same disulfide connectivity (Cys1-Cys6, Cys2-Cys10, Cys5-Cys13) and overall fold.

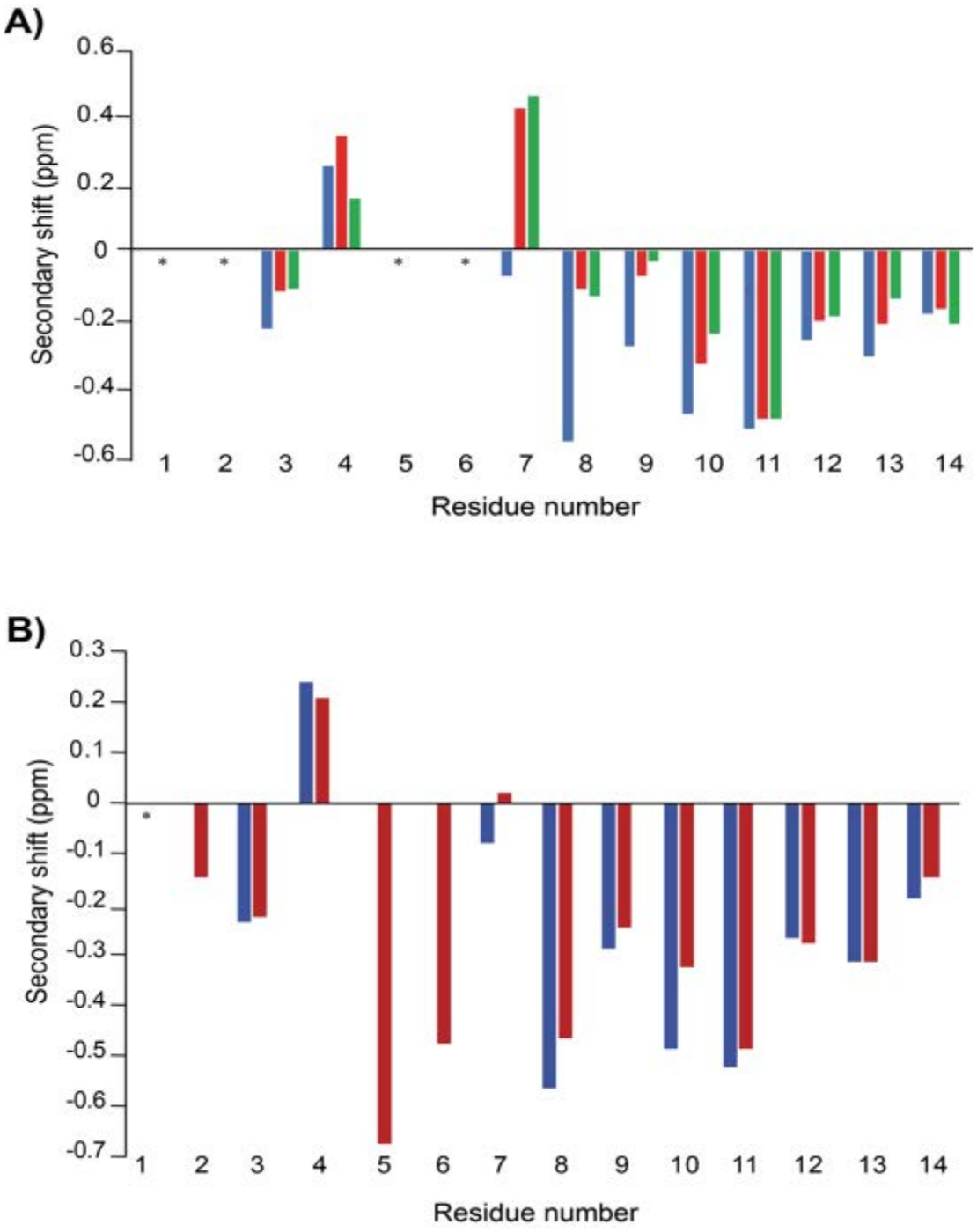

Figure 3.2. Secondary shift analysis. The secondary shifts were calculated by subtracting the random coil shifts from the αH shifts (25). A) MC12-linaclotide (blue), Linaclotide (red) and STh (6-19) (green); Residues that were not able to be assigned are marked with an asterisk. (B) Comparison of secondary shifts of MC12-linaclotide derived from spectra recorded in aqueous solution (blue) and 100 mM SDS (red). The N-terminal residue is marked with an asterisk as it could not be assigned in the spectra recorded in SDS.

One-dimensional NMR spectra were recorded for MC12-linaclotide over the pH range 3.5 to 6 to determine if the missing resonances were evident. Peaks corresponding to the amide protons of residues 1, 2, 5 and 6 were not present in any of the spectra. Most of the amide protons were not evident in the one-dimensional spectrum at pH 6.

The three-dimensional structure of MC12-lincalotide was calculated based on NOE and dihedral angle restraint data (30). Although the N-terminal region is disordered a turn of 3_{10} helix from residues 7-10 was present based on analysis with CYANA(26). A superposition of the 20 lowest energy structures is given in Figure 3.3.A, which highlights the disorder at the N- and C-termini despite the high proportion of disulfide bonds in the peptide. The structure statistics are provided Table 3.1.

Table 3.1. Structural statistics for the MC12-linaclotide ensemble

Experimental restraints	
Interproton distance restraints	62
Intraresidue	30
Sequential	22
Medium range (i-j < 5)	9
Long range (i-j ≥5)	1
Dihedral-angle restraints	6
R.m.s. deviations from mean coordinate structure (Å)	
Backbone atoms (residue 1-14)	1.68 ± 0.69
All heavy atoms (residue 1-14)	2.54 ± 0.7
Backbone atoms (residue 6-11)	1.54 ± 0.84
All heavy atoms	1.28 ± 0.82
Ramachandran Statistics	
% in most favoured region	36.4%
% in additionally allowed region	62.4%

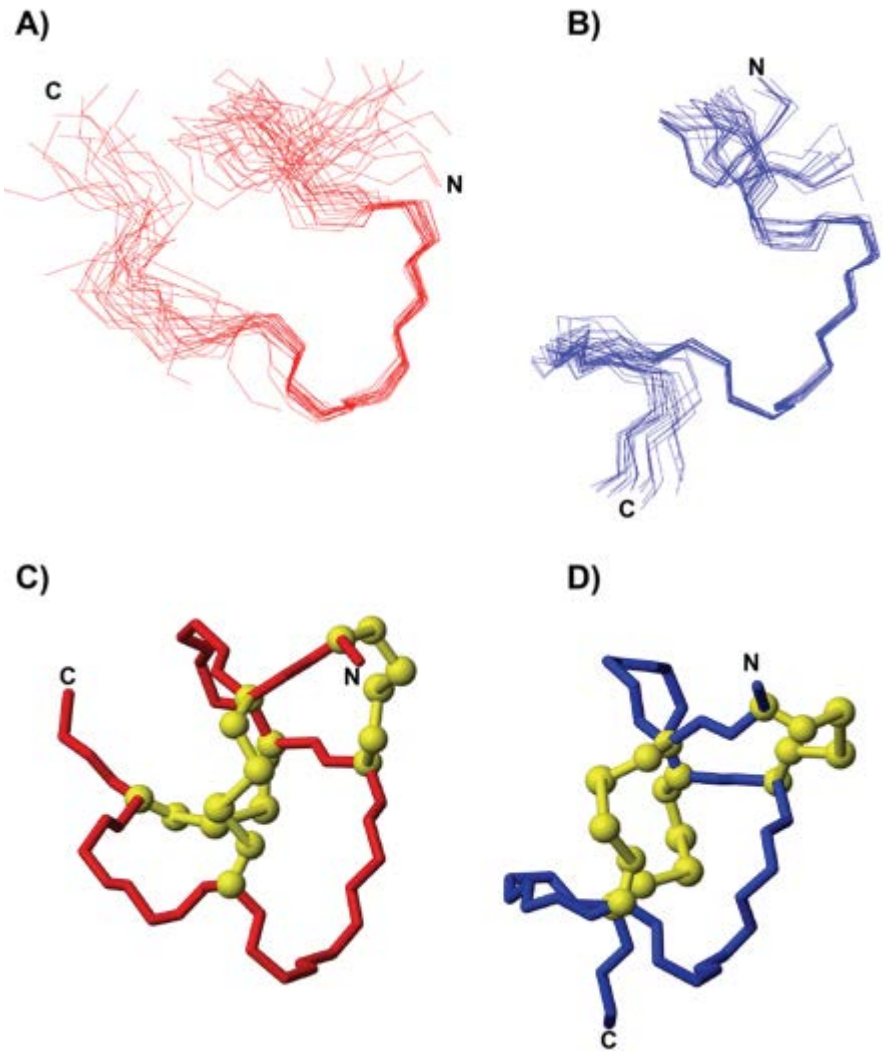

Figure 3.3. Three-dimensional structures of MC12-linaclotide. A superposition of the 20 lowest energy structure of MC12-linaclotide determined in (A) aqueous solution and (B)100 mM SDS. (C) The lowest energy structure of MC12-linaclotide in (C) aqueous solution and (D) 100 mM SDS, with the disulfide bonds shown in ball-and-stick format. The figure was generated using MOLMOL (27)

To determine if a non-aqueous environment stabilizes the structure, spectra were recorded in the presence of 100 mM deuterated SDS. A comparison of the secondary shifts in aqueous solution and in SDS is given in Figure 3.2B. The shifts are similar between the two peptides

indicating that SDS does not significantly influence the overall fold. However, a larger number of NOEs were evident in the NOESY spectra and enabled a more well-defined structure to be calculated as shown in Figure 3.3B.

3.4.3. TNBS mouse colitis model

The effect of MC12-linaclotide in a TNBS induced colitis mouse model was assessed. Mice were either left untreated (naïve), treated with TNBS alone or were treated with peptides at a dose of 3 mg/kg five hours prior to administration of TNBS. On day 3, mice were humanely euthanased using gas asphyxiation and examined for assessment of protection against colitis.

The TNBS treated mice lost weight and did not recover during the experiment, consistent with inflammation and colonic mucosa damage. By contrast, MC12-linaclotide treated mice displayed significant protective effects in the TNBS assay as shown in Figure 3.4A, showing statistically significant effects in reducing weight loss. MC12-linaclotide also showed statistically better macroscopic scores than TNBS only treated mice as shown in Figure 3. 4B. No difference is colon length was observed (results not shown). By contrast, linaclotide did not display protective effects, indicating that the grafting of the MC-12 sequence was responsible for the bioactivity.

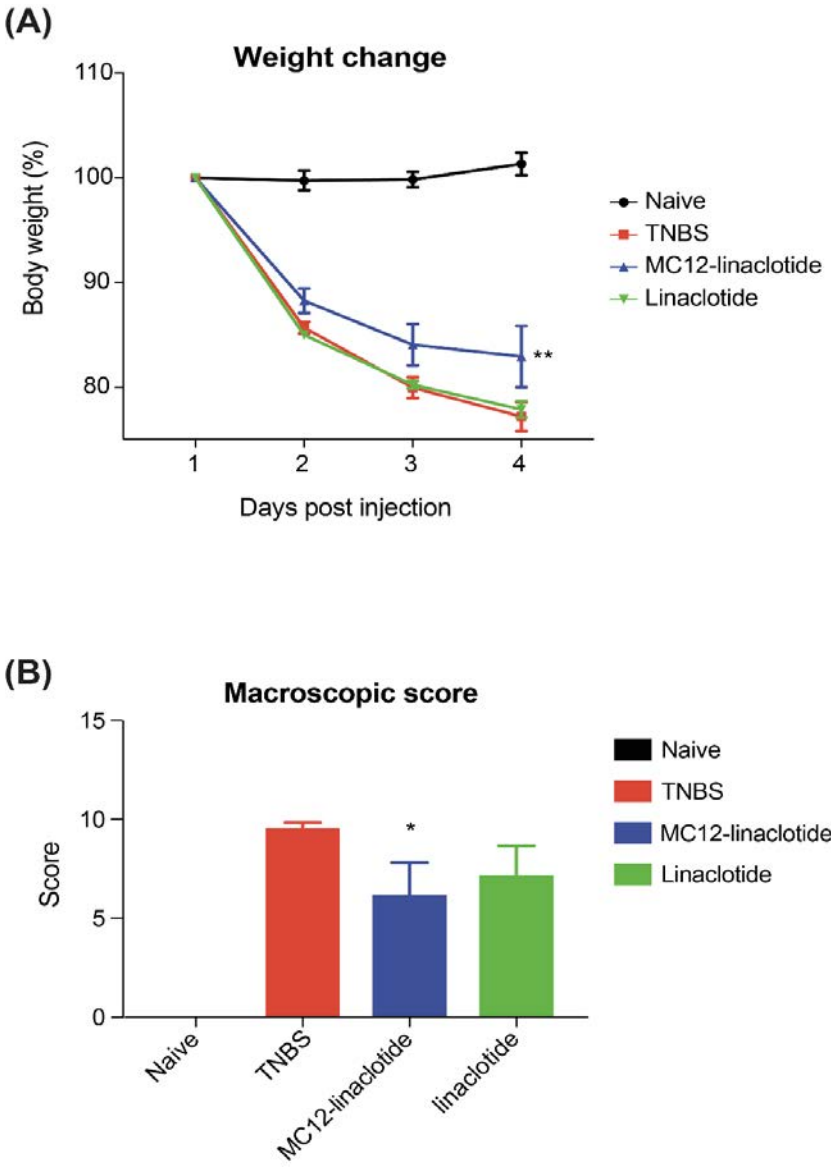

Figure 3.4. Protective effects of MC12-linaclotide against colitic weight loss and macroscopic pathology induced by intra-rectal administration of TNBS. Mice (5 per group) were untreated (naïve) or treated with TNBS following intra-peritoneal administration of peptides (3 mg/kg) or saline vehicle control (TNBS only). A) Percentage weight change (**P= 0.0018); B) Macroscopic pathology score (*P= 0.0238). Data was analysed using GraphPad Prism. Statistical analyses of weights were performed using the 2-way ANOVA, with multiple comparisons of the groups over different days. Macroscopic score was analysed using unpaired Mann-Whitney non-parametric tests. All values are expressed as mean ± SEM. Results were considered significant when $P < 0.05$.

3.4.4. Tissue p-IκB-α (Ser32) and p-NF-κB p65 (Ser536) measurements

Analysis of colon tissue homogenates for phosphorylated transcription factor levels in mice illustrates that linaclotide-treated mice (MC12-linaclotide +TNBS) have levels of phospho-NF-κB p65 (Ser536) and phospho-IκBα (Ser32) that are not statistically different to the TNBS-only treated mice. There appears to be a trend for lower levels of phosphorylated NFκB in mice treated with MC12-linaclotide plus TNBS which might suggest that the peptide is able to reduce the production of pro-inflammatory cytokines but larger sample sizes may be required to reach statistical significance.

3.5. Discussion

Grafting bioactive sequences into peptide scaffolds is proving to be a useful approach for the design of novel drug leads (15,31,32). Here we show for the first time that the highly disuflide-rich peptide, linaclotide, can be used as a scaffold to confer anti-inflammatory activity in a TNBS mouse model of colitis.

The MC-12 tri-peptide has previously been shown to have effects in mouse models of colitis (33), and we have shown that grafting it into the SFTI-1 scaffold improves the potency and stability of the peptide (15). Our current study confirms the importance of the MC-12 tri-peptide sequence (QAW) as linaclotide alone did not alleviate the symptoms of colitis, in contrast to the grafted MC12-linaclotide peptide which had a moderate but statistically significant influence on weight loss and macroscopic score. MC-12 is thought to interact with NF-κB and it is likely that the grafted peptide has the same mechanism of action but this has yet to be explored.

Analysis of the structures of the grafted MC12-linaclotide and linaclotide with NMR spectroscopy has been complicated due to the lack of spectral data in the N-terminal of both peptides. The missing peaks are most likely the result of structural flexibility in this region. Despite the incomplete assignments, the NMR analysis indicates that the synthetic forms of MC12-linaclotide and linaclotide used in the current study have similar overall folds. Comparison of the secondary shifts of linaclotide and MC12-linaclotide with a peptide closely related to linaclotide, a heat stable enterotoxin from the human strain of enterotoxigenic E. coli named ST Ib (6-19) (29), highlights the similarly with the synthetic peptides used in this study. ST Ib (6-19) also has incomplete assignment for residues 1, 2, 5 and 6, suggesting that

apparent flexibility in the N-terminal region is characteristic of this family of peptides. Overall, the NMR analysis indicates that our synthetic peptides have the same cysteine connectivity (Cys1-Cys6, Cys2-Cys10, Cys5-Cys13) as previously reported for linaclotide (34)

The three-dimensional structure of MC12-linaclotide was determined and as expected was disordered at the N-terminus, but displayed a relatively well defined region corresponding to the grafted MC-12 sequence as shown in Figure 3.3A. The disorder at the N-terminus clearly results from the lack of assignments in the region, but this apparent flexibility is intriguing given the high percentage of cysteine residues in this peptide.

Comparison of the secondary shifts of MC12-linaclotide in aqueous solution and 100 mM SDS (Figure 3.2B) highlights the similarity between the two conditions. However, in the presence of SDS the α-protons of residues 2, 5 and 6 could be assigned, in contrast to the spectra recorded in aqueous solution. Peaks corresponding to these residues were not present in the aqueous solution data, and were broad in the SDS spectra. The structures determined in the presence of SDS are more well defined than those in aqueous solution indicating that SDS is having an impact on the dynamics of the peptide. Comparison of the three-dimensional structure of MC12-linaclotide in SDS with the crystal structure of a related peptide, STp(5-17), also highlights the similarity between the grafted peptide and peptides with similar sequences to linaclotide, as shown in Figure 3.5.

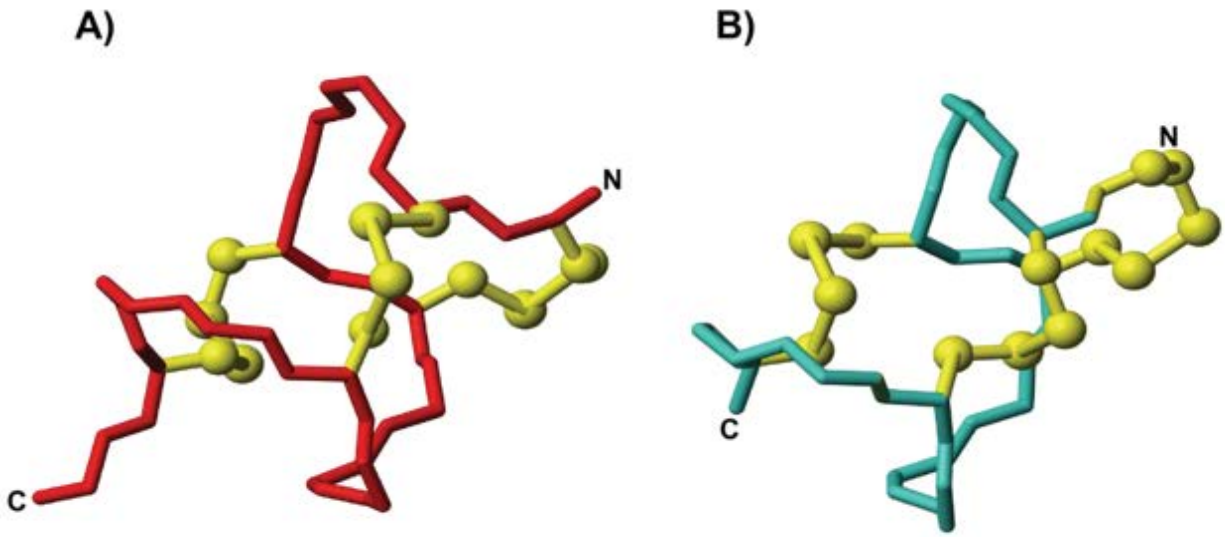

Figure 3.5. Three-dimensional structures of MC12-linaclotide and ST Ib. A) MC12-linaclotide determined in the presence of 100mM SDS and B) crystal structure of STp (5-17), PDB code: 1ETN. The figure was generated using MOLMOL (27)

In summary, we have shown that linaclotide can serve as a scaffold to accommodate a small bioactive sequence and allow appropriate binding to a biological target. In particular, linaclotide is an interesting scaffold for the design of novel lead molecules for inflammatory bowel disease. Overall, this study provides further insight into grafting bioactive sequences into stable peptide scaffolds.

3.6. References

1. Yang, Y. L., Hua, K. F., Chuang, P. H., Wu, S. H., Wu, K. Y., Chang, F. R., and Wu, Y. C. (2008) New cyclic peptides from the seeds of Annona squamosa L. and their anti-inflammatory activities. J. Agric. Food Chem. 56, 386-392

2. Svangard, E., Goransson, U., Hocaoglu, Z., Gullbo, J., Larsson, R., Claeson, P., and Bohlin, L. (2004) Cytotoxic cyclotides from Viola tricolor. J. Nat. Prod. 67, 144-147

3. Gustafson, K. R., McKee, T. C., and Bokesch, H. R. (2004) Anti-HIV cyclotides. Curr. Protein Peptide Sci. 5, 331-340

4. Tam, J. P., Lu, Y. A., Yang, J. L., and Chiu, K. W. (1999) An unusual structural motif of antimicrobial peptides containing end-to-end macrocycle and cystine-knot disulfides. Proc. Natl. Acad. Sci. U. S. A. 96, 8913-8918

5. Pinto, M. F. S., Fensterseifer, I. C. M., Migliolo, L., Sousa, D. A., de Capdville, G., Arboleda-Valencia, J. W., Colgrave, M. L., Craik, D. J., Magalhaes, B. S., Dias, S. C., and Franco, O. L. (2012) Identification and Structural Characterization of Novel Cyclotide with Activity against an Insect Pest of Sugar Cane. J. Biol. Chem. 287, 134-147

6. Adessi, C., and Soto, C. (2002) Converting a peptide into a drug: Strategies to improve stability and bioavailability. Curr. Med. Chem. 9, 963-978

7. Cemazar, M., Kwon, S., Mahatmanto, T., Ravipati, A. S., and Craik, D. J. (2012) Discovery and Applications of Disulfide-Rich Cyclic Peptides. Curr. Top. Med. Chem. 12, 1534-1545

8. Silverman, A. P., Levin, A. M., Lahti, J. L., and Cochran, J. R. (2009) Engineered Cystine-Knot Peptides that Bind alpha(v)beta(3) Integrin with Antibody-Like Affinities. J. Mol. Biol. 385, 1064-1075

9. Chan, L. Y., Gunasekera, S., Henriques, S. T., Worth, N. F., Le, S. J., Clark, R. J., Campbell, J. H., Craik, D. J., and Daly, N. L. (2011) Engineering pro-angiogenic peptides using stable, disulfide-rich cyclic scaffolds. Blood 118, 6709-6717

10. Miljanich, G. P. (2004) Ziconotide: Neuronal calcium channel blocker for treating severe chronic pain. Curr. Med. Chem. 11, 3029-3040

11. Basus, V. J., Nadasdi, L., Ramachandran, J., and Miljanich, G. P. (1995) Solution structure of ω-conotoxin MVIIA using 2D NMR spectroscopy. FEBS Lett. 370, 163-169

12. Ito, C., Ribeiro, R. C., Behm, F. G., Raimondi, S. C., Pui, C. H., and Campana, D. (1996) Cyclosporine a induces apoptosis in childhood acute lymphoblastic leukemia cells. Blood 88, 261-261

13. Rao, S. S. C., Quigley, E. M. M., Shiff, S. J., Lavins, B. J., Kurtz, C. B., MacDougall, J. E., Currie, M. G., and Johnston, J. M. (2014) Effect of Linaclotide on Severe Abdominal Symptoms in Patients With Irritable Bowel Syndrome With Constipation. Clin. Gastroenterol. Hepatol. 12, 616-623

14. Chey, W. D., Lembo, A. J., Lavins, B. J., Shiff, S. J., Kurtz, C. B., Currie, M. G., MacDougall, J. E., Jia, X. D., Shao, J. Z., Fitch, D. A., Baird, M. J., Schneier, H. A., and Johnston, J. M. (2012) Linaclotide for Irritable Bowel Syndrome With Constipation: A 26-Week, Randomized, Double-blind, Placebo-Controlled Trial to Evaluate Efficacy and Safety. Am. J. Gastroenterol. 107, 1702

15. Cobos Caceres, C., Bansal, P. S., Navarro, S., Wilson, D., Don, L., Giacomin, P., Loukas, A., and Daly, N. L. (2017) An engineered cyclic peptide alleviates symptoms of inflammation in a murine model of inflammatory bowel disease. J. Biol. Chem. 292, 10288-10294

16. Luckett, S., Garcia, R. S., Barker, J. J., Konarev, A. V., Shewry, P. R., Clarke, A. R., and Brady, R. L. (1999) High-resolution structure of a potent, cyclic proteinase inhibitor from sunflower seeds. J. Mol. Biol. 290, 525-533

17. Daly, N. L., Chen, Y. K., Foley, F. M., Bansal, P. S., Bharathi, R., Clark, R. J., Sommerhoff, C. P., and Craik, D. J. (2006) The absolute structural requirement for a proline in the P3 '-position of Bowman-Birk protease inhibitors is surmounted in the minimized SFTI-1 scaffold. J. Biol. Chem. 281, 23668-23675

18. Lesner, A., Legowska, A., Wysocka, M., and Rolka, K. (2011) Sunflower Trypsin Inhibitor 1 as a Molecular Scaffold for Drug Discovery. Curr. Pharm. Des. 17, 4308-4317

19. Ament, M. E. (1975) Inflammatory disease of colon - ulcerative-colitis and crohns colitis. J. Pediatr. 86, 322-334

20. Navarro, S., Ferreira, I., and Loukas, A. (2013) The hookworm pharmacopoeia for inflammatory diseases. Int. J. Parasitol. 43, 225-231

21. Molnar, T., Farkas, K., Szepes, Z., Nagy, F., Szucs, M., Nyari, T., Balint, A., and Wittmann, T. (2014) Long-term outcome of cyclosporin rescue therapy in acute, steroid-refractory severe ulcerative colitis. United European Gastroenterol J. 2, 108-112

22. Wangchuk, P., Navarro, S., Shepherd, C., Keller, P. A., Pyne, S. G., and Loukas, A. (2015) Diterpenoid alkaloids of Aconitum laciniatum and mitigation of inflammation by 14-O-acetylneoline in a murine model of ulcerative colitis. Sci. Rep. 5, 10

23. Leoni, G., Neumann, P. A., Kamaly, N., Quiros, M., Nishio, H., Jones, H. R., Sumagin, R., Hilgarth, R. S., Alam, A., Fredman, G., Argyris, I., Rijcken, E., Kusters, D., Reutelingsperger, C., Perretti, M., Parkos, C. A., Farokhzad, O. C., Neish, A. S., and Nusrat, A. (2015) Annexin A1-containing extracellular vesicles and polymeric nanoparticles promote epithelial wound repair. J. Clin. Invest. 125, 1215-1227

24. Wuthrich, K. (2003) NMR studies of structure and function of biological macromolecules (Nobel Lecture). J. Biomol. NMR 27, 13-39

25. Yap, K. L. (2001) Empirical analysis of backbone chemical shifts in proteins.

26. Ikeya, T., Terauchi, T., Guntert, P., and Kainosho, M. (2006) Evaluation of stereo-array isotope labeling (SAIL) patterns for automated structural analysis of proteins with CYANA. Magn. Reson. Chem. 44, S152-S157

27. Koradi, R., Billeter, M., and Wuthrich, K. (1996) MOLMOL: A program for display and analysis of macromolecular structures. J. Mol. Graph. 14, 51-55

28. Ferreira, I., Smyth, D., Gaze, S., Aziz, A., Giacomin, P., Ruyssers, N., Artis, D., Laha, T., Navarro, S., Loukas, A., and McSorley, H. J. (2013) Hookworm excretory/secretory products induce interleukin-4 (IL-4)(+) IL-10(+) CD4(+) T cell responses and suppress pathology in a mouse model of colitis. Infect. Immun. 81, 2104-2111

29. Gariepy, J., Lane, A., Frayman, F., Wilbur, D., Robien, W., Schoolnik, G. K., and Jardetzky, O. (1986) Structure of the toxic domain of Escherichia coli heat-stable enterotoxin ST I. Biochemistry 25, 7854-7866

30. Shen, Y., Delaglio, F., Cornilescu, G., and Bax, A. (2009) TALOS plus : a hybrid method for predicting protein backbone torsion angles from NMR chemical shifts. J. Biomol. NMR 44, 213-223

31. Gunasekera, S., Foley, F. M., Clark, R. J., Sando, L., Fabri, L. J., Craik, D. J., and Daly, N. L. (2008) Engineering Stabilized Vascular Endothelial Growth Factor-A Antagonists: Synthesis, Structural Characterization, and Bioactivity of Grafted Analogues of Cyclotides. J. Med. Chem. 51, 7697-7704

32. Wang, C. K., Gruber, C. W., Cemazar, M., Siatskas, C., Tagore, P., Payne, N., Sun, G. Z., Wang, S. H., Bernard, C. C., and Craik, D. J. (2014) Molecular Grafting onto a Stable Framework Yields Novel Cyclic Peptides for the Treatment of Multiple Sclerosis. ACS Chem. Biol. 9, 156-163

33. Ouyang, N. T., Zhu, C. H., Zhou, D. Y., Nie, T., Go, M. F., Richards, R. J., and Rigas, B. (2012) MC-12, an annexin A1-based peptide, is effective in the treatment of experimental colitis. PLoS One 7, 11

34. Gariepy, J., Lane, A., Frayman, F., Wilbur, D., Robien, W., Schoolnik, G. K., and Jardetzky, O. (1986) Structure of the toxic domain of the escherichia-coli heat-stable enterotoxin ST-I. Biochemistry 25, 7854-7866

4. CHAPTER 4

Peptides derived from hookworm anti-inflammatory proteins suppress inducible colitis in mice and inflammatory cytokine production by human cells

Claudia Cobos Caceres, Paramjit S. Bansal, David Wilson, Linda Jones, Matthew A. Field, Ramon M. Eichenberger, Rachael Y. M. Ryan, Champa N. Ratnatunga, John J. Miles, Paul Giacomin, Severine Navarro, Alex Loukas, Norelle L. Daly

4.1. Abstract

A decline in the prevalence of parasites such as hookworms appears to be correlated with the rise in autoimmune conditions in developed countries. This correlation has led to studies that have identified hookworm proteins with activity in inflammatory bowel disease (IBD) and asthma. Hookworms secrete a family of netrin-domain containing proteins referred to as AIPs (Anti-Inflammatory Proteins), but there is no information on the structure-function relationships. Here we have applied a downsizing approach to the hookworm AIPs to derive peptides of 20 residues or less, some of which display significant anti-inflammatory effects when co-cultured with human peripheral blood mononuclear cells and/or in a TNBS mouse model of colitis. Our results indicate that a conserved helical region is responsible, at least in part, for the anti-inflammatory effects. This helical region has potential in the design of new leads for treating IBD and possibly other inflammatory conditions.

4.2. Introduction

A decline in the prevalence of parasites such as hookworms appears to be correlated with the rise in autoimmune conditions in developed countries (1-3). This correlation has led to studies of parasite excreted proteins in autoimmune conditions such as inflammatory bowel disease (IBD) and asthma. IBDs affect the gastrointestinal track and can be sub-classified into two main conditions: ulcerative colitis (UC) and Crohn's disease (CD) (4). The causes of IBD are still unknown, but a combination of immune responses and environmental factors appear to be involved (5). Asthma primarily affects the respiratory tract and its incidence is rising in industrialized and developing countries, generating a burden on their health services (6). Current treatments for both IBD and asthma have significant limitations (7,8) and consequently new drug leads are required.

The excretory/secretory (ES) products in hookworms are a diverse source of compounds with potential in the treatment of both IBD and asthma (9,10). The ES products comprise a complex mixture of proteins, carbohydrates, small molecules and lipids secreted by the parasite (11). Proteomic profiling of ES products of the dog hookworm, *Ancylostoma caninum*, indicated the presence of 250 different proteins (11,12). Several of these proteins have sequence homology to a family of mammalian proteins known as tissue inhibitors of matrix-metalloproteinases (TIMPs), including *Ac*-TMP-1 and *Ac*-TMP-2 (13). Despite sequence and predicted structural similarity to TIMPs, these hookworm proteins do not seem to possess MMP inhibitory activity, and their netrin domains likely perform unrelated functions (13). *Ac*-TMP-1 and *Ac*-TMP-2 have subsequently been referred to as *Ac*-AIP-1 and *Ac*-AIP-2, and have been tested in mouse models of colitis (14) and asthma (15) respectively. Recombinant forms of both proteins significantly alleviate the disease symptoms in these models, reduce immunopathology and

suppress expression of inflammatory cytokines. However, the biological targets of these proteins are not known, and there is no information available on the structure-function relationships.

Analysis of three-dimensional protein structures can provide clues to regions important in activity, and insight into the process of "downsizing" proteins (16,17). This process can be valuable for the design of peptide-based drug leads that have lower immunogenicity, greater tissue penetration, and are cheaper to manufacture than larger proteins (18,19). Here we have applied the downsizing approach to selected hookworm TIMP-like proteins from three different species with a focus on developing peptides with potential in treating colitis.

The three proteins chosen for this study are *Ace*ES-2 from *Ancylostoma ceylanicum*, *Ac*-AIP-2 from *A. caninum*, and NECAME 07191 from *Necator americanus* (this protein will be subsequently referred to as *Na*-AIP-1 for consistency). We have used the crystal structure of *Ace*ES-2 (20) and modelled structures of *Ac*-AIP-2 and *Na*-AIP-1, as there are no experimental structures available, as the basis for our peptide design studies. We were primarily interested in the analysis of discrete elements of secondary structure, and have shown a small helical region, conserved amongst these hookworm proteins, can alleviate symptoms in a chemically-induced mouse model of colitis and supress cytokine secretion by human peripheral blood mononuclear cells *in vitro*.

4.3. Experimental Procedures

4.3.1. Peptide synthesis and purification

Peptides were synthesised using solid phase peptide synthesis (SPPS) on a Protein Technologies PS3 synthesiser using fluorenylmethyloxycarbonyl (Fmoc) chemistry on a 0.1 mmole scale. The resin used for the peptides was 2-chlorotrityl chloride resin on a 0.1 mmole scale. Amino acids (2 equiv.) were activated in 5 equiv HBTU and 10 equiv. DIPEA in DMF (1.5 mL). Deprotection was carry out in two repetitions: Starting with 2 min of 20% pipiridine in DMF (5ml), followed by 3 mins of the same solution. The C-terminal amino acid was coupled manually to the resin, and the rest of the sequence was assembled using a Protein Technologies PS3 synthesiser. Following complete assembly of the peptides, all peptides were cleaved from the resin using a mixture of trifluoroacetic acid (TFA)/water/triisopropylsilane (95:2.5:2.5) for 2-3 h, and then each peptide was precipitated with diethylether. After precipitation they were dissolved in 50% acetonitrile/0.05% TFA and finally lyophilised. Purification was performed with RP-HPLC on a C_{18} preparative column (Phenomenex Jupiter 250 x 21.2 mm, 10 µm, 300 Å) using a 1% gradient of solvent B (solvent A: 0.05% TFA; solvent B: 90% acetonitrile, 0.05% TFA). Masses were analysed using MALDI-TOF mass spectrometry.

4.3.2. NMR spectroscopy and structural analysis

Lyophilized and purified peptides were resuspended to a final concentration of ~0.2 mM in 90%H_2O:10%D_2O. 2D ^{1}H-^{1}H TOCSY, ^{1}H-^{1}H NOESY, ^{1}H-^{1}H DQF-COSY, ^{1}H-^{15}N HSQC, and ^{1}H-^{13}C HSQC spectra were acquired at 290 K using a 600 MHz AVANCE III NMR

spectrometer (Bruker, Karlsruhe, Germany). NOESY spectra were acquired with mixing times of 200-300 ms, and TOCSY spectra were acquired with isotropic mixing periods of 80 ms. Standard Bruker pulse sequences were used with an excitation sculpting scheme for solvent suppression. Spectra were referenced to internal 4,4-dimethyl-4-silapentane-1-sulfonic acid (DSS).

The assignments were made using established protocols (21) and the secondary shifts derived by subtracting the random coil αH shift from the experimental αH shifts (22). The 2D NOESY spectra of AIP2-20 were automatically assigned and an ensemble of structures calculated using the program CYANA (23). Torsion-angle restraints from TALOS+ (24) were used in the structure calculations. The final structures were visualized using MOLMOL (25).

4.3.3. TNBS colitis

Experiments were conducted in accordance with the James Cook University Animal Ethics Committee approved guidelines under the project #A2012. All experiments were performed with C57BL/6 strain mice in groups of five males (5 weeks old). Mice were purchased from the Animal Resources Centre (Perth, Australia) and housed in the animal care facility unit at James Cook University under specific pathogen free conditions. After arriving at our facility, mice were placed inside plastic cages with unlimited access to food and water.

Mice were divided randomly into different groups: Naïve, 2,4,6-trinitrobenzenesulfonic acid (TNBS), AIP peptides and SFTI-1. Mice received intraperitoneal (i.p.) injections of peptides and protein at a dose of 1.0 mg/kg 5 hours prior to administration of TNBS. Ketamine/xylazine solution was used to anaesthetise the mice prior to administration of TNBS. Mice received 100

μL of 5% (w/v) TNBS solution in 60% ethanol by intra-colonic instillation using a 20 gauge soft catheter (Terumo), which was inserted into the colon. Mice were monitored daily for piloerection, survival, stool consistency, body weight, rectal bleeding and decreased motor activity. The effective induction of TNBS-induced colitis was confirmed by weight loss during the course of the experiment; this occurs due to inflammation and colonic mucosa damage. On day 3 of the experiment, the mice were euthanased using gas asphyxiation and examined for assessment of protection against colitis. A score of macroscopic pathology was calculated for each colon. This macroscopic pathology was made by harvesting the colon and opening it longitudinally, then washing the colon with sterile phosphate buffer saline. The colon was then visualised using a stereomicroscope (Olympus SZ61, 0.67-4.5x). Tissues were assessed and scored for pathological changes as follows: presence of adhesions (0 to 3), bowel wall thickening (0 to 3), mucosal oedema (0 to 3), ulceration (0 to 3), and colon length as described previously.(10) All animal experiments were conducted in duplicate to ensure reproducibility of the findings. Graphs and statistical analysis were produced using GraphPad Prism version 7.02 (GraphPad Software Inc).

4.3.4. Histological evaluation of colitis

Tissue for histological analysis was fixed in formalin and then transferred to a solution of 70% alcohol. The tissue was embedded in paraffin and sectioned longitudinally for histology at 4 μm thickness. Periodic acid-Schiff (PAS) stain was used to assess goblet cell destruction. Scoring of the images was determined in a blinded fashion following the scoring method of Hong et al. (26) High resolution images were scored as follows: Ulceration: no ulcers = 0; 1 ulcer = 1; 2 ulcers = 2; 3 ulcers = 3; and >3 ulcers = 4. Infiltration: 0 = no infiltrate, 1 = infiltrate at crypt bases, 2 = infiltrate reaching to muscularis mucosa, 3 = extensive infiltration reaching

the muscularis, and 4 = infiltration of the submucosa with oedema. Epithelium was scored: 0 = normal morphology, 1 = loss of goblet cells in one area, 2 = loss of goblet cells in more than one area, 3 = loss of crypts in one area, and 4 = loss of crypts in more than one area. Lymphoid follicles: none = 0, 1 = 1, 2 = 2, 3 = 3, > 3 = 4

4.3.5. Bioactivity on human immune cells

The human blood used for this project was donated by healthy volunteers. Written informed consent was obtained from each donor at the time of blood draw. Ethical approval for this research was obtained from the James Cook University Human Ethics Committee (Australia). PBMCs were isolated from whole blood by density gradient centrifugation using Ficoll-Paque media. For induction of T cell cytokines, PBMCs were activated with a cell stimulation cocktail of 50 ng/ml of phorbol 12-myristate 13-acetate (PMA) and 1 µg/ml of ionomycin (eBioscience). PMA + ionomycin-stimulated cells were treated with 0.1-100 µg/ml of hookworm AIP peptide or remained untreated. For stimulation of myeloid-associated cytokines, PBMCs were activated with 10 ng/ml lipopolysaccharide (LPS) (Sigma-Aldrich). LPS-stimulated PBMCs were treated with 0.1-100 µg/ml of AIP peptide or remained untreated. The cell culture plates were incubated overnight at 37°C and 6.5% CO_2. After incubation, the samples were centrifuged at 1,500 x *g* for 5 minutes and the culture supernatants were collected for cytokine analysis. Toxicity assays were performed with the LIVE/DEAD Cell Viability Assay (Thermo Fisher Scientific) and readout using flow cytometry. This dye binds to amines in cells with compromised cell membranes but cannot enter healthy cells.

4.3.6. BD™ cytometric bead array

Interleukin (IL)-1β, IL-2, IL-6, IL-8, IFN-γ and tumour necrosis factor (TNF)-α from PBMC culture supernatant were quantified using **BD**™ Cytometric Bead Array (CBA) (BD Biosciences). The CBA assays were performed according to the manufacturer's instruction using a five laser Special Order LSRFortessa™ with HTS (BD Biosciences). Cytokine concentrations (pg/ml) were calculated based on the sample MFI compared to the cytokine standard curves. **BD**™ FCAP Array software version 3.0 was used for data analysis. Graphs and statistical analysis were produced using GraphPad Prism version 7.02 (GraphPad Software Inc).

4.3.7. Serum stability assay

The serum stability of the peptides was tested using human male AB plasma (Sigma-Aldrich) following methods previously described.(27) The peptides were tested at a concentration of 200 μM, incubated in serum or PBS at 37°C and 40 μL aliquots were taken at 0 h, 3 h and 8 h. The aliquots of serum were quenched with 40 μL of 20% TFA and incubated for 10 minutes at 4°C to precipitate serum proteins. PBS received the same treatment as serum. The samples were then centrifuged at 17000 *g* for 10 min and 90 μL of supernatant analysed by RP-HPLC at a flow rate of 0.3 mL/min using a Phenomenex Jupiter Proteo C_{12} analytical column (150 x 2.00 mm, 4 μm, 90 Å) using a linear 1% min^{-1} acetonitrile gradient (0-50% solvent B). The eluent was observed using a dual wavelength UV detector set to 214 and 280 nm

.

4.4. Results

4.4.1. Molecular models

The structures of *Ac*-AIP-2 and *Na*-AIP-1, were modelled using I-TASSER protein structure and function prediction software, which involves: threading template identification, iterative structure assembly simulation, model selection and refinement, and structure-based function annotation (28). The templates with the highest scores for the model of *Ac*-AIP-2 and *Na*-AIP-1 were the human TIMP-2 protein (PDB code 1BR9.pdb) (29) and the TIMP-3 protein (PDB code 3CKI.pdb)(30), highlighting the similarities between these TIMP proteins.

The crystal structure of *Ace*ES-2 (20) along with the modelled structures of *Ac*-AIP-2 and *Na*-AIP-1 with the highest C-score (-2.57 and -0.51 respectively) are shown in Figure 4.1. All of the proteins contain several β-sheets at the core of the protein, and a conserved helical region is present at the C-termini of *Na*-AIP-1 and *Ace*ES-2. *Ac*-AIP-2 contains a similar helical region but has an extended C-terminal region compared to the other two proteins. The conservation of this helical region indicated it might be functionally important as helices are often involved in protein-protein interactions. Analysis of protein complexes submitted to the PDB showed that 62% contain a helix at the interface (31).

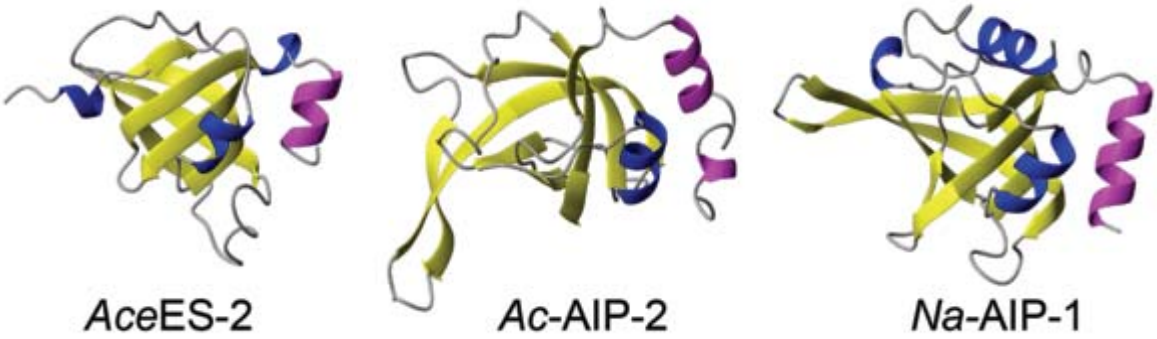

Figure 4.1. Structures of hookworm proteins. A) Crystal structure of *Ace*ES-2 (PDB code 3NSW); B) The modelled structure of *Ac*-AIP-2; C) The modelled structure of *Na*-AIP-1. The conserved C-terminal helical region is shown in magenta. The extended C-terminal tail in *Ac*-AIP-2 has been removed for clarity. The figure was made using MOLMOL (25).

4.4.2. Synthesis and characterisation of peptides

Peptides corresponding to the conserved C-terminal helical region were designed and the sequences are shown in Table 1. The peptides are named based on the residue numbers corresponding to the N- and C-termini. A mutant form of AIP2-20 - AIP2-20D6P, where Asp6 was replaced with a proline residue - was included in the suite of peptides synthesised. The rationale for this peptide was based on the structural data obtained for AIP2-20 (see below). The peptides were synthesised using Fmoc chemistry on a 0.1 mmole scale, purified using RP-HPLC and the mass analysed using MALDI mass spectrometry.

Table 4.1. Sequences of synthetic peptides

Protein	Residue numbers	Peptide name	Sequence*
Ac-AIP-2	(115-134)	AIP2-20	TPEEHDLLMDLMGDPKKAEE
Ac-AIP-2	(115-134)	AIP2-20D6P	TPEEHPLLMDLMGDPKKAEE
Na-AIP-1	(125-137)	AIP1-13	PSKEKADLGKYKA
AceES-2	(93-102)	ES-10	SQKEKDLLKE

* The EXXXL motif is highly conserved amongst the proteins.

The structures of the peptides were analysed in aqueous solution using NMR spectroscopy. The peptides displayed sharp peaks in solution indicating they were in a monomeric state. Two-dimensional TOCSY and NOESY spectra allowed assignment of the resonances, and the secondary chemical shifts (secondary shifts) were determined by subtracting random coil chemical shifts (22) from the αH chemical shifts. A comparison of the secondary shifts is given in Figure 4.2. Chemical shift analysis often provides an indication of the type of secondary structure present in peptides, with consecutive shifts more negative than -0.1 indicating the presence of helical structure (32). AIP2-20 displayed consecutive negative chemical shifts in the N-terminal region of the peptide, and AIP1-13 and ES-10 have consecutive negative secondary shifts for a large proportion of the molecules, albeit with some of the shifts being relatively close to random coil values. The negative shifts present in AIP2-20 are disrupted in AIP2-20D6P at residues 5 and 6. Overall, this analysis indicates a modest propensity for helical structure in the isolated peptides with the exception of AIP2-20D6P where the disruption of negative shifts indicates that the helical region would also be disrupted.

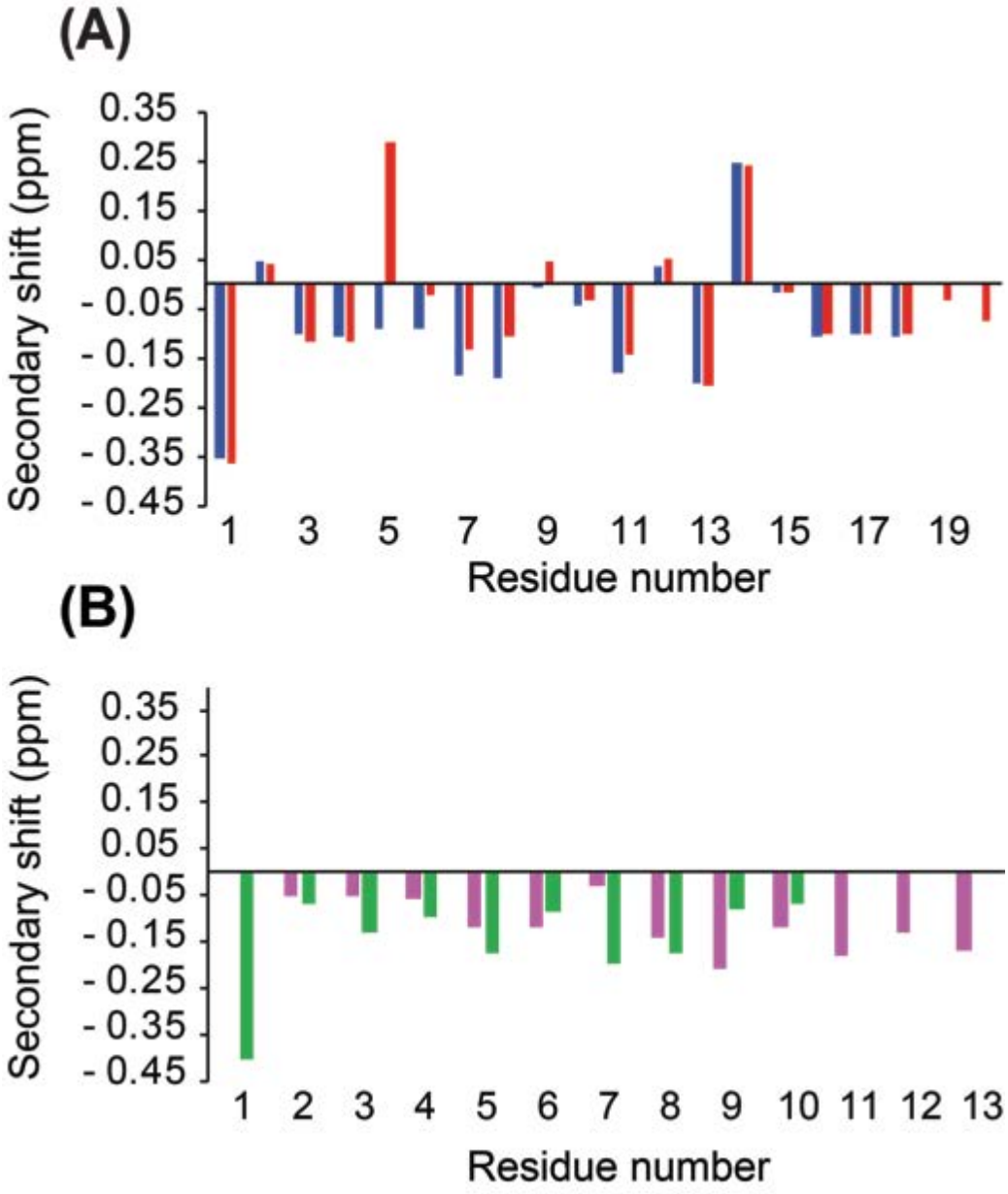

Figure 4.2. Secondary shift analysis of the peptides. The secondary shifts of AIP2-20, AIP1-13 ES-10 and AIP2-20D6P were calculated by subtracting the random coil shifts (22) from the αH shift

To determine if helical structure is actually present in the peptides, analysis of the NOESY spectra, dihedral angle prediction using TALOS+ (24), and determination of the slowly exchanging amide protons was carried out. Analysis of the NOESY spectra of AIP2-20

indicated the presence of several medium range NOEs indicative of helical turns and several slowly exchanging amide protons were identified in D_2O exchange experiments. The three-dimensional structures of AIP2-20 were calculated using CYANA, initially based on the NOESY data and dihedral angle restraints predicted using TALOS+. Based on the preliminary structures and slowly exchanging amide protons (Leu8, Gly9, Tyr11, Lys12, Ala13), hydrogen bond restraints were included. The final ensemble of AIP2-20 structures is shown in Figure 4.3. The N-terminal region displays a well-defined α-helical region (Figure 4.3A), in contrast to the C-terminal region, which does overlay to some extent but does not possess regular secondary structure (Figure 4.3B).

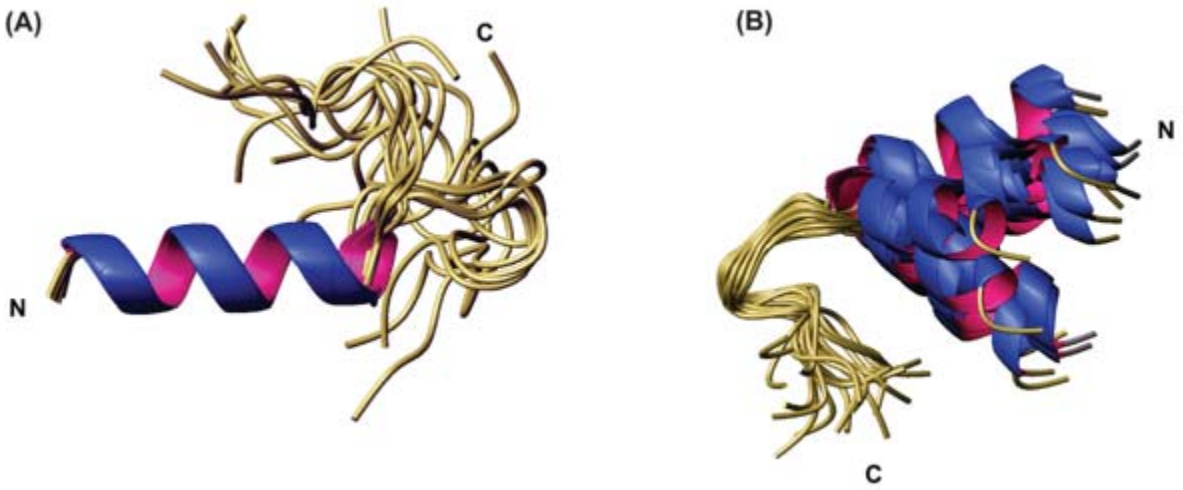

Figure 4.3. Three-dimensional structure of AIP2-20. The 20 lowest energy structures of *Ac*-AIP-2 determined based on NMR spectroscopy data. (A) Superposition of structures over the backbone atoms of residues 2-11 (RMSD 0.126 Å). (B) Superposition of structures of the backbone atoms of residues 11-18 (RMSD 1.003 Å). The figure was made using MOLMOL(25).

Proline residues generally have a low propensity for helix formation and can result in disruption of helical secondary structure. A proline residue was introduced into the helical region of AIP2-20 to determine if this change disrupted the structure and influenced the activity. The NOESY spectra of AIP2-20D6P showed limited medium or long range NOEs and the TALOS+ analysis did not provide any definitive prediction for the dihedral angles, but slowly exchanging amide protons were evident in the D_2O exchange experiments. The presence of slowly exchanging amide protons is generally indicative of hydrogen bonds suggesting that the peptide is structured in solution. However, the structure calculations for AIP2-20D6P resulted in flexible structures with no defined secondary structure. This lack of structure is a direct result of limited experimental restraints to define the structure but indicates that the D6P mutation disrupts the structure.

Analysis of the NMR data for the peptides AIP1-13 and ES-10 demonstrated that both peptides had limited medium or long range NOEs, TALOS+ analysis did not provide any definitive prediction of the dihedral angles, and both peptides displayed slowly exchanging amide protons in the D_2O exchange experiments. AIP1-13 showed slowly exchanging amide protons for five residues for 30 minutes following resuspension in D_2O. All amide protons exchanged within 60 minutes. ES-10 showed the amide protons of eight residues still present after 30 minutes. The conserved Leu 8 residue was particularly slowly exchanging compared to the other residues, and was still evident in spectra recorded 2.5 hours after dissolution of the peptide in D_2O. The lack of NOEs and dihedral angle restraints prevented the determination of the structures of AIP1-13 and ES-10 and suggests that the peptides are not well structured in solution. However, similar to AIP2-20D6P, the presence of slowly exchanging amide protons suggests the peptides have a propensity for forming hydrogen bonds.

4.4.3. TNBS-induced weight loss, macroscopic pathology and colon shortening

AIP2-20, AIP1-13 and ES-10 displayed significant protective effects against TNBS-induced intestinal inflammation as shown in Figure 4. AIP2-20 ($P<0.001$), AIP1-13 ($P<0.01$) and ES-10 ($P<0.01$) protected against TNBS-induced weight loss (Figure 4A) compared to the control peptide SFTI-1 which, consistent with previous studies, showed no protective effect (33). Treatment of mice with both ES-10 and AIP2-20 resulted in significant protection ($P<0.05$) against TNBS-induced colon shortening (Figure 4B) compared to TNBS mice, whereas SFTI-1 was not statistically different to the TNBS-only treated mice. The clinical scores for mice treated with all three peptides were significantly lower than the TNBS-only treated mice (Figure 4C). An additional peptide corresponding to residues 34-51 in *Ac*-AIP-2 was synthesised with terminal cysteine residues, which were oxidised to form a disulfide bond. This peptide was tested in the TNBS model and did not display protective effects (results not shown), indicating that not all regions of the AIP proteins display activity in the colitis model.

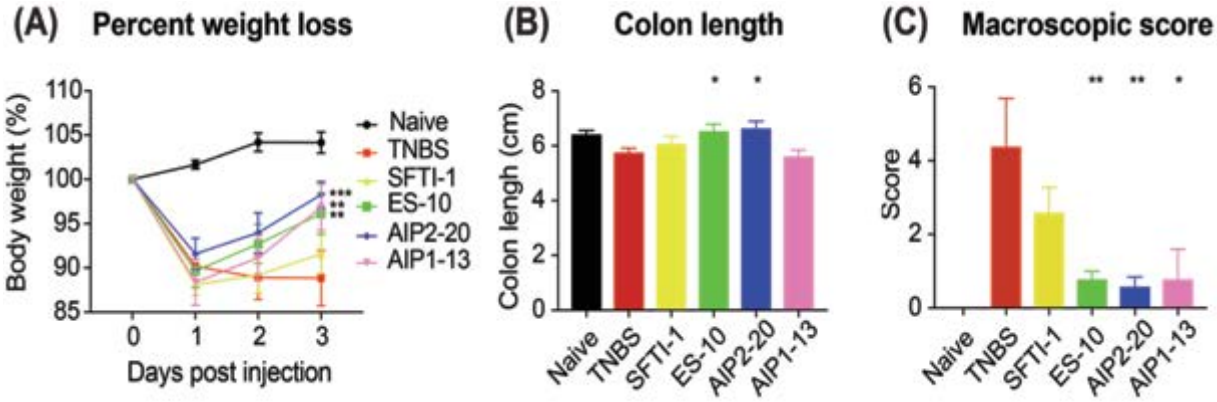

Figure 4.4. Protective effects of the peptides against weight loss and clinical symptoms induced by TNBS colitis. Mice were untreated (naïve) or treated with TNBS following administration of peptides, or saline vehicle control (TNBS). A) Body weight percentage change; B) Colon length; C) Macroscopic Score (the details of how the macroscopic score was evaluated are given in the Materials and Methods); (*P <0.05; ** P < 0.01; *** P < 0.001).

Treatment of mice with AIP2-20D6P did not confer protection against any of the parameters measured of TNBS-induced colitis (as shown in Figure 4.5 for weight loss), indicating that Asp6 is important for bioactivity. Alternatively, the structural changes observed as a consequence of this mutation could result in the changes observed for the bioactivity.

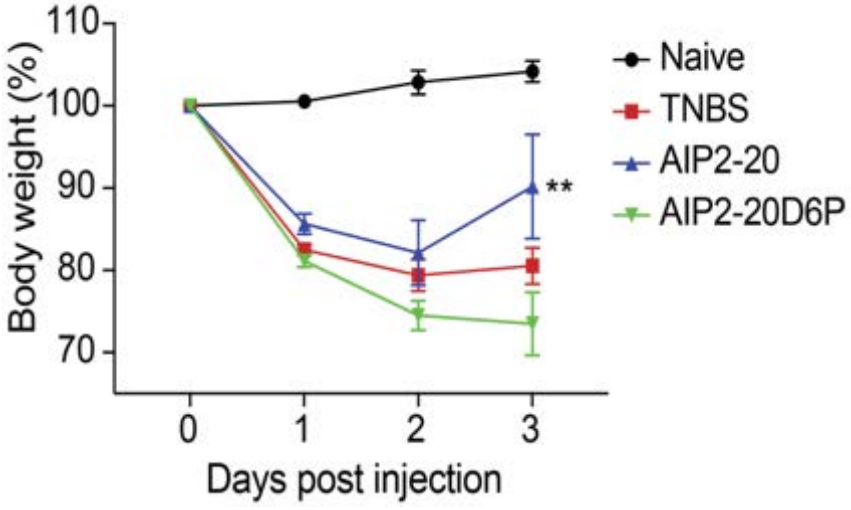

Figure 4.5. Percent change in body weight following treatment with AIP2-20 and AIP2-20D6P in a TNBS colitis model. Mice were untreated (naïve) or treated with TNBS following i.p. administration of peptides (1 mg/kg), or saline vehicle control (TNBS). AIP2-20D6P did not protect against the symptoms of colitis in contrast to AIP2-20. ** $P < 0.01$.

4.4.4. Histological evaluation of colitis

Inflammatory cell infiltration into the lamina propria was visible in the Periodic acid–Schiff (PAS) stain of the colon tissue from the TNBS-only mice (Figure 4.6A). Colons from mice that received TNBS only displayed lesions and histological damage characterised by epithelial hyperplasia, goblet cell loss, thickening of the lamina propria and colon walls with extensive ulcerations. By contrast, the mice treated with AIP peptides showed decreased histological signs of colitis (Figure 4.6A) with retained epithelial integrity, minimal focal inflammatory cell

infiltrates in the mucosa, larger numbers of goblet cells (Figure 4.6C) and no ulceration. Histological scoring showed that mice treated with AIP2-20, AIP1-13 and ES-10 had significantly less ($P<0.05$) histopathology compared with TNBS-only treated mice (Figure 4.6B). The control peptide, SFTI-1, was not statistically different to the TNBS-only treated mice.

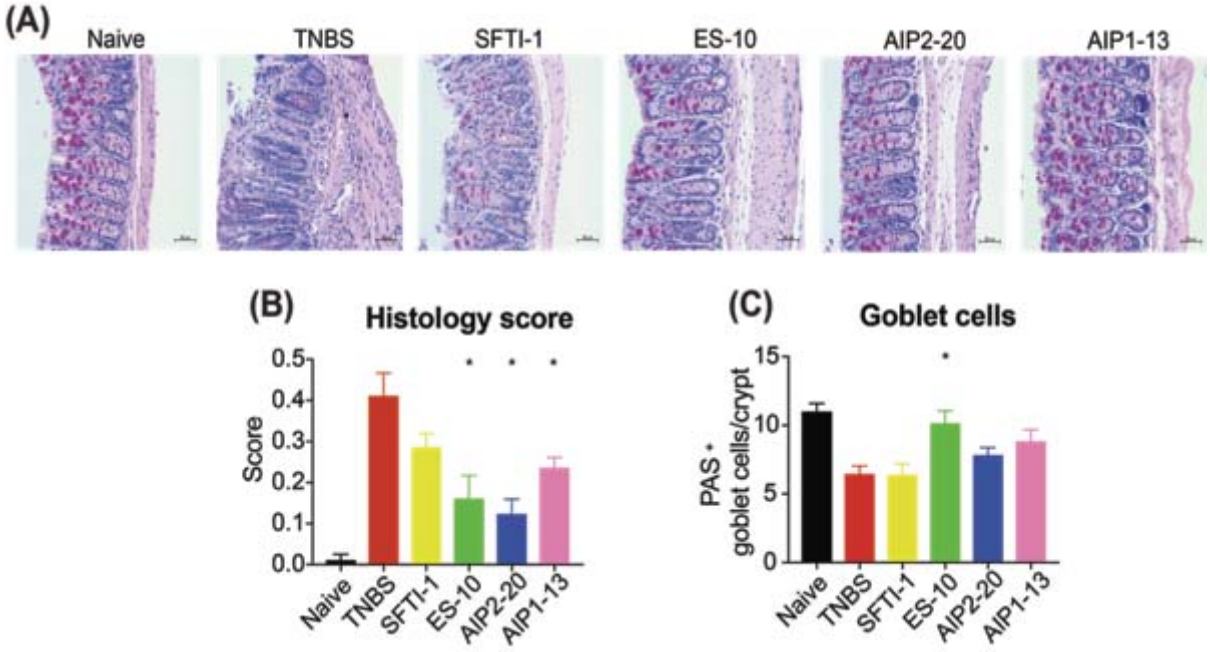

Figure 4.6. Histological evaluation of colitis. A) Representative micrograph of periodic acid schiff-stained colonic tissue sections; B) Histology scoring; C) Goblet cell scoring. Treatment groups were compared against TNBS only group. Statistical analyses were performed using unpaired Mann-Whitney non-parametric tests. All values are expressed as mean ± SEM. (*P <0.05)

4.4.5. Bioactivity on primary human lymphocytes

Human PBMCs were stimulated with either PMA/ionomycin (for T cell activation) or LPS (for myeloid cell activation) in the presence or absence of AIP2-20, AIP1-13 and ES-10. During PMA/ionomycin stimulation of PBMCs, addition of ES-10 but not the other AIP peptides resulted in significant reduction in IFN-γ ($P<0.001$), TNF-α ($P<0.001$), IL-2 ($P<0.01$) and IL-8 ($P<0.05$) (Figure 4.7A). During LPS stimulation, addition of ES-10 but not the other AIP or control peptides resulted in significant reduction in TNF-α ($P<0.01$), IL-8 ($P<0.01$), IL-1β ($P<0.05$) and IL-6 ($P<0.05$) (Figure 4.7B). A dose response analysis of TNF-α production by LPS-stimulated PBMCs in the presence of ES-10 showed a dose-dependent effect with as little as 1.0 µg/ml final concentration of peptide (Figure 4.7C). Analysis of ES-10 activity across genetically unrelated donors showed that PBMCs from 5 of 6 donors responded to *ex vivo* treatment with ES-10 (Figure 4.7D). Using LIVE/DEAD viability staining on PBMCs, ES-10 was shown to be non-toxic at 1.0 µg/ml (93% viability), 10 µg/ml (92% viability) and 100 µg/ml (92% viability). The untreated controls exhibited 92% viability (data not shown). Collectively, these data show ES-10 is non-toxic to human lymphocytes at high concentrations and displays bioactivity on both T cell and myeloid lineages.

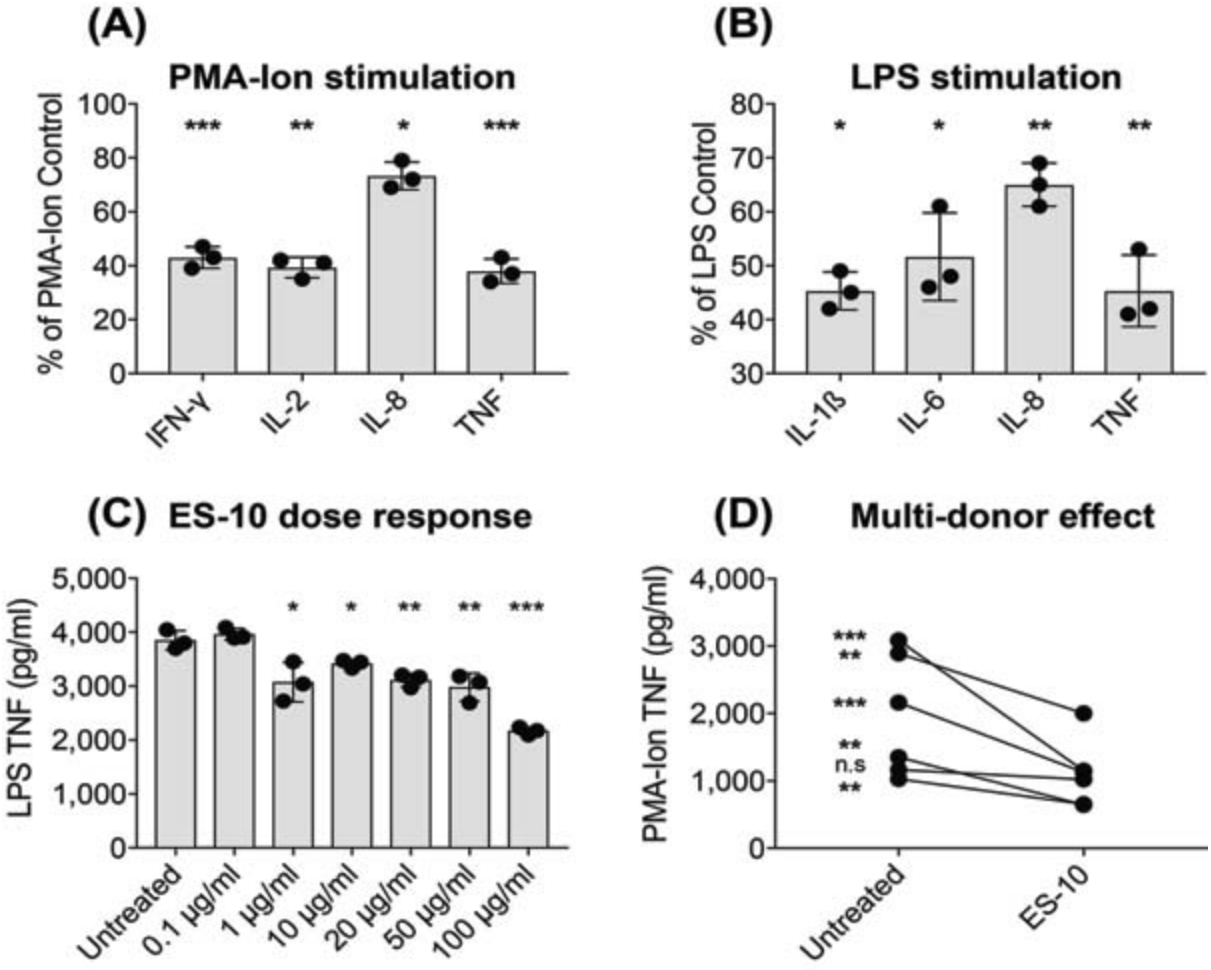

Figure 4.7. ES-10 suppresses cytokine production by human T cells and myeloid cells. ES-10 (100 µg/ml) was added to $1x10^6$ PBMCs stimulated with (A) 50 ng/ml of PMA and 1 µg/ml of ionomycin or (B) 10 ng/ml of LPS. After overnight incubation, cytokines from culture supernatants were quantified by CBA. (C) A ES-10 dose response from 0.1-100 µg/ml was performed on $1x10^6$ PBMCs stimulated with 10 ng/ml of LPS. (D) ES-10 effects across genetically unrelated donors. All results were performed in triplicate. *P <0.05; ** P < 0.01; *** P < 0.001.

4.4.6. Serum stability assay

The stability of the peptides in human serum was assessed over a 24-hour period. The percentage of peptide remaining was determined using RP-HPLC and the degradation profiles are shown in Figure 8. AIP2-20 degraded slower than AIP1-13 and ES-10. The latter two peptides had less than 10% peptide remaining within 4 hours, whereas AIP2-20 had more than 50% remaining at the 8-hour time-point and could still be detected after 24 hours. AIP2-20D6P degraded slower than AIP1-13 and ES-10 but was less stable than AIP2-20.

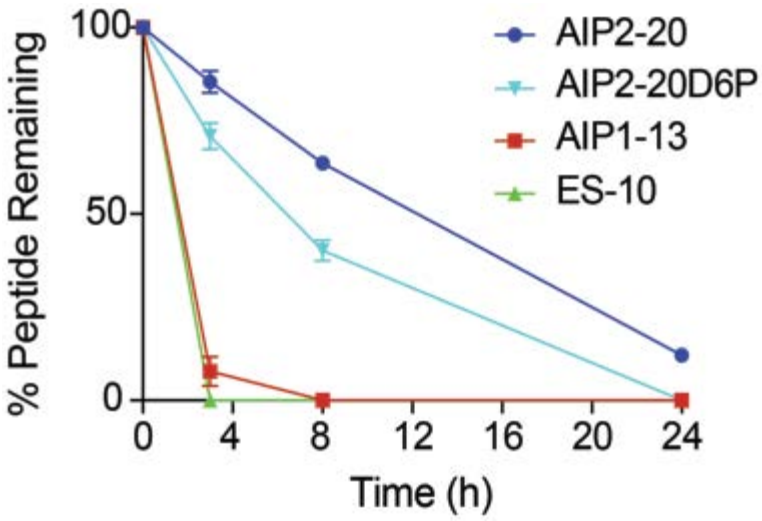

Figure 4.8. Stability of the peptides in human serum. The percentage of peptide remaining in the serum stability assay was assessed by RP-HPLC. All data are represented as mean ± SD and were recorded in triplicate

4.5. Discussion

This study provides the first insight into the structure-function relationships of AIPs derived from hookworms. We have applied a downsizing approach to *Ace*ES-2, *Ac*-AIP-2, and *Na*-AIP-1 to derive peptides of 20 residues or less, with significant protective effects in a mouse model of colitis and anti-inflammatory activity of one of these peptides with human PBMCs *ex vivo*. Our results indicate that a conserved helical region in the proteins is responsible, at least in part, for the anti-inflammatory effects observed in this family of hookworm proteins.

To date, only *Ac*-AIP-1 and *Ac*-AIP-2 have been reported to have anti-inflammatory activity from this protein family (14,15). Neither *Na*-AIP-1 nor *Ace*ES-2 have been reported to have activity in anti-inflammatory assays. However, given that peptides derived from *Ace*ES-2, *Ac*-AIP-2, and *Na*-AIP-1 all displayed significant effects on symptoms in a TNBS mouse model of colitis, our results indicate that anti-inflammatory activity is characteristic of this family of proteins.

Although peptides derived from the three different proteins all displayed activity in the TNBS mouse model, only ES-10 displayed bioactivity with human PBMCs. The peptides analysed in the current study were chosen based on structural alignment of the full-length proteins, but there is sequence diversity amongst the peptides. This sequence diversity is presumably responsible for the differences observed with the human cells.

Despite the sequence diversity, the peptides all contain a EXXXL motif as highlighted in Table 1. A hydrogen bond is present in the crystal structure of *Ace*ES-2 and in the modelled structures of *Ac*-AIP-2 and *Na*-AIP-1, between the conserved E and L residues. This hydrogen bond is

also present in the structures of AIP2-20, implying that this interaction is an important feature for stabilizing the structure. Indeed, it is interesting to speculate that this conserved motif might play a key role in the structure-function relationships, but further study is required to confirm this hypothesis.

Comparison of the structures of the active peptides highlighted some intriguing differences. The structure of AIP2-20 contains a well-defined helix over residues 2-11, consistent with the modelled structure of *Ac*-AIP-2 and the structures of the related proteins. Furthermore, the presence of slowly exchanging amide protons is consistent with hydrogen bonds stabilizing the structure. In contrast, structures for the other peptides were unable to be determined due to a lack of NOEs in the NOESY spectra and dihedral angle restraints. ES-10 and AIP1-13 are considerably shorter than AIP2-20, and this small size can have a substantial impact on the quality of the NOESY spectra given the relationship between molecular weight and NOE intensity (34). However, in this case, strong peaks corresponding to the sequential connections are present suggesting that the lack of medium and long-range NOEs is not simply a function of the mixing time.

Despite the lack of medium and long range NOEs for ES-10 and AIP1-13, these peptides have similar secondary shifts to AIP2-20, with a proportion of negative shifts indicating the presence of helical structure. Perhaps more compelling is the presence of slowly exchanging amide protons in ES-10 and AIP1-13 indicative of hydrogen bonds stabilizing the structure. Therefore, based on the chemical shifts and slowly exchanging amide protons it would be expected that AIP1-13 and ES-10 would also display well-defined helical structures in solution, but this is not the case as the structures could not be defined.

The apparent discrepancy between NOEs, and chemical shifts, and slowly exchanging amide protons has been previously observed in an unrelated protein (35). Similar to our results, cytochrome b_{562} showed chemical shifts and slowly exchanging amide protons consistent with the presence of helical structure, but was not supported by the NOE data. Relaxation analysis indicated the presence of conformational exchange as the likely reason for the discrepancy. It is possible that similar conformational exchange could be occurring with ES-10 and AIP1-13, but further study is required to confirm this suggestion.

The serum stability results also highlight a difference between the peptides. AIP2-20 is more stable than AIP1-13 and ES-10, which are degraded rapidly. The reasonably high stability of AIP2-20 is consistent with the well-defined helical structure present in solution, whereas degradation of ES-10 and AIP1-13 is consistent with a lack of secondary structure. It is unclear how conformational exchange in ES-10 and AIP1-13 could impact the serum stability, but overall it appears that the longer peptide (AIP2-20) has the most stable structure. AIP2-20D6P has improved stability in serum compared to AIP1-13 and ES-10, but is less stable than AIP2-20, indicating that the introduction of a proline residue in the helical region decreases the biological stability.

There are no significant differences in the protective effects of the AIP peptides in the TNBS assay. However, the cell based assay showed ES10 has significant reduction in IFN-γ ($P<0.001$), TNF-α ($P<0.001$), IL-2 ($P<0.01$) and IL-8 ($P<0.05$), whereas 2HE did not. This suggests that the more structured peptide, 2HE, is not necessarily the more active peptide in human cells.

Some netrin domain-containing proteins, including TIMPs, have biological functions that are unrelated to MMP inhibition, including inhibition of cell migration (36). The mechanism of action of AIP proteins has yet to be determined, but depletion of either $CD11c^+$ dendritic cells or $Foxp3^+$ regulatory T cells ablated AIP-2-induced protection against asthma and associated lung pathology in mice (15,37). The bioactivity that we detected with ES-10 on human PBMCs indicated that the peptide suppressed cytokine production by myeloid cells (possibly dendritic cells and/or macrophages). We also detected ES-10-induced suppression of T cell cytokine production after stimulation of PBMCs with PMA-ionomycin, but whether this was dependent on myeloid cell presence is unclear.

In summary, a small helical region present in hookworm netrin domain-containing AIPs appears to play a role in bioactivity. This region is relatively solvent exposed in the hookworm proteins and therefore has the potential to be involved in protein-protein interactions. Consequently, we have identified a promising starting point for the design of peptide-based lead molecules for the treatment of inflammatory diseases such as IBD.

4.6. Acknowledgements

I would like to acknowledge Cairns Base Hospital for the histological analysis of the tissue samples. CCC would like to thank James Cook University for a PhD scholarship. This work was supported by the Australian Research Council and National Health and Medical Research Council via a Future Fellowship to NLD (110100226), a senior principal research fellowship to AL (1117504) and program grant to AL (1037304), and Janssen R&D, US.

4.7. References

1. Molodecky, N. A., Soon, I. S., Rabi, D. M., Ghali, W. A., Ferris, M., Chernoff, G., Benchimol, E. I., Panaccione, R., Ghosh, S., Barkema, H. W., and Kaplan, G. G. (2012) Increasing Incidence and Prevalence of the Inflammatory Bowel Diseases With Time, Based on Systematic Review. Gastroenterology 142, 46-54

2. Prescott, S., and Allen, K. J. (2011) Food allergy: Riding the second wave of the allergy epidemic. Pediatr. Allergy Immunol. 22, 155-160

3. Weinstock, J. V., Summers, R. W., Elliott, D. E., Qadir, K., Urban, J. F., and Thompson, R. (2002) The possible link between de-worming and the emergence of immunological disease. J. Lab. Clin. Med. 139, 334-338

4. Bouma, G., and Strober, W. (2003) The immunological and genetic basis of inflammatory bowel disease. Nat. Rev. Immunol. 3, 521-533

5. Podolsky, D. K. (2002) Inflammatory bowel disease. N. Engl. J. Med. 347, 417-429

6. To, T., Stanojevic, S., Moores, G., Gershon, A. S., Bateman, E. D., Cruz, A. A., and Boulet, L. P. (2012) Global asthma prevalence in adults: findings from the cross-sectional world health survey. BMC Public Health 12

7. Choby, G. W., and Lee, S. (2015) Pharmacotherapy for the treatment of asthma: current treatment options and future directions. Int. Forum Allergy Rhinol. 5, S35-S40

8. Badorrek, P., Hohlfeld, J. M., Krug, N., Joshi, A., and Raut, A. (2015) Efficacy and safety of a novel nasal steroid, S0597, in patients with seasonal allergic rhinitis. Ann. Allergy, Asthma Immunol. 115, 325-+

9. Navarro, S., Pickering, D. A., Ferreira, I. B., Jones, L., Ryan, S., Troy, S., Leech, A., Hotez, P. J., Zhan, B., Laha, T., Prentice, R., Sparwasser, T., Croese, J., Engwerda, C. R., Upham, J. W., Julia, V., Giacomin, P. R., and Loukas, A. (2016) Hookworm recombinant protein promotes regulatory T cell responses that suppress experimental asthma. Science Translational Medicine 8

10. Ferreira, I., Smyth, D., Gaze, S., Aziz, A., Giacomin, P., Ruyssers, N., Artis, D., Laha, T., Navarro, S., Loukas, A., and McSorley, H. J. (2013) Hookworm excretory/secretory products induce interleukin-4 (IL-4)(+) IL-10(+) CD4(+) T cell responses and suppress pathology in a mouse model of colitis. Infect. Immun. 81, 2104-2111

11. Mulvenna, J., Hamilton, B., Nagaraj, S. H., Smyth, D., Loukas, A., and Gorman, J. J. (2009) Proteomics Analysis of the Excretory/Secretory Component of the Blood-feeding Stage of the Hookworm, Ancylostoma caninum. Mol. Cell. Proteomics 8, 109-121

12. Morante, T., Shepherd, C., Constantinoiu, C., Loukas, A., and Sotillo, J. (2017) Revisiting the Ancylostoma Caninum Secretome Provides New Information on Hookworm-Host Interactions. Proteomics 17

13. Cantacessi, C., Hofmann, A., Pickering, D., Navarro, S., Mitreva, M., and Loukas, A. (2013) TIMPs of parasitic helminths - a large-scale analysis of high-throughput sequence datasets. Parasit. Vectors 6

14. Ferreira, I. B., Pickering, D. A., Troy, S., Croese, J., Loukas, A., and Navarro, S. (2017) Suppression of inflammation and tissue damage by a hookworm recombinant protein in experimental colitis. Clin. Transl. Immunology 6, e157

15. Navarro, S., Pickering, D. A., Ferreira, I. B., Jones, L., Ryan, S., Troy, S., Leech, A., Hotez, P. J., Zhan, B., Laha, T., Prentice, R., Sparwasser, T., Croese, J., Engwerda, C. R., Upham, J. W., Julia, V., Giacomin, P. R., and Loukas, A. (2016) Hookworm recombinant protein promotes regulatory T cell responses that suppress experimental asthma. Sci. Transl. Med. 8, 14

16. Harrison, R. S., Shepherd, N. E., Hoang, H. N., Ruiz-Gomez, G., Hill, T. A., Driver, R. W., Desai, V. S., Young, P. R., Abbenante, G., and Fairlie, D. P. (2010) Downsizing human, bacterial, and viral proteins to short water-stable alpha helices that maintain biological potency. Proc. Natl. Acad. Sci. U. S. A. 107, 11686-11691

17. Reid, R. C., Yau, M. K., Singh, R., Hamidon, J. K., Reed, A. N., Chu, P. F., Suen, J. Y., Stoermer, M. J., Blakeney, J. S., Lim, J., Faber, J. M., and Fairlie, D. P. (2013) Downsizing a human inflammatory protein to a small molecule with equal potency and functionality. Nat. Commun. 4

18. Fosgerau, K., and Hoffmann, T. (2015) Peptide therapeutics: current status and future directions. Drug Discov. Today 20, 122-128

19. Sachdeva, S. (2017) Peptides as 'Drugs': The Journey so Far. Int. J. Pept. Res. Ther. 23, 49-60

20. Kucera, K., Harrison, L. M., Cappello, M., and Modis, Y. (2011) Ancylostoma ceylanicum Excretory-Secretory Protein 2 Adopts a Netrin-Like Fold and Defines a Novel Family of Nematode Proteins. J. Mol. Biol. 408, 9-17

21. Wuthrich, K. (2003) NMR studies of structure and function of biological macromolecules (Nobel Lecture). J. Biomol. NMR 27, 13-39

22. (2001).

23. Ikeya, T., Terauchi, T., Guntert, P., and Kainosho, M. (2006) Evaluation of stereo-array isotope labeling (SAIL) patterns for automated structural analysis of proteins with CYANA. Magn. Reson. Chem. 44, S152-S157

24. Shen, Y., Delaglio, F., Cornilescu, G., and Bax, A. (2009) TALOS plus : a hybrid method for predicting protein backbone torsion angles from NMR chemical shifts. J. Biomol. NMR 44, 213-223

25. Koradi, R., Billeter, M., and Wuthrich, K. (1996) MOLMOL: A program for display and analysis of macromolecular structures. J. Mol. Graph. 14, 51-&

26. Hong, T., Yang, Z., Lv, C. F., and Zhang, Y. (2012) Suppressive effect of berberine on experimental dextran sulfate sodium-induced colitis. Immunopharmacol. Immunotoxicol. 34, 391-397

27. Chan, L. Y., Gunasekera, S., Henriques, S. T., Worth, N. F., Le, S. J., Clark, R. J., Campbell, J. H., Craik, D. J., and Daly, N. L. (2011) Engineering pro-angiogenic peptides using stable, disulfide-rich cyclic scaffolds. Blood 118, 6709-6717

28. Yang, J. Y., Yan, R. X., Roy, A., Xu, D., Poisson, J., and Zhang, Y. (2015) The I-TASSER Suite: protein structure and function prediction. Nat. Methods 12, 7-8

29. Tuuttila, A., Morgunova, E., Bergmann, U., Lindqvist, Y., Maskos, K., Fernandez-Catalan, C., Bode, W., Tryggvason, K., and Schneider, G. (1998) Three-dimensional structure of human tissue inhibitor of metalloproteinases-2 at 2.1 angstrom resolution. J. Mol. Biol. 284, 1133-1140

30. Wisniewska, M., Goettig, P., Maskos, K., Belouski, E., Winters, D., Hecht, R., Black, R., and Bode, W. (2008) Structural determinants of the ADAM inhibition by TIMP-3: Crystal structure of the TACE-N-TIMP-3 complex. J. Mol. Biol. 381, 1307-1319

31. Bullock, B. N., Jochim, A. L., and Arora, P. S. (2011) Assessing helical protein interfaces for inhibitor design. J Am Chem Soc 133, 14220-14223

32. Mielke, S. P., and Krishnan, V. V. (2009) Characterization of protein secondary structure from NMR chemical shifts. Prog. Nucl. Magn. Reson. Spectrosc. 54, 141-165

33. Cobos Caceres, C., Bansal, P. S., Navarro, S., Wilson, D., Don, L., Giacomin, P., Loukas, A., and Daly, N. L. (2017) An engineered cyclic peptide alleviates symptoms of inflammation in a murine model of inflammatory bowel disease. J. Biol. Chem. 292, 10288-10294

34. D. Neuhaus, M. W. (1989) The Nuclear Overhauser Effect in Structural and Conformational Analysis, VCH Publishers

35. D'Amelio, N., Bonvin, A., Czisch, M., Barker, P., and Kaptein, R. (2002) The C terminus of apocytochrome b(562) undergoes fast motions and slow exchange among ordered conformations resembling the folded state. Biochemistry 41, 5505-5514

36. Stetler-Stevenson, W. G. (2008) Tissue Inhibitors of Metalloproteinases in Cell Signaling: Metalloproteinase-Independent Biological Activities. Science Signaling 1

37. Cuellar, C., Wu, W. H., and Mendez, S. (2009) The Hookworm Tissue Inhibitor of Metalloproteases (Ac-TMP-1) Modifies Dendritic Cell Function and Induces Generation of CD4 and CD8 Suppressor T Cells. PLoS Negl. Trop. Dis. 3

5. CHAPTER 5

Engineering of an Anti-Inflammatory Peptide Based on MHC-II Binding Predictions

Claudia Cobos Caceres, Paramjit S. Bansal, Linda Jones, Ramon Marc Eichenberger, David Wilson, Alex Loukas, Severine Navarro*, Norelle L. Daly*

5.1. Abstract

Hookworm proteins have significant potential in the design of anti-inflammatory agents, highlighted by *Ac*-AIP proteins excreted by *Ancylostoma caninum*, having efficacy in mouse models of asthma and colitis. However, there is limited information on the structure/function relationships. Here we used a novel approach based on MHC II peptide binding prediction to identify a bioactive sequence derived from *Ac*-AIP2. A peptide corresponding to residues 69-85 in *Ac*-AIP2 displayed significant protective effects on symptoms in a TNBS mouse model of colitis, indicating that this region is in part responsible for the bioactivity of this protein.

5.2. Introduction

The incidence of autoimmune diseases has been rising sharply during the past few decades (1-4). One in five children experience diseases such as asthma, dermatitis or rhinitis in developed countries (5). Furthermore, inflammatory bowel diseases have increased in younger populations of industrialised countries/regions such as Australia, New Zealand, Northern Europe and USA (6). The hypothesis behind why this is happening, termed the "hygiene hypothesis", relates to an inverse correlation between levels of parasites and the incidence of autoimmune diseases (7-9).

The hygiene hypothesis has led to studies aimed at characterizing parasite excretory/secretory (ES) products and analysing their potential as novel drug leads for autoimmune diseases (10). Several parasite proteins have been shown to have therapeutic potential including proteins derived from hookworms. Proteomic analysis of the hookworm *Ancylostoma caninum* ES proteins has revealed the relative abundance of two Tissue Inhibitor of Metalloprotease (TIMP)-like proteins, anti-inflammatory protein *Ac*-AIP1 and *Ac*-AIP2 (11), neither of which appear to have the protease inhibitory properties that characterise the TIMP family (12). We have shown that *Ac*-AIP2 supresses airway proliferation in a mouse model of asthma and ex vivo of T cells from human subjects (13). More recently we have shown that hookworm AIP proteins have therapeutic efficacy in a mouse model of acute colitis and promote a regulatory immune environment in treated mice (14). The current treatments for diseases such as asthma and IBD have significant limitations (15-17) and the AIP proteins have potential as new therapeutic agents.

To facilitate the development of AIP protein-based drug leads a better understanding of the structure/function relationships is required. In particular, elucidating the bioactive region(s) could be useful for developing smaller lead molecules that are less likely to be immunogenic and could be produced using synthetic procedures rather than recombinant technologies. Several approaches have been applied to elucidating bioactive regions of proteins, which primarily involve mutational and truncation studies. In the current study we have used a truncation approach guided by prediction of a peptide likely to be presented as a peptide-MHC II complex. Our hypothesis was that a peptide from *Ac*-AIP-2 predicted to form an MHC II complex could be presented to T cells and regulate the immune response, and ultimately result in a lead peptide for the design of new anti-inflammatory agents. In support of this hypothesis, we have identified a 17-residue peptide that displays protection against chemically induced-colitis in a mouse model.

5.3. Experimental Procedures

5.3.1. Peptide design

The Immune Epitope Database Analysis Resource was used to predict peptide sequences from *Ac*-AIP2 that could be presented in MHC-II complexes. The selected species/locus for the comparison was mouse allele H-2-I. Selected MHC alleles were H2-IAd. The peptides were sorted by percentile rank, with the lowest percentile more likely to bind to MHC II.

5.3.2. Peptide synthesis and purification

AIP2(69-85) was synthesised using solid phase peptide synthesis in a Protein Technologies PS3 synthesiser using fluorenylmethyloxycarbonyl (Fmoc) chemistry with 2-chlorotrityl chloride as resin on a 0.1 mmole scale. Amino acids (2 equiv.) were activated in 5 equiv HBTU and 10 equiv. DIPEA in DMF (1.5 mL). Deprotection was carry out in two repetitions: Starting with 2 min of 20% pipiridine in DMF (5ml), followed by 3 mins of the same solution. First amino acid was coupled manually to the resin, the rest of the amino acids were added using the peptide sinthesiser. After that, the peptide was cleaved from the resin using a mixture of trifluoroacetic acid (TFA)/water/triisopropylsilane (95:2.5:2.5) for 2-3 h, and precipitated with diethylether after cleavage. Subsequently, the peptide was dissolved in 50% acetonitrile/0.05% TFA, and finally lyophilised. RP-HPLC was used for purification on a C_{18} preparative column (Phenomenex Jupiter 250 x 21.2 mm, 10 µm, 300 Å) with a 1% gradient of solvent B (solvent A: 0.05% TFA; solvent B: 90% acetonitrile, 0.05% TFA). The mass was analysed using MALDI-TOF mass spectrometry. SFTI-1 was used as a control peptide and was synthesized as previously reported (18-20)

5.3.3. NMR Spectroscopy and Structural Analysis

AIP2(69-85) was resuspended in 90%H_2O:10%D_2O at a concentration of ~0.2 mM. 2D ^{1}H-^{1}H TOCSY, ^{1}H-^{1}H NOESY, ^{1}H-^{1}H DQF-COSY, ^{1}H-^{15}N HSQC, and ^{1}H-^{13}C HSQC spectra were acquired at 290 K using a 600 MHz AVANCE III NMR spectrometer (Bruker, Karlsruhe, Germany). NOESY spectra were acquired with mixing times of 200-300 ms, and TOCSY spectra were acquired with isotropic mixing periods of 80 ms. Standard Bruker pulse sequences were used with an excitation sculpting scheme for solvent suppression. Spectra were referenced to internal 4,4-dimethyl-4-silapentane-1-sulfonic acid (DSS).

Established protocols were used for the NMR assignments (21), and the secondary shifts derived by subtracting the random coil αH shift from the experimental αH shifts (22). Slow exchanging amide protons was carried out. Numerous slowly exchanging amide protons were identified in D_2O exchange experiments. AIP2(69-85) showed slowly exchanging amide protons for 5 residues after 30 minutes of resuspension in D_2O. After 2 hrs, Trp4 and Val14 were particularly slowly exchanging compared to the other residues. Slow exchanging amides for these residues suggest that the peptides have a propensity for forming hydrogen bonds.

5.3.4. TNBS colitis assay

All experiments were conducted following James Cook University Animal Ethics Committee approved guidelines. C57BL/6 strain of mice 5 weeks old were divided in groups of five males per group. Mice came from the Animal Resources Centre (Perth, Australia) and housed in the animal care facility unit at James Cook University under specific pathogen free conditions.

After arriving at our facility, mice were placed inside plastic cages with unlimited access to food and water, and with daily health checks.

Mice were divided randomly into different groups of 5: Naïve, 2,4,6trinitrobenzenesulfonic acid (TNBS), a control peptide SFTI-1and AIP2(69-85). Mice received intraperitoneal (i.p) injections of peptides. Prior to administration of TNBS mice were anaesthetised with a solution of ketamine/xylazine. Mice received 100 μL of 5% (w/v) TNBS solution in 60% ethanol by intra-colonic instillation using a 20 gauge soft catheter (Terumo), which was inserted into the colon. Mice were monitored daily for different variables such as: piloerection, survival, stool consistency, body weight, rectal bleeding and decreased motor activity. Macroscopic score was made after culling the mice to analyse the pathology scoring for each colon. Following this, tissues were assessed and scored for pathological changes as follows: adhesion (0 to 3), bowel wall thickening (0 to 3), mucosal oedema (0 to 3), ulceration (0 to 3), and colon length as described previously (23). All animal experiments were conducted in duplicate to ensure reproducibility of the findings.

5.3.5. Histological evaluation of colitis

Histology tissue was fixed using formalin and transferred to a solution of 70% alcohol. Tissue was embedded in paraffin and sectioned longitudinally for histology at 4 μm thickness. PAS staining was used to assess goblet cell destruction. Scoring of the images was determined in a blinded fashion following the scoring method of Hong et al (24). High resolution images were scoring as follow: Ulceration: no ulcers = 0; 1 ulcer = 1; 2 ulcers = 2; 3 ulcers = 3; and >3 ulcers = 4. Infiltration: 0 = no infiltrate, 1 = infiltrate at crypt bases, 2 = infiltrate reaching to muscularis mucosa, 3 = extensive infiltration reaching the muscularis, and 4 = infiltration of

the submucosa with oedema. Epithelium was scored: 0 = normal morphology, 1 = loss of goblet cells in one area, 2 = loss of goblet cells in more than one area, 3 = loss of crypts in one area, and 4 = loss of crypts in more than one area. Lymphoid follicles: none = 0, 1 = 1, 2 = 2, 3 = 3, > 3 = 4

5.3.6. Serum stability assay

The serum stability of the peptides was tested using human male AB plasma (Sigma-Aldrich) following methods previously described (19). The final concentration for the peptide was 200 μM, which was firstly incubated in serum or PBS at 37°C. 40 μL aliquots taken at 0 h, 3 h and 8 h. The aliquots of serum were quenched with 40 μL of 20% TFA and incubated for 10 minutes at 4°C to precipitate serum proteins. PBS received the same treatment as serum. The samples were then centrifuged at 17000 *g* for 10 min and 90 μL of supernatant analysed by RP-HPLC at a flow rate of 0.3 mL/min using a Phenomenex Jupiter Proteo C_{12} analytical column (150 x 2.00 mm, 4 μm, 90 Å) using a linear 1% min^{-1} acetonitrile gradient (0-50% solvent B). The eluent was observed using a dual wavelength UV detector set to 214 and 280 nm.

5.4. Results

5.4.1. Peptide design and synthesis

The three *highest*-ranking sequences from *Ac*-AIP2 predicted to bind to MHC II, using the Immune Epitope Database, are given in Table 5.1. To encompass all of the residues predicted to be involved we synthesized a 17-residue peptide corresponding to residues 69-85 of *Ac*-AIP2. The peptide, termed AIP2(69-85), was synthesised using Fmoc chemistry on a 0.1 mmole scale, purified using RP-HPLC and the mass analysed using MALDI mass spectrometry.

Table 5.1. Peptide sequences from *Ac*-AIP2 predicted to have MHC II binding*

Residue numbers	Sequence	Percentile Rank
(70-84)	HVWHMRTWKGPVVDT	3.4
(71-85)	VWHMRTWKGPVVDTS	3.41
(69-83)	YHVWHMRTWKGPVVD	4.14

***Prediction method: Immune Epitope Database Analysis Resource was used to predict the sequences.**

The program predicts binding affinities for each peptide of 15 amino acids, and compares the affinity for the predicted peptides with a set of randomly selected peptides, to derive the percentile rank. A low percentile rank is predicted to have improved binding to the MHC II**.**

5.4.2. Structural analysis

Despite the large proportion of aromatic and methyl containing residues, AIP2(69-85) was highly soluble, and NMR spectra were recorded in aqueous solution. Two-dimensional

TOCSY and NOESY spectra allowed assignment of the resonances, and the secondary chemical shifts, shown in Figure 5.1, were determined by subtracting random coil chemical shifts from the αH chemical shifts (22). Secondary shifts can provide an indication of the type of secondary structure present in peptides. This chemical shift analysis showed consecutive shifts more negative than -0.1, which can indicate the presence of helical structure (25). In support of regular secondary structure, the peptide displayed slowly exchanging amide protons in the D_2O exchange experiments for five residues. By contrast, no medium or long range NOEs were observed in the NOESY spectra and the TALOS+ analysis did not provide any definitive prediction of the dihedral angles, which is consistent with an unstructured peptide. The lack of NOEs and dihedral angle restraints prevented a structure from being determined for AIP2(69-85).

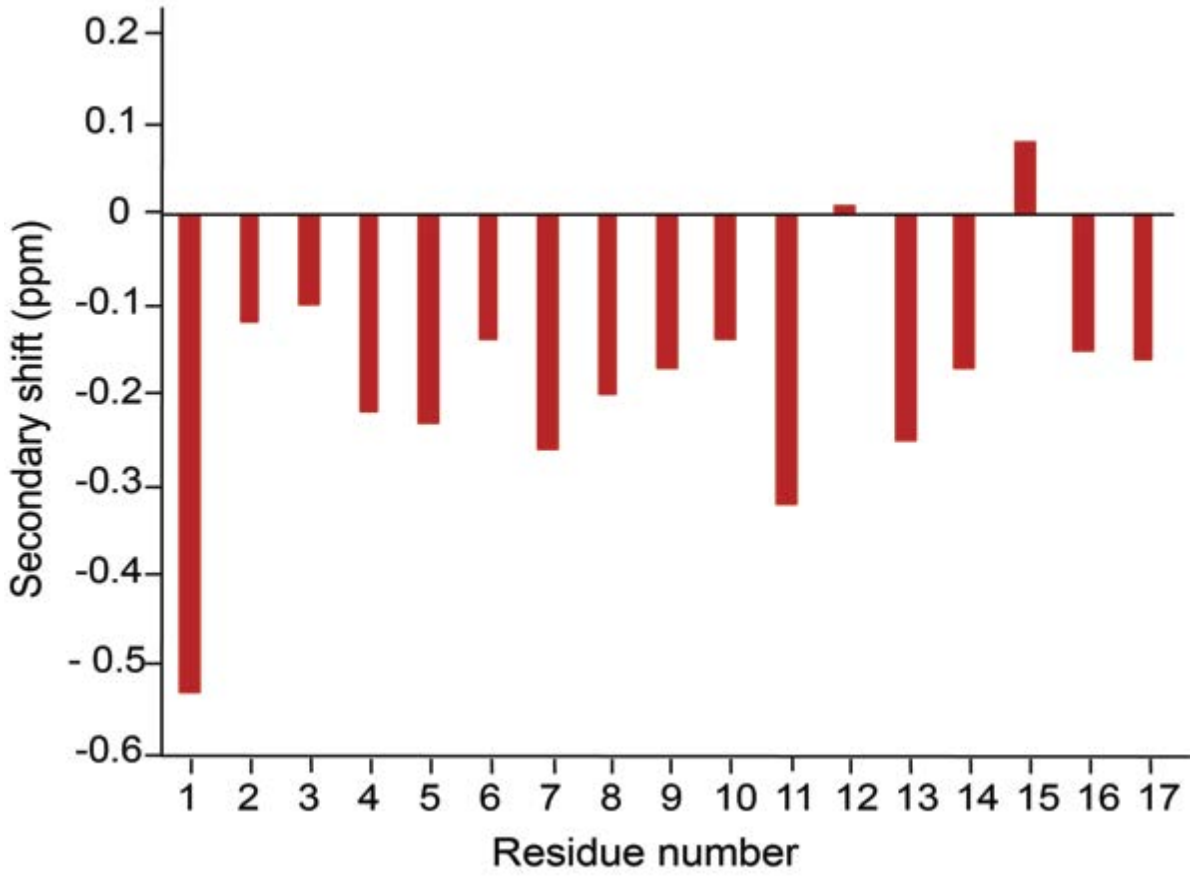

Figure 5.1. Chemical shift analysis of the AIP2(69-85). The secondary shifts of AIP2(69-85) were calculated by subtracting the random coil shifts from the αH shifts (22) and are indicative of helical structure.

To provide insight into the structure AIP2(69-85) might adopt in the full length protein the structure of *Ac*-AIP2 was modelled using I-TASSER protein structure and function prediction software, based on the human tissue inhibitor of metalloproteinase-2 protein (PDB code 1BR9.pdb) as a template (26). The region corresponding to AIP2(69-85) is shown in Figure5.2. In the modelled structure this peptide is involved in a β-strand.

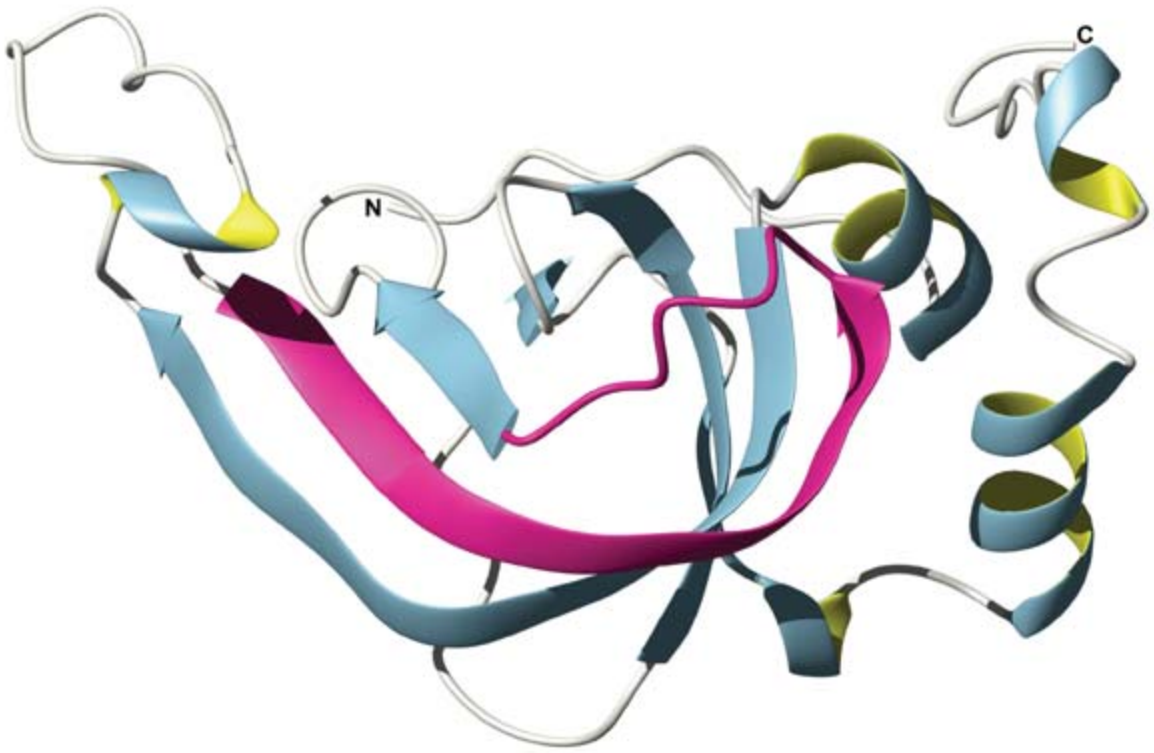

Figure 5.2. The modelled structure of Ac-AIP2. The sequence corresponding to AIP2(69-95) is shown in magenta. The extended C-terminal tail in Ac-AIP2 has been removed for clarity. The figure was made using MOLMOL(28).

5.4.3. TNBS mouse colitis model

The effect of AIP2(69-85) in a TNBS induced colitis mouse model was accessed. Mice were either left untreated (naïve), treated with TNBS alone or were treated with peptides at a dose of 1 mg/kg five hours prior to administration of TNBS. On day 3, mice were humanely euthanased using gas asphyxiation and examined for assessment of protection against colitis.

The TNBS-only treated mice initially lost weight and did not recover during the experiment, consistent with inflammation and colonic mucosa damage. By contrast, AIP2(69-85) displayed significant protective effects in the TNBS assay as shown in Figure 5.3, with statistically significant effects in reducing weight loss. Following culling of the mice, each colon was removed and scored macroscopically using these parameters: adhesion, bowel wall thickening, mucosal oedema, ulceration, necrosis, and colon length. AIP2(69-85) showed statistically longer colons and lower clinical scores than TNBS-only treated mice. Furthermore, consistent with previous results, a control peptide, SFTI-1 showed no protective effects against TNBS-treated mice (18).

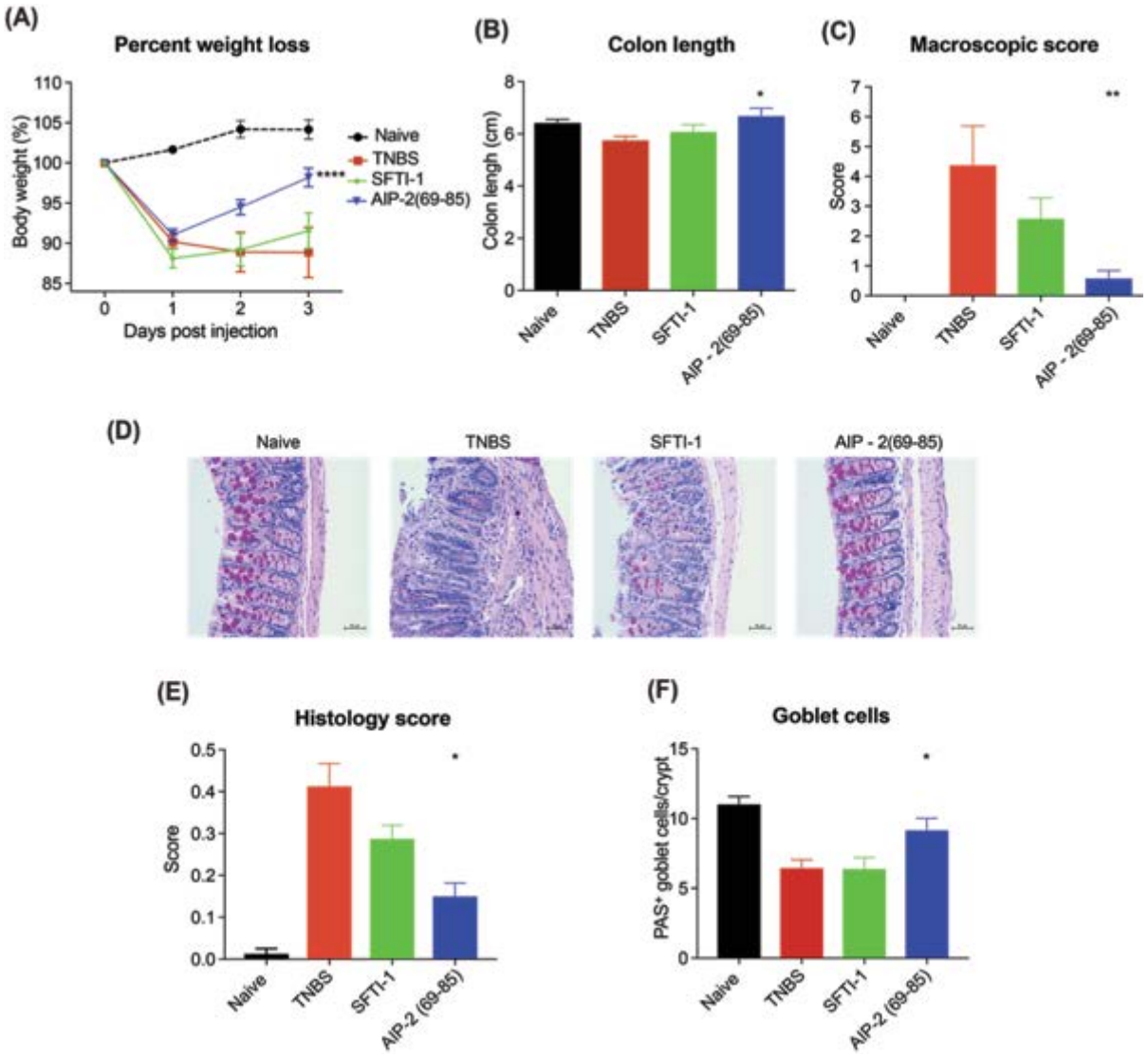

Figure 5.3. Protective effects of AIP2 (69-85) against weight loss and clinical symptoms in a TNBS colitis mouse model. Mice were untreated (naïve) or treated with TNBS following administration of peptides, or saline vehicle control (TNBS). A) Percentage weight loss; B) Colon length; C) Macroscopic Score; D) Representative microscopy PAS stained colonic tissue sections; E) Histology scoring; E) Goblet cells scoring counting.

5.4.4. Histological evaluation of colitis

Inflammatory cell infiltration into the lamina propria is visible in the Periodic acid–Schiff (PAS) stain of the colon tissue from the TNBS-only treated mice. The tissue displayed

epithelial hyperplasia, goblet cells loss, thickening of the lamina propria and colon wall with extensive ulcerations. By contrast, AIP2(69-85) tissue showed lessened colitis features. The epithelium appears intact and with minimal focal inflammatory cell infiltrates in the mucosa. More globet cells were visible in the tissue treated with AIP2(69-85) compared with TNBS treated mice, which indicates that the peptide was protective against colitis. Overall, the histological score is indicative of reduced pathology of AIP2(69-85) -treated mice compared with TNBS-only treated mice.

5.4.5. Serum stability assay

The *in vitro* stability of the peptide in human serum was assessed over a 24-hour period. The percentage of peptide remaining was determined using RP-HPLC. AIP2 (69-85) was degraded within 3 hours as shown in Figure 5.4.

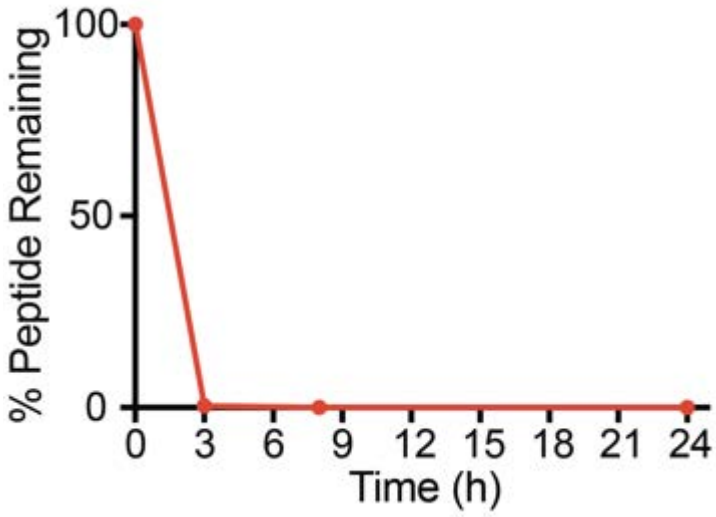

Figure 5.4. Stability of the peptides in human serum. The percentage of peptide remaining in the serum stability assay was assessed by RP-HPLC. All data are represented as mean ± SD and were recorded in triplicate.

5.5. Discussion

Some hookworm proteins have significant potential in the design of anti-inflammatory agents, but there is limited information on the structure/function relationships. Here we used a novel approach based on MHC II peptide binding prediction to identify a bioactive sequence derived from *Ac*-AIP2. A peptide corresponding to residues 69-85 in *Ac*-AIP2 displayed significant protective effects on symptoms in a TNBS mouse model of colitis, indicating that this region is in part responsible for the bioactivity of this protein.

Although we can show that this region of *Ac*-AIP2 has bioactivity in isolation, analysis of the structure has been complicated. Based on a lack of medium and long range NOEs and a lack of predicted dihedral angle restraints the peptide appears to be unstructured in solution. This lack of structure is consistent with the full-length protein of *Ac*-AIP2, which indicates that residues 69-85 are involved in a β-strand that interacts with residues 35-48. It appears unlikely that residues 69-85 would be structured in isolation as the inter-strand interactions cannot form. The lack of stability in serum is also consistent with the peptide being unstructured in solution.

By contrast, analysis of the secondary shifts indicates a propensity for AIP2(69-85) to form helical structure and the presence of slowly exchanging amide protons indicates the presence of hydrogen bonds stabilizing the secondary structure. The discrepancy between NOEs, and chemical shifts and slowly exchanging amide protons is similar to that observed in an unrelated protein (27). Similar to our results, cytochrome b_{562} showed chemical shifts and slowly exchanging amide protons consistent with the presence of helical structure, but was not supported by the NOE data. Relaxation analysis indicated the presence of conformational

exchange as the likely reason for the discrepancy. It is possible that similar conformational exchange could be happening with AIP2(69-85).

Determination of an experimental structure of *Ac*-AIP2 is likely to resolve the question of what structure residues 69-85 have in the full-length protein. However, it is possible that the peptide behaves differently, in terms of structure and activity, in isolation than in the full-length protein. Regardless of the structural features, the bioactivity displayed for AIP2(69-85) suggests that it is an interesting lead molecule for the design of novel anti-inflammatory agents. Our results support our hypothesis that a MHC II presented peptide is useful for the design of a novel bioactive peptide, but further studies are required to confirm if it is binding to MHC II.

5.6. Acknowledgements

The James Cook University NMR facility was partially funded by the Australian Research Council (LE120100015, LE160100218).

5.7. References

1. Eder, W., Ege, M. J., and von Mutius, E. (2006) The Asthma Epidemic. N. Engl. J. Med. 355, 2226-2235

2. Patterson, C. C., Dahlquist, G. G., Gyürüs, E., Green, A., and Soltész, G. (2009) Incidence trends for childhood type 1 diabetes in Europe during 1989–2003 and predicted new cases 2005–20: a multicentre prospective registration study. The Lancet 373, 2027-2033

3. Cosnes, J., Gower–Rousseau, C., Seksik, P., and Cortot, A. (2011) Epidemiology and Natural History of Inflammatory Bowel Diseases. Gastroenterology 140, 1785-1794.e1784

4. Ananthakrishnan, A. N. (2015) Epidemiology and risk factors for IBD. Nat. Rev. Gastroenterol. Hepatol. 12, 205-217

5. Beasley, R., Keil, U., von Mutius, E., Pearce, N., Ait-Khaled, N., Anabwani, G., Anderson, H. R., Asher, M. I., Bjorkstein, B., Burr, M. L., Clayton, T. O., Crane, J., Ellwood, P., Lai, C. K. W., Mallol, J., Martinez, F. D., Mitchell, E. A., Montefort, S., Robertson, C. F., Shah, J. R., Sibbald, B., Stewart, A. W., Strachan, D. P., Weiland, S. K., Williams, H. C., and Int Study Asthma Allergies, C. (1998) Worldwide variation in prevalence of symptoms of asthma, allergic rhinoconjunctivitis, and atopic eczema: ISAAC. Lancet 351, 1225-1232

6. M'koma, A. E. (2013) Inflammatory Bowel Disease: An Expanding Global Health Problem. Clin. Med. Insights Gastroenterol. 6, CGast.S12731

7. Bach, J.-F. (2017) The hygiene hypothesis in autoimmunity: the role of pathogens and commensals. Nat. Rev. Immunol. 18, 105

8. Briggs, N., Weatherhead, J., Sastry, K. J., and Hotez, P. J. (2016) The Hygiene Hypothesis and Its Inconvenient Truths about Helminth Infections. PLoS Negl. Trop. Dis. 10, e0004944

9. Versini, M., Jeandel, P.-Y., Bashi, T., Bizzaro, G., Blank, M., and Shoenfeld, Y. (2015) Unraveling the Hygiene Hypothesis of helminthes and autoimmunity: origins, pathophysiology, and clinical applications. BMC Med. 13, 81

10. Wu, Z., Wang, L., Tang, Y., and Sun, X. (2017) Parasite-Derived Proteins for the Treatment of Allergies and Autoimmune Diseases. Front. Microbiol. 8

11. Mulvenna, J., Hamilton, B., Nagaraj, S. H., Smyth, D., Loukas, A., and Gorman, J. J. (2009) Proteomics analysis of the excretory/secretory component of the blood-feeding stage of the hookworm, Ancylostoma caninum. Mol Cell Proteomics 8, 109-121

12. Cantacessi, C., Hofmann, A., Pickering, D., Navarro, S., Mitreva, M., and Loukas, A. (2013) TIMPs of parasitic helminths - a large-scale analysis of high-throughput sequence datasets. Parasit Vectors 6, 156

13. Navarro, S., Pickering, D. A., Ferreira, I. B., Jones, L., Ryan, S., Troy, S., Leech, A., Hotez, P. J., Zhan, B., Laha, T., Prentice, R., Sparwasser, T., Croese, J., Engwerda, C. R., Upham, J. W., Julia, V., Giacomin, P. R., and Loukas, A. (2016) Hookworm recombinant

protein promotes regulatory T cell responses that suppress experimental asthma. Sci Transl Med 8, 362ra143

14. Ferreira, I. B., Pickering, D. A., Troy, S., Croese, J., Loukas, A., and Navarro, S. (2017) Suppression of inflammation and tissue damage by a hookworm recombinant protein in experimental colitis. Clin Transl Immunology 6, e157

15. Rutgeerts, P. J. (2001) Review article: the limitations of corticosteroid therapy in Crohn's disease. Aliment. Pharmacol. Ther. 15, 1515-1525

16. Coskun, M., Vermeire, S., and Nielsen, O. H. (2017) Novel Targeted Therapies for Inflammatory Bowel Disease. Trends Pharmacol. Sci. 38, 127-142

17. Haselkorn, T., Chen, H., Miller, D. P., Fish, J. E., Peters, S. P., Weiss, S. T., and Jones, C. A. (2010) Asthma control and activity limitations: insights from the Real-world Evaluation of Asthma Control and Treatment (REACT) Study. Ann. Allergy, Asthma Immunol. 104, 471-477

18. Cobos Caceres, C., Bansal, P. S., Navarro, S., Wilson, D., Don, L., Giacomin, P., Loukas, A., and Daly, N. L. (2017) An engineered cyclic peptide alleviates symptoms of inflammation in a murine model of inflammatory bowel disease. J. Biol. Chem. 292, 10288-10294

19. Chan, L. Y., Gunasekera, S., Henriques, S. T., Worth, N. F., Le, S. J., Clark, R. J., Campbell, J. H., Craik, D. J., and Daly, N. L. (2011) Engineering pro-angiogenic peptides using stable, disulfide-rich cyclic scaffolds. Blood 118, 6709-6717

20. Gunasekera, S., Aboye, T. L., Madian, W. A., El-Seedi, H. R., and Goransson, U. (2013) Making ends meet: Microwave-accelerated synthesis of cyclic and disulfide rich proteins via in situ thioesterification and native chemical ligation. Int. J. Pept. Res. Ther. 19, 43-54

21. Wuthrich, K. (2003) NMR studies of structure and function of biological macromolecules (Nobel Lecture). J. Biomol. NMR 27, 13-39

22. Yap, K. L. (2001) Empirical analysis of backbone chemical shifts in proteins.

23. Ferreira, I., Smyth, D., Gaze, S., Aziz, A., Giacomin, P., Ruyssers, N., Artis, D., Laha, T., Navarro, S., Loukas, A., and McSorley, H. J. (2013) Hookworm excretory/secretory products induce interleukin-4 (IL-4)(+) IL-10(+) CD4(+) T cell responses and suppress pathology in a mouse model of colitis. Infect. Immun. 81, 2104-2111

24. Hong, T., Yang, Z., Lv, C. F., and Zhang, Y. (2012) Suppressive effect of berberine on experimental dextran sulfate sodium-induced colitis. Immunopharmacol. Immunotoxicol. 34, 391-397

25. Mielke, S. P., and Krishnan, V. V. (2009) Characterization of protein secondary structure from NMR chemical shifts. Prog. Nucl. Magn. Reson. Spectrosc. 54, 141-165

26. Tuuttila, A., Morgunova, E., Bergmann, U., Lindqvist, Y., Maskos, K., Fernandez-Catalan, C., Bode, W., Tryggvason, K., and Schneider, G. (1998) Three-dimensional structure

of human tissue inhibitor of metalloproteinases-2 at 2.1 angstrom resolution. J. Mol. Biol. 284, 1133-1140

27. Koradi, R., Billeter, M., and Wuthrich, K. (1996) MOLMOL: A program for display and analysis of macromolecular structures. J. Mol. Graph. 14, 51-55

28. D'Amelio, N., Bonvin, A., Czisch, M., Barker, P., and Kaptein, R. (2002) The C terminus of apocytochrome b(562) undergoes fast motions and slow exchange among ordered conformations resembling the folded state. Biochemistry 41, 5505-5514

6. CHAPTER 6

Conclusions and Future Directions

6.1. Conclusions

Peptides have gained increased interest as therapeutics during recent years. This thesis has presented new strategies and broadened knowledge regarding the development of new peptide-based drug leads for the treatment of inflammatory bowel diseases.

Stabilising small bioactive compounds or downsizing proteins are useful tools for the generation of new treatments, as shown in this study for inflammatory bowel diseases. However, these approaches can be applied to different diseases when tailored to appropriate peptide and targets.

The hypotheses for Chapters 2 and 3 were based on the premise that disulfide-rich peptides can be used as scaffolds to generate valuable drug leads based on their intrinsic stability and ability to adopt novel bioactivities. The specific aims of these chapters focussed on the design and synthesis of grafted disulfide-rich peptides incorporating a small bioactive sequence with anti-inflammatory activity, and subsequently analysing the structure and bioactivity of the final grafted peptides.

The aims of Chapters 2 and 3 were successfully completed and the studies confirmed that grafting a small bioactive sequence such as MC-12 into two different disulfide-rich scaffolds can enhance the potency and stability of the original peptide. Specifically, these studies showed that the overall fold of the structure was maintained, and therefore grafting the small sequence was not disrupting the structure of the original peptide. Biological assays confirmed that the grafted peptides improved the therapeutic efficacy, relative to the tri-peptide, in a murine model of chemically-induced acute colitis.

The positive outcomes from these studies suggest that using cyclic or disulfide-rich peptides as structural scaffolds, is a promising approach for developing treatments of IBD. Also, this approach, which has been previously been used for other peptide scaffolds and applications, could be extended to other chronic inflammatory conditions.

The overall objective for Chapters 4 and 5 related to downsizing proteins into bioactive peptides. The main focus for these studies was TIMP-like proteins (AIP proteins), with the central idea to downsize the AIP proteins into peptides with anti-inflammatory activity and potential as lead molecules for clinical development in IBD. The hypothesis for these two chapters was that AIP peptides hold significant promise as therapeutics, as they are likely to be more stable than the full-length proteins, less immunogenic and cheaper to manufacture. The specific aims were to design and characterise AIP peptides and analyse their activity as anti-inflammatory agents.

In Chapter 4, the study was based on a small helical region, conserved amongst the hookworm proteins, and comprising the conserved EXXXL sequence motif. The final results showed that peptides corresponding to these regions can alleviate symptoms in a chemically-induced mouse model of colitis. In vitro only ES-10 suppressed cytokine secretion by human peripheral blood mononuclear cell. These results confirm that analyse of conserved regions in different proteins with anti-inflammatory activity is one approach that can be used to elucidate the structure/function relationships associated with the anti-inflammatory activity. Not all of the peptides could be structurally characterised, most likely as a result of conformational exchange. The final findings in Chapter 4, give insight into the structure/function relationships for the AIP-proteins.

For Chapter 5, although it was a continuation of the same idea as Chapter 4, the elucidation of a bioactive region in an AIP protein was guided by prediction of a peptide likely to be presented as a peptide-MHC II complex, and consequently regulate the immune response. The study identified a peptide with significant protective effects on symptoms in a TNBS mouse model of colitis, confirming that this region is in part responsible for the bioactivity of this protein. This tool might help to elucidate structure/function relationships for proteins and their targets. Although the synthetic peptide appears to be unstructured in solution, the analysis of the secondary shifts indicates a propensity to form helical structure, but similarly to the AIP peptides from Chapter 4, appears to have conformation exchange. Despite this finding, in Chapter 5 the final outcome confirmed that a peptide predicted to be involved in an MHC-II complex, is able to reverse inflammatory indicators in a induced-colitis mouse model. This approach has the potential for downsizing other proteins into peptides.

Chapters 4 and 5 identified different regions of the AIP proteins but they both had bioactivity in the TNBS mouse model of colitis. These regions have significantly different properties in terms of sequence, with the peptide identified in Chapter 5 having a large proportion of aromatic residues in contrast to the peptides identified in Chapter 4. Furthermore, the peptides characterised in Chapter 4 have a conserved helical region in the full-length proteins, whereas the peptide from Chapter 5 is predicted to be involved in a β-sheet structure. These differences in composition suggest that the two classes of peptides might be acting on different targets, despite the same macroscopic effects in the mouse model. However, further study is required to determine the biological targets of these peptides, and the target(s) of the proteins.

In summary, this thesis confirms that peptides have potential as drug leads that could benefit patients with diseases such as IBD. My thesis also highlights the potential of peptide-based engineering studies or downsizing protein approaches, in the rational design of peptides as therapeutic treatments.

6.2. Future directions

Perhaps the most obvious direction for future studies in this area is to address the lack of knowledge of the biological target and mechanism of action of the anti-inflammatory peptides. The studies on the MC-12 peptide suggest that grafted peptides are likely to inhibit NF-kB activity, but studies have yet to be carried out. Regarding the AIP peptides, insight into the cell type involved in the mechanism of the full-length proteins has been gained by studies using AIP-2 administration to modify mesenteric dendritic cell function. Identification of a specific protein as the molecular target, could be used to develop *in vitro* assays that could accelerate the elucidation of structure/function relationships and limit the animal studies required to develop new drug leads.

The effects of the ES-10 peptide on cytokine secretion by human peripheral blood mononuclear cells could also be further explored. Mutational analysis of ES-10 could be used to discern the residues important for effects on human cells. In particular, mutation of the conserved Glu and Leu in the EXXXL motif could provide insight into whether this motif is conserved from a functional or structural perspective.

More in depth structural analysis could give us a better understanding of structure-activity relationship with the target. The structures of AIP-1 and AIP-2 were modelled as there are no experimental structures available. The use of isotopically labelled protein with NMR spectroscopy, or X-ray crystallography could be used to determine the three-dimensional structures of these proteins. Experimental determination of the structure of AIP-2 is also likely to shed light on the apparent discrepancy of the propensity of the AIP2(69-85) peptide to form

helical structure in solution (secondary shift analysis and slow exchange data) but is predicted to be in a β-sheet structure in the full-length protein.

The AIP peptides identified in this thesis might also be useful for inflammatory diseases other than IBD. The AIP-2 protein has been shown to have effects in asthma, and consequently it is of significant interest to also test the AIP peptides in models of asthma. More broadly, inflammation can also be important for a range of disease states such as peripheral artery disease and further study could involve testing the AIP peptides in a range of disease models.

Another possible direction for study involves the oral administration of the peptides. The peptides used in this study were injected intraperitoneally, but the pharmaceutical industry, and indeed patients, prefer orally available drugs rather than agents that require injection. Therefore, one of the next steps is to study the oral efficacy of these peptides. Interestingly, the MC-12 tri-peptide was shown to have oral activity by Ouyang et al, albeit at very high concentrations. The oral efficacy of such a small peptide provides promise for the peptides designed in this study, particularly the grafted peptides that incorporate the MC-12 sequence but have improved *in vitro* stability. However, a range of approaches can also be used to further enhance stability of peptides such as the incorporation of non-natural amino acids, N-methylation and albumin binding tags.

There are several animal models of colitis and analysis of the anti-inflammatory peptides in additional models might provide further insight into the potential of these peptides. The TNBS model has the advantage of being a relatively short model (3 days), and requires limited quantities of test compound, but models such as the T-cell transfer model (animals genetically programmed to develop IBD when receiving injections of the sorted T-cells from naïve mice).

The disadvantage of this model is that takes 8 weeks and would require multiple injections of the peptides.

More dramatic changes in mouse models might also be a future avenue of study. We study human diseases in mouse models where the mice are kept in pristine laboratory environments, free of pathogens, which could potentially impair the immune system, and clearly does not represent the lifestyle of humans. It has been suggested that the use of pathogen free mice might be related to the poor relationship between animal model results and human trial results. Recent studies have started to explore the use of “dirty mice” models where the mice are not raised in pathogen free environments, to determine if models using these mice represent more realistic models of disease. Such studies could give us a better understanding of diseases and models that are closer data to human diseases and could have significant implications for autoimmune diseases such as IBD (doi: 10.1038/d41586-018-03916-9)

These future directions might help realise the potential of peptides as drug leads for the treatment of inflammatory bowel diseases.

7. Appendix

7.1. Appendix 1. Chapter 2 publication

Cobos Caceres, C., Bansal, P. S., Navarro, S., Wilson, D., Don, L., Giacomin, P., Loukas, A., and Daly, N. L. (2017) An engineered cyclic peptide alleviates symptoms of inflammation in a murine model of inflammatory bowel disease. J. Biol. Chem. 292, 10288-10294.

JBC ARTICLE

An engineered cyclic peptide alleviates symptoms of inflammation in a murine model of inflammatory bowel disease

Received for publication, February 2, 2017, and in revised form, April 20, 2017 Published, Papers in Press, May 4, 2017, DOI 10.1074/jbc.M117.779215

Claudia Cobos Caceres, Paramjit S. Bansal, Severine Navarro, David Wilson, Laurianne Don, Paul Giacomin, Alex Loukas[1], and Norelle L. Daly[2]

From the Centre for Biodiscovery and Molecular Development of Therapeutics, AITHM, James Cook University, Cairns, Queensland 4870, Australia

Edited by Wolfgang Peti

Inflammatory bowel diseases (IBDs) are a set of complex and debilitating diseases for which there is no satisfactory treatment. Recent studies have shown that small peptides show promise for reducing inflammation in models of IBD. However, these small peptides are likely to be unstable and rapidly cleared from the circulation, and therefore, if not modified for better stability, represent non-viable drug leads. We hypothesized that improving the stability of these peptides by grafting them into a stable cyclic peptide scaffold may enhance their therapeutic potential. Using this approach, we have designed a novel cyclic peptide that comprises a small bioactive peptide from the annexin A1 protein grafted into a sunflower trypsin inhibitor cyclic scaffold. We used native chemical ligation to synthesize the grafted cyclic peptide. This engineered cyclic peptide maintained the overall fold of the naturally occurring cyclic peptide, was more effective at reducing inflammation in a mouse model of acute colitis than the bioactive peptide alone, and showed enhanced stability in human serum. Our findings suggest that the use of cyclic peptides as structural backbones offers a promising approach for the treatment of IBD and potentially other chronic inflammatory conditions.

The authors declare that they have no conflicts of interest with the contents of this article.

This article contains supplemental Tables 1 and 2.

The atomic coordinates and structure factors (codes 5VAV and 5VFW) have been deposited in the Protein Data Bank (http://wwpdb.org/).

The chemical shifts are available in the Biological Magnetic Resonance Data Bank under accession numbers 30274 and 30281.

[1] Recipient of fellowship support from National Health and Medical Research Council NHMRC (1020114). To whom correspondence should be addressed. Tel.: 61-7-4232-1608; Email: alex.loukas@jcu.edu.au.

[2] Recipient of fellowship support from Australian Research Council (FF110100226). To whom correspondence should be addressed. Tel.: 61-7-42321815; E-mail: norelle.daly@jcu.edu.au.

[3] The abbreviations used are: IBD, inflammatory bowel disease; SFTI-1, sunflower trypsin inhibitor-1; DMF, dimethylformamide; TNBS, 2,4,6-trinitrobenzenesulfonic acid; Fmoc, fluorenylmethyloxycarbonyl; TOCSY, total correlation spectroscopy; RP-HPLC, reverse-phase HPLC.

Content has been removed
due to copyright restrictions

Content has been removed
due to copyright restrictions

Content has been removed
due to copyright restrictions

Content has been removed
due to copyright restrictions

Content has been removed
due to copyright restrictions

Content has been removed
due to copyright restrictions

7.3. Appendix 2. RP-HPLC purity and NMR spectra

7.3.1. Chapter 2

7.3.1.1. c-MC12 peptide

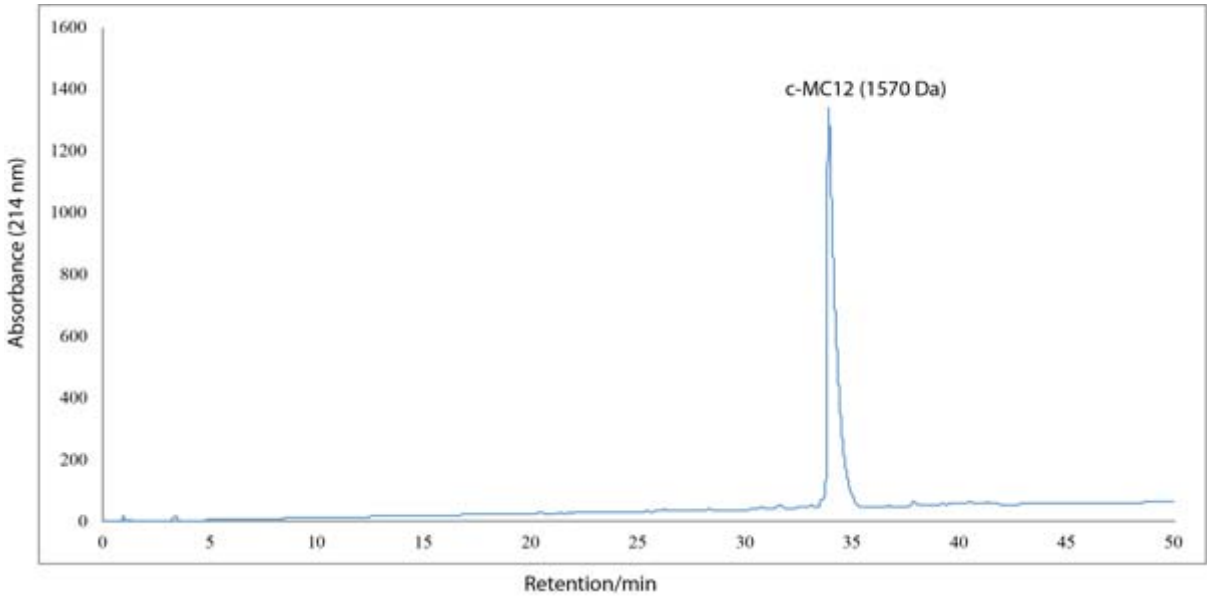

8.1 Reverse Phase High Performance Liquid Chromatography (RP-HPLC)

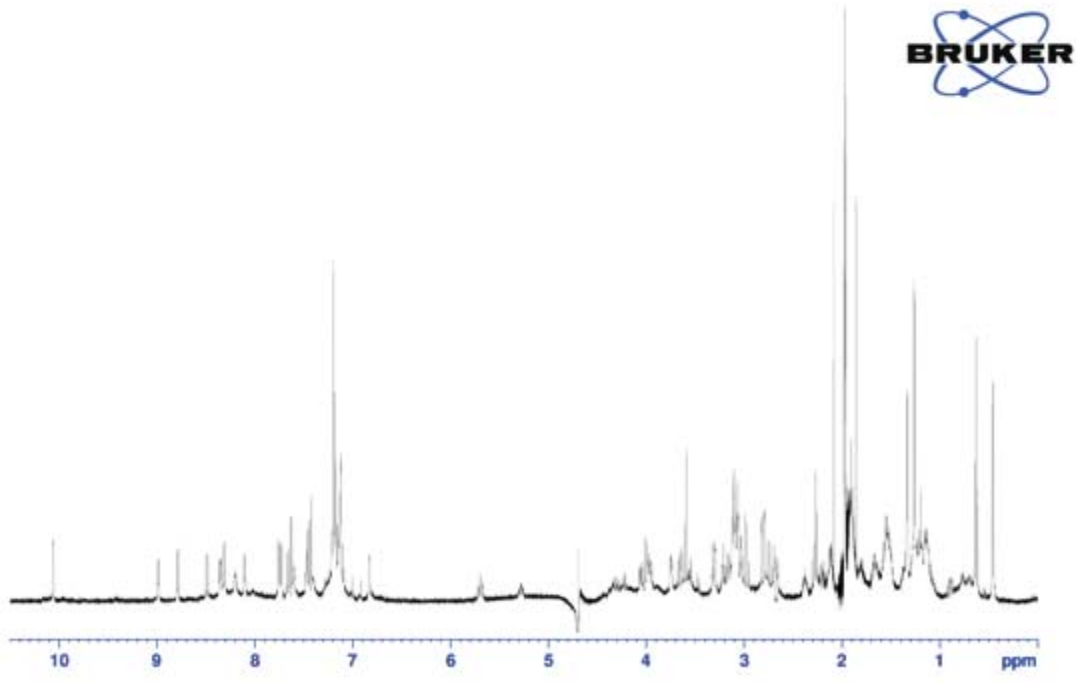

8.2 ^{1}H NMR in D_2O

7.3.2. Chapter 3

7.3.2.1. MC12-linaclotide peptide

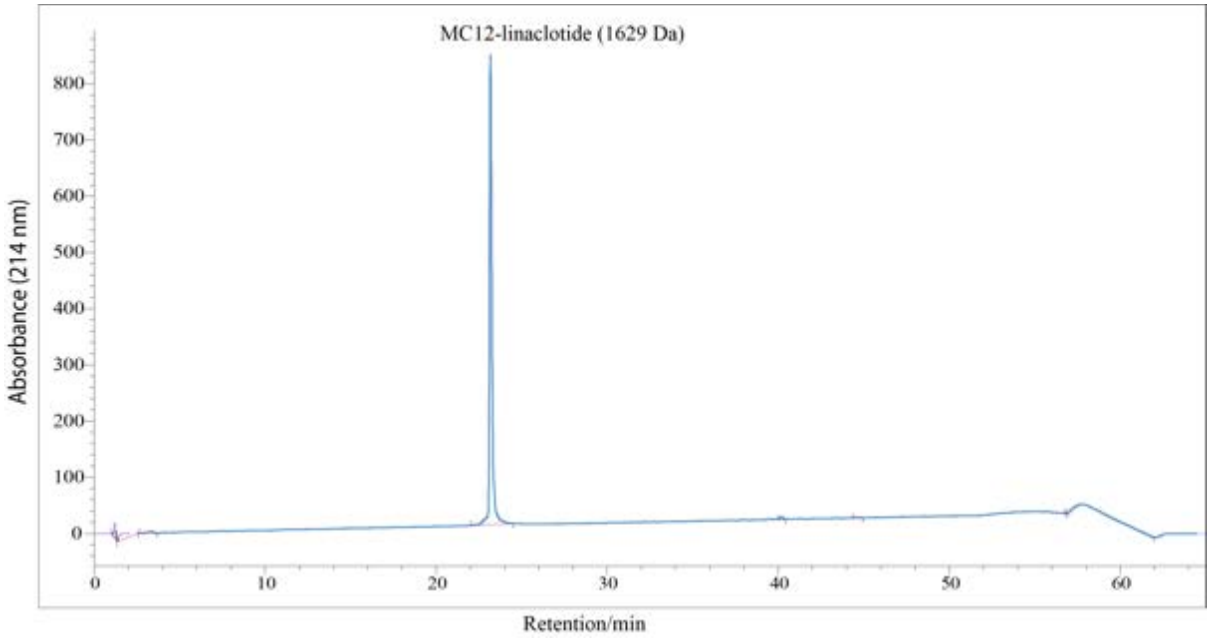

8.3 Reverse Phase High Performance Liquid Chromatography (RP-HPLC)

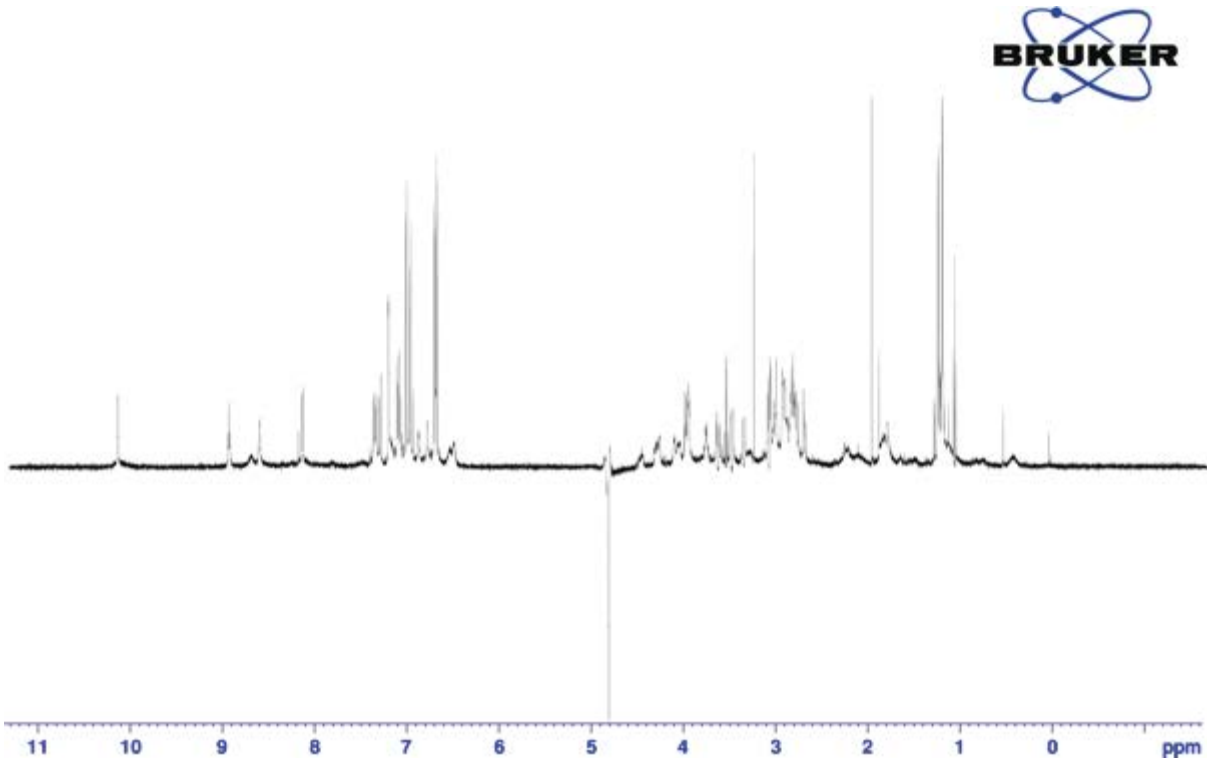

8.4. ^{1}H NMR in D_2O

7.3.3. Chapter 4

7.3.3.1. AIP2-20 peptide

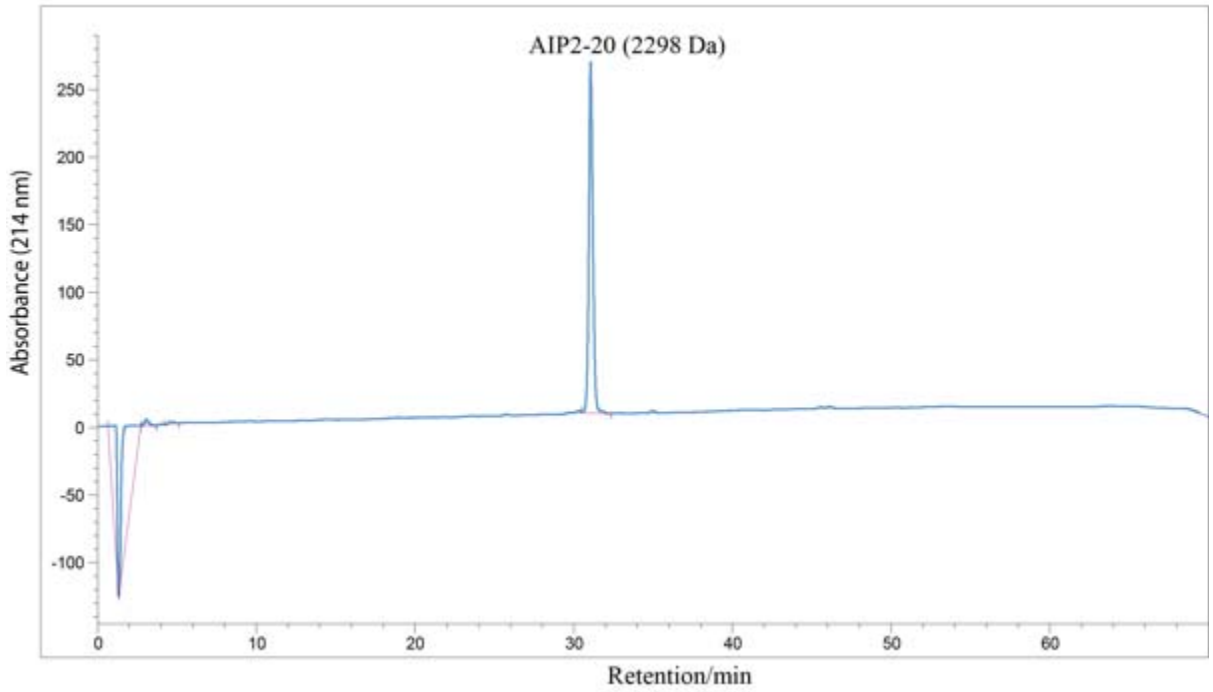

8.5. Reverse Phase High Performance Liquid Chromatography (RP-HPLC)

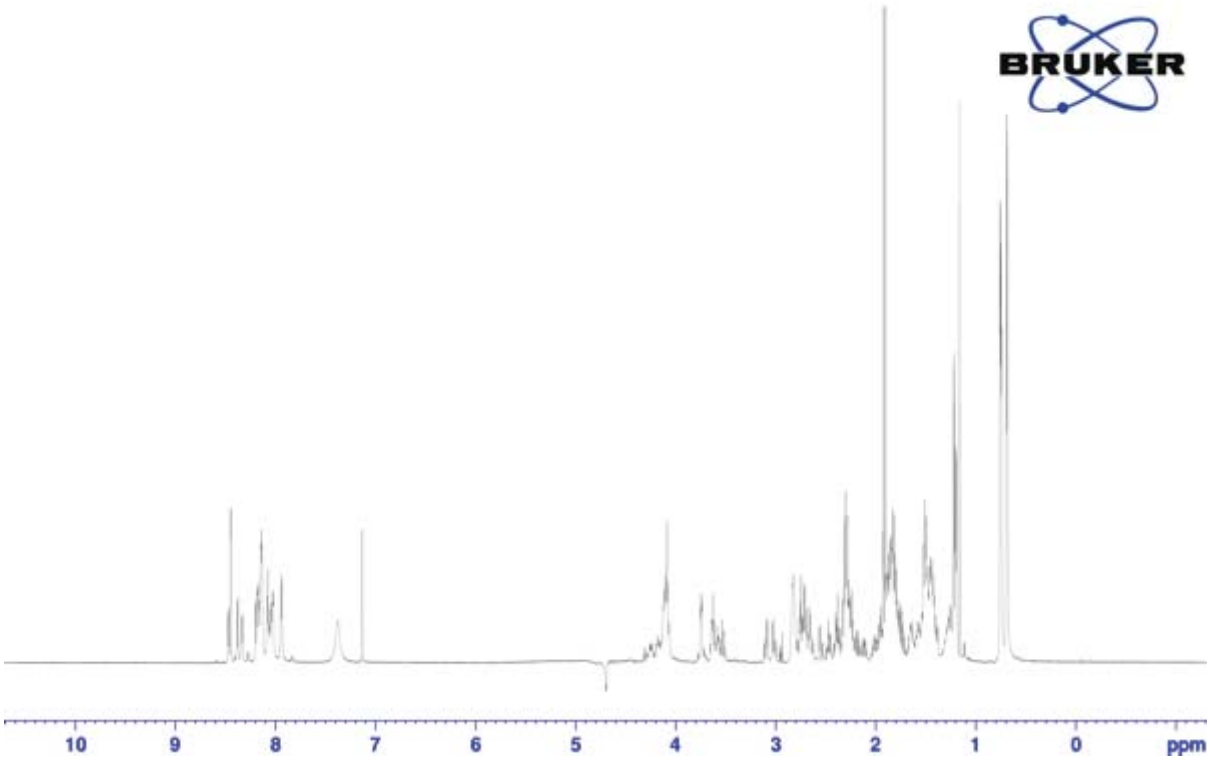

8.6. ^{1}H NMR in D_2O

7.3.3.2. AIP2-20D6P peptide

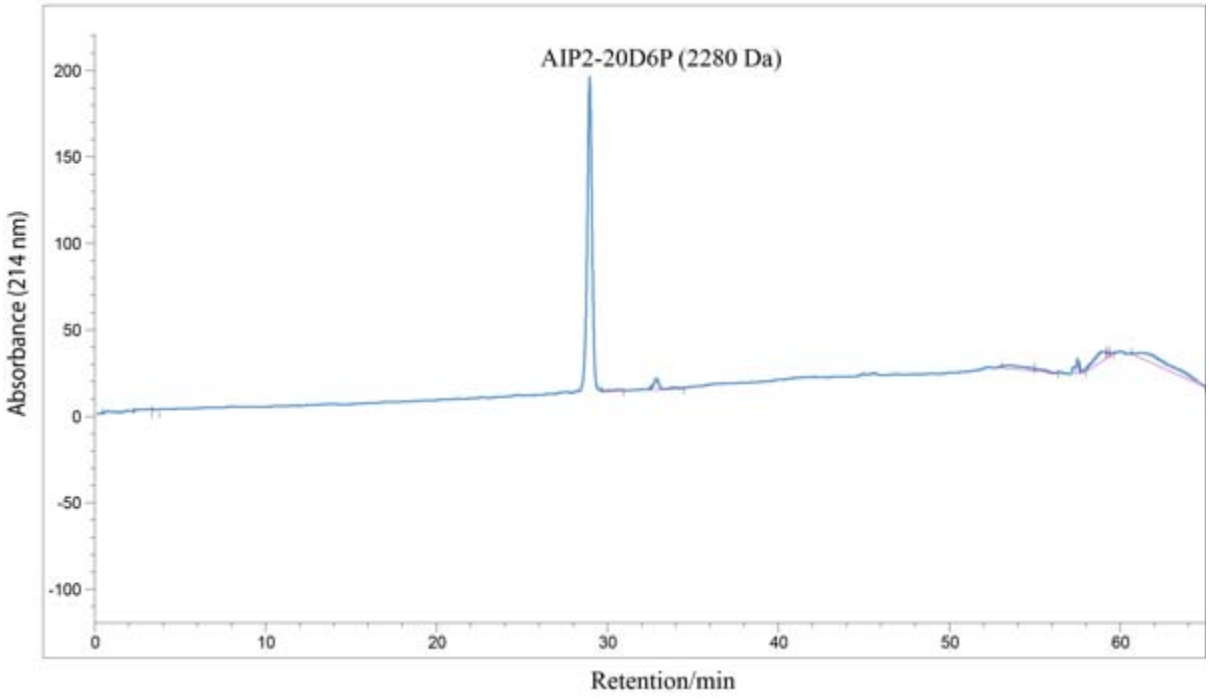

8.7. Reverse Phase High Performance Liquid Chromatography (RP-HPLC)

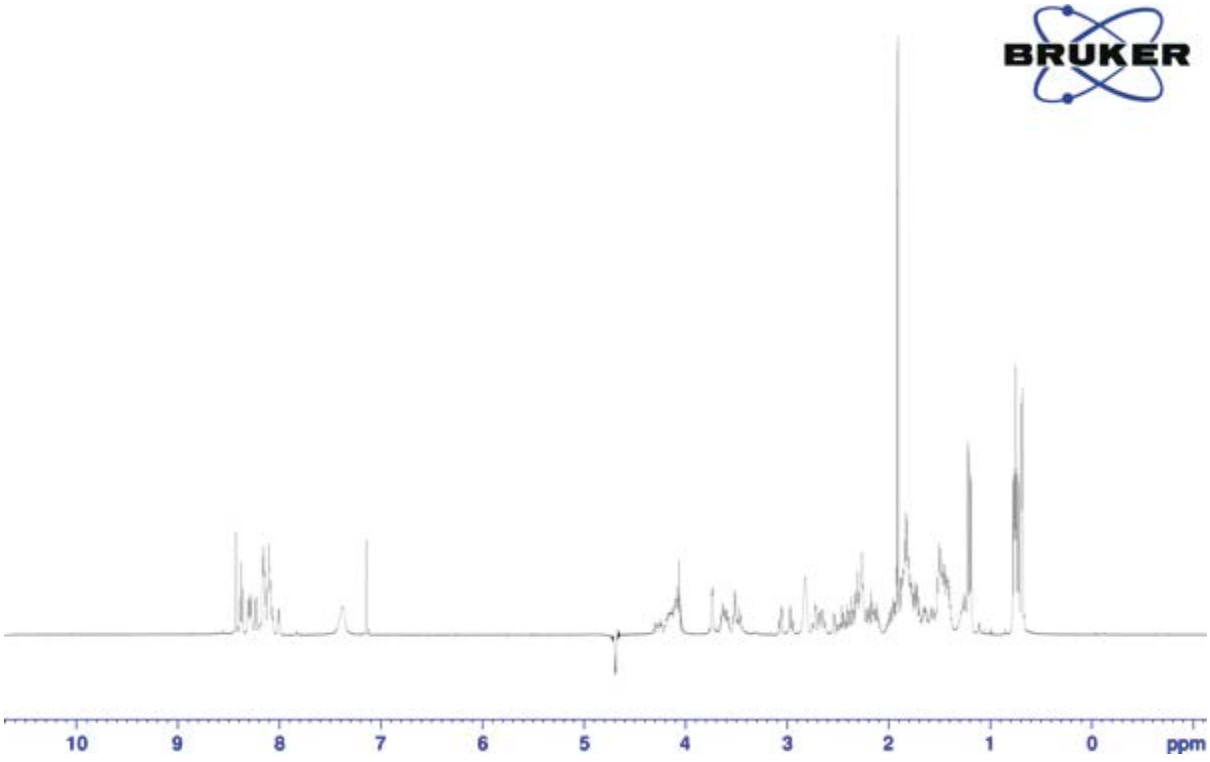

8.8. ^{1}H NMR in D_2O

7.3.3.3. AIP1-13 peptide

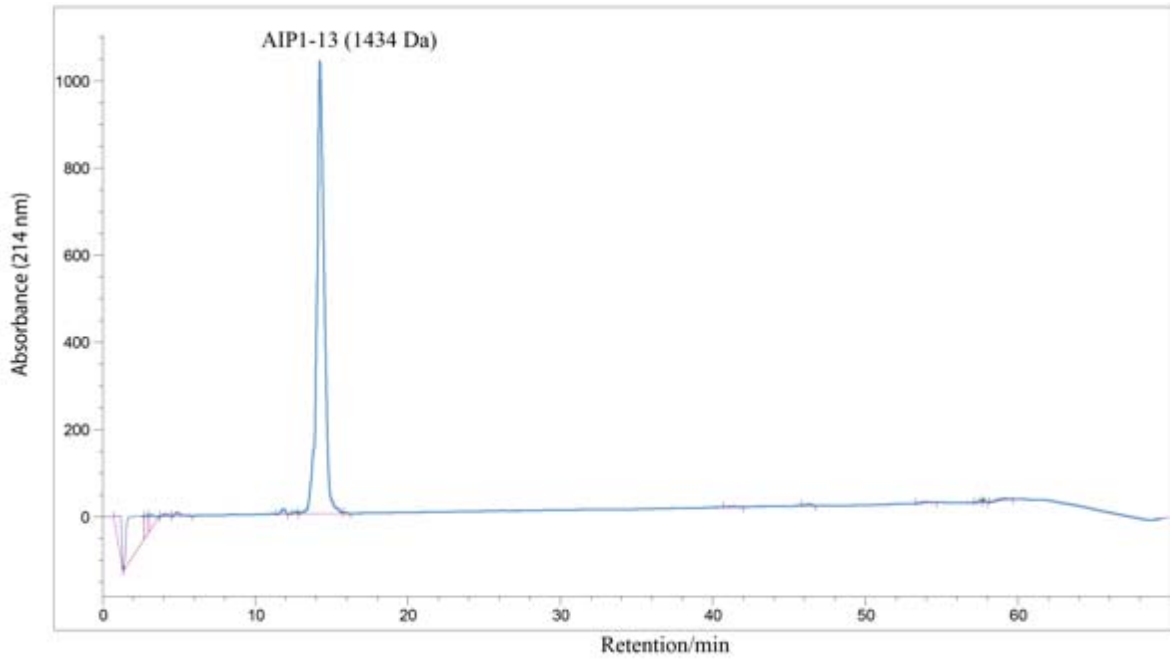

8.9. Reverse Phase High Performance Liquid Chromatography (RP-HPLC)

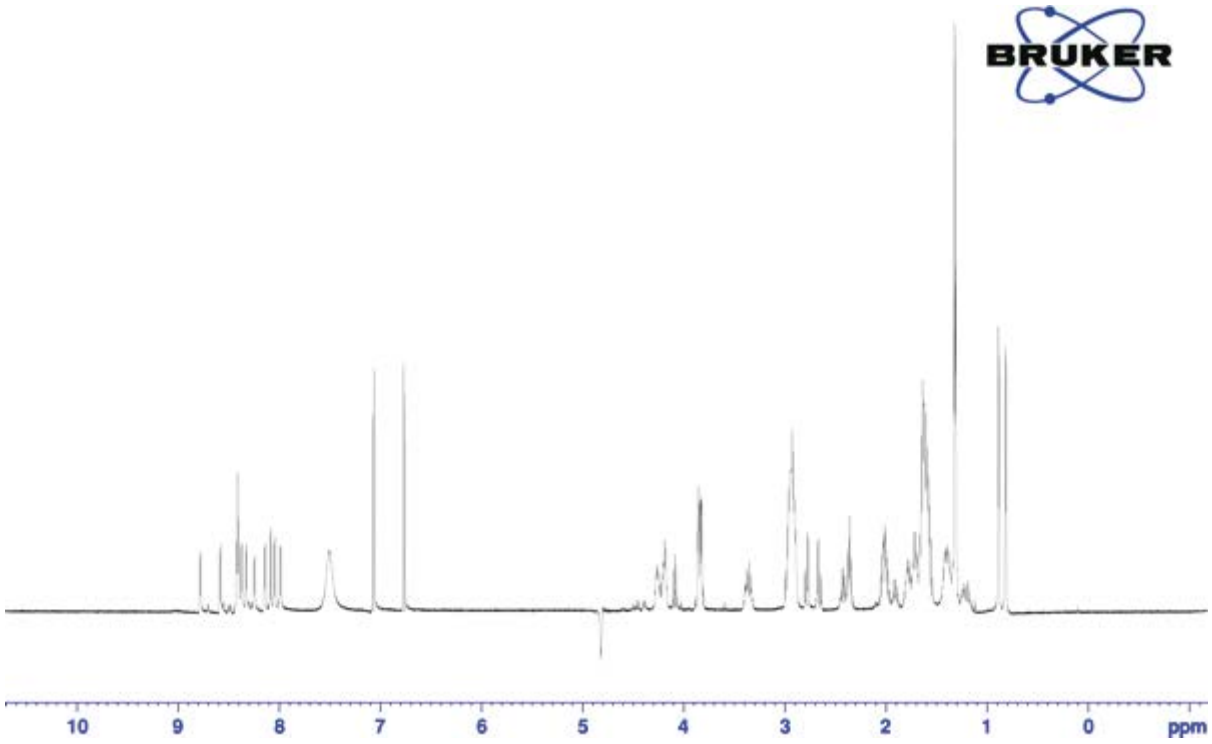

9.1. ^{1}H NMR in D_2O

7.3.3.4. ES-10

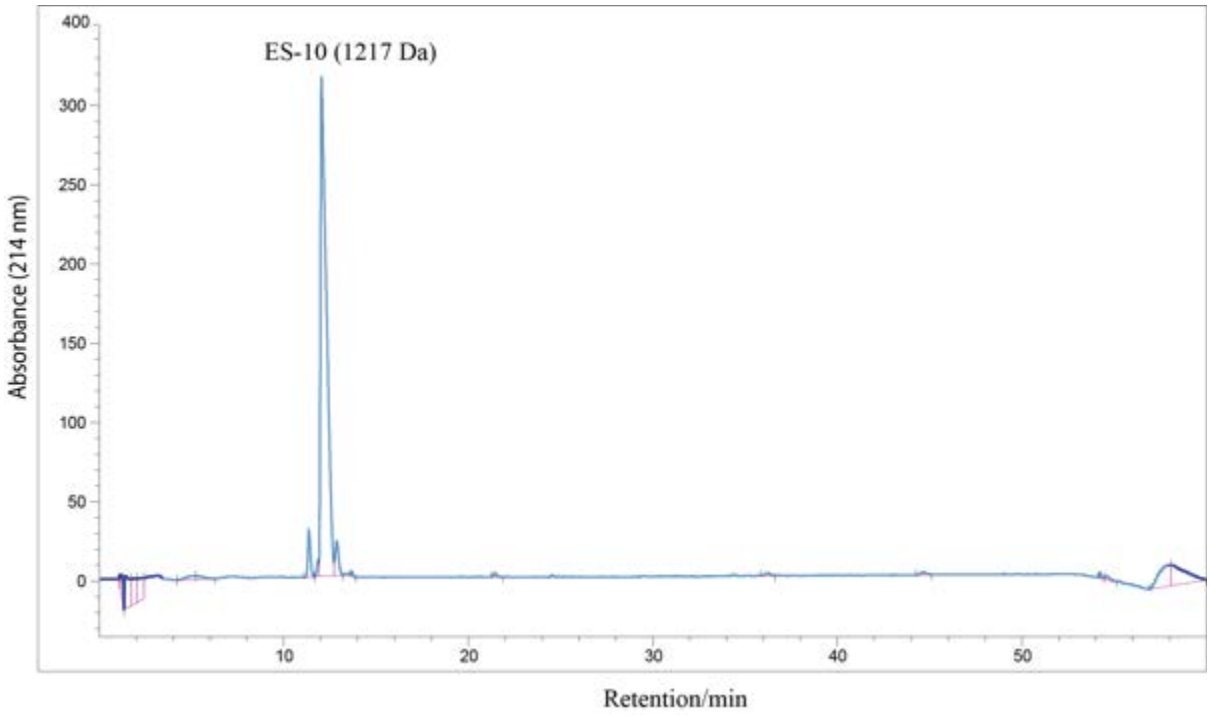

9.2. Reverse Phase High Performance Liquid Chromatography (RP-HPLC)

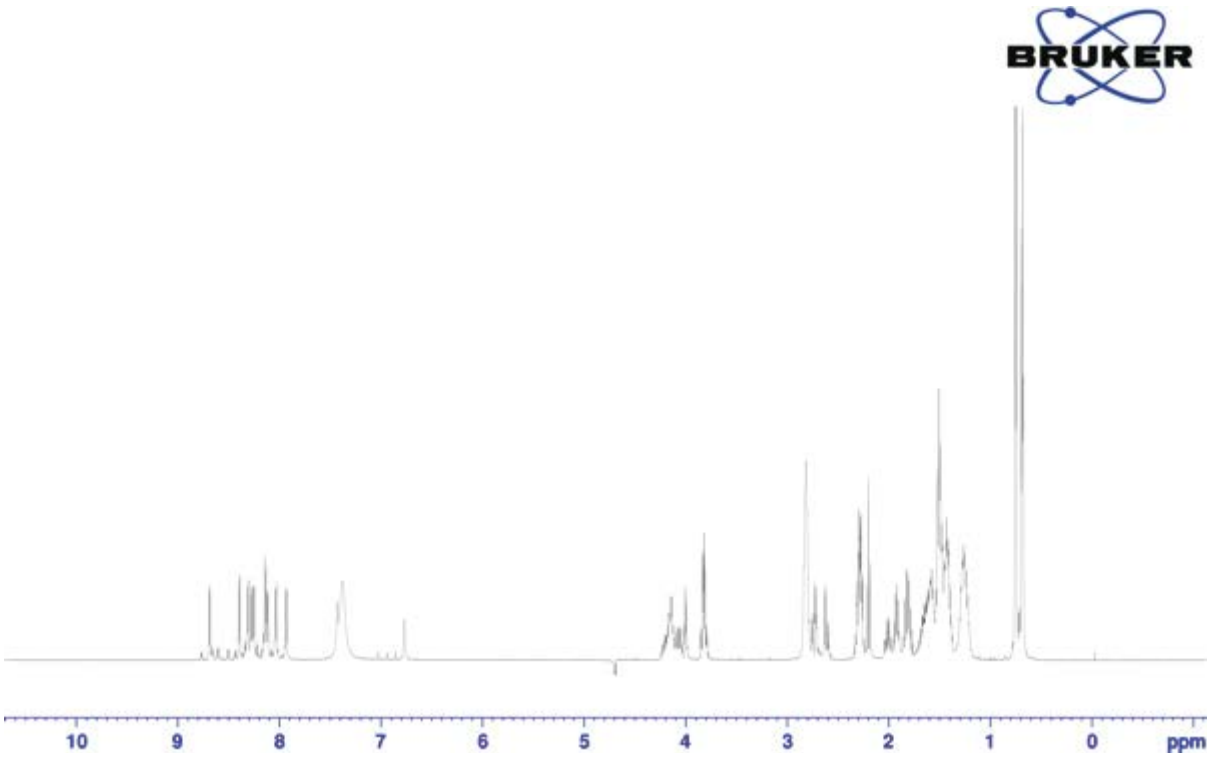

9.3. ^{1}H NMR in D_2O

7.3.4. Chapter 5.

7.3.4.1. 4.1 AIP2(69-95) peptide

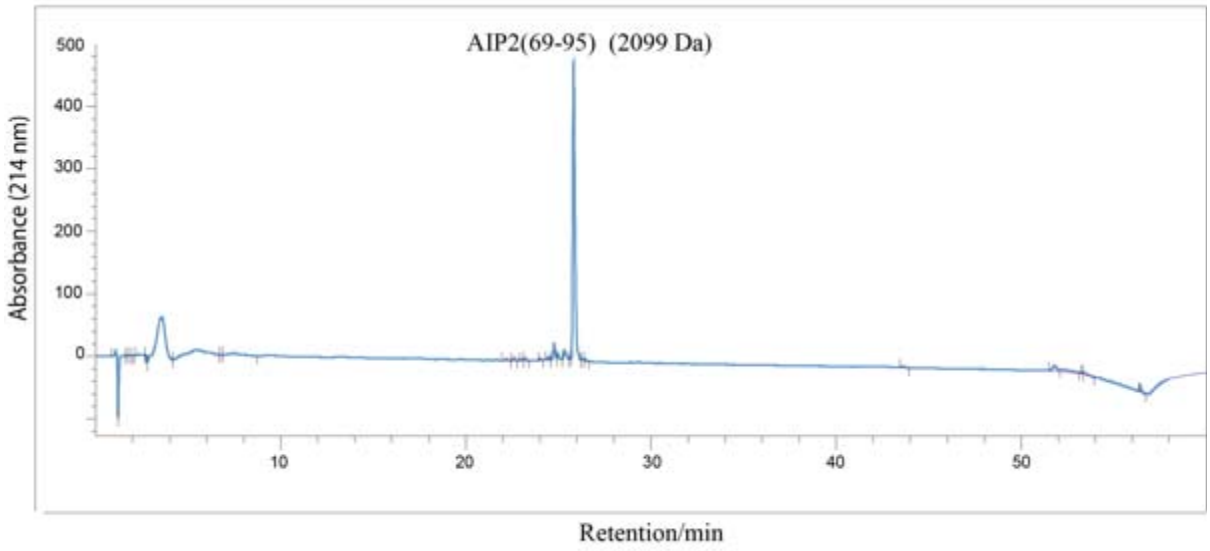

9.4. Reverse Phase High Performance Liquid Chromatography (RP-HPLC)

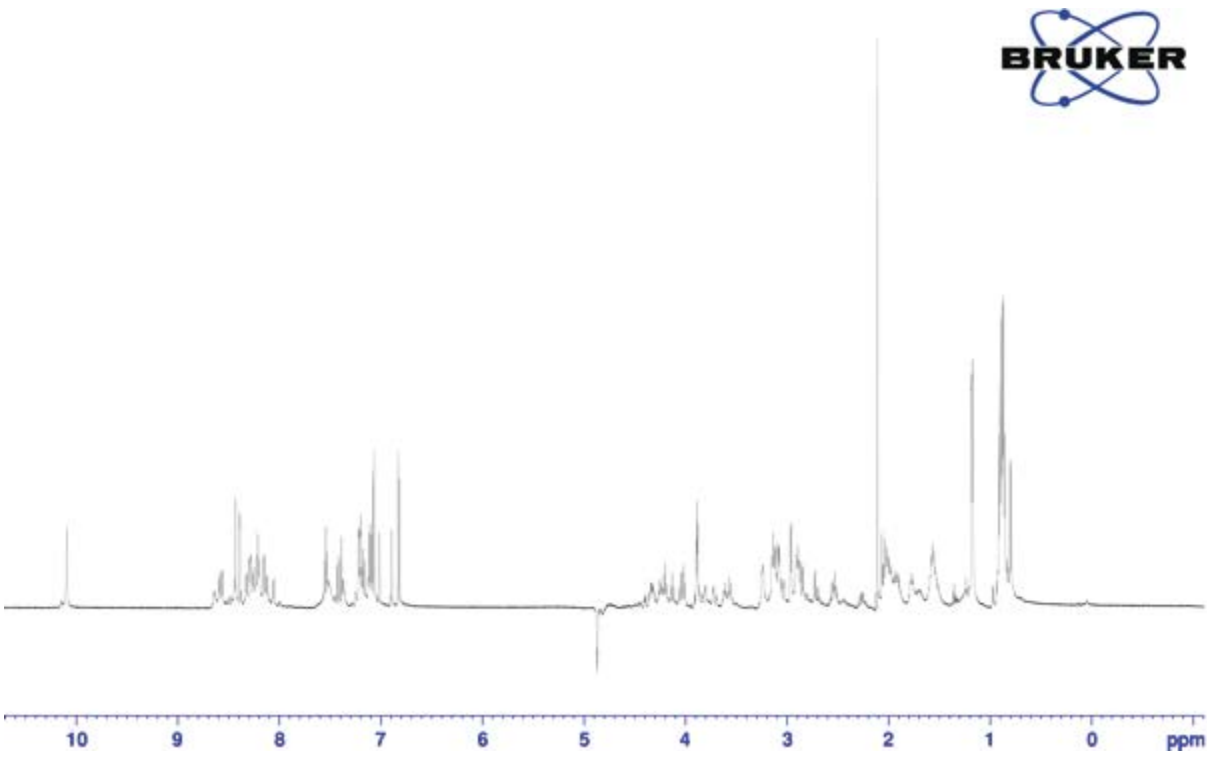

9.5. ^{1}H NMR in D_2O